XVir-N-31-based glioma-oncovirotherapy and its combination with an immune checkpoint inhibition that targets PD-1/PD-L1: Assessment of immune responses

Dissertation

zur Erlangung des Grades eines
Doktors der Naturwissenschaften

der Mathematisch-Naturwissenschaftlichen Fakultät
und
der Medizinischen Fakultät
der Eberhard-Karls-Universität Tübingen

vorgelegt
von

Moritz Dominik Klawitter

aus Heilbronn, Deutschland

2023

Tag der mündlichen Prüfung: 10.03.23

Dekan der Math.-Nat. Fakultät: Prof. Dr. Thilo Stehle

Dekan der Medizinischen Fakultät: Prof. Dr. Bernd Pichler

1. Berichterstatter: Prof. Dr. / PD Dr. / Dr. Ulrike Naumann

2. Berichterstatter: Prof. Dr. / PD Dr. / Dr. Ulrich Lauer

Prüfungskommission: Prof. Dr. / PD Dr. / Dr. Ulrike Naumann

Prof. Dr. / PD Dr. / Dr. Ulrich Lauer

Prof. Dr. / PD Dr. / Dr. Stephan Huber

Prof. Dr. / PD Dr. / Dr. Karin Schilbach

Erklärung / Declaration:

Ich erkläre, dass ich die zur Promotion eingereichte Arbeit mit dem Titel:

„XVir-N-31-based glioma-oncovirotherapy and its combination with an immune checkpoint inhibition that targets PD-1/PD-L1: Assessment of immune responses“

selbständig verfasst, nur die angegebenen Quellen und Hilfsmittel benutzt und wörtlich oder inhaltlich übernommene Stellen als solche gekennzeichnet habe. Ich versichere an Eides statt, dass diese Angaben wahr sind und dass ich nichts verschwiegen habe. Mir ist bekannt, dass die falsche Abgabe einer Versicherung an Eides statt mit Freiheitsstrafe bis zu drei Jahren oder mit Geldstrafe bestraft wird.

I hereby declare that I have produced the work entitled "……", submitted for the award of a doctorate, on my own (without external help), have used only the sources and aids indicated and have marked passages included from other works, whether verbatim or in content, as such. I swear upon oath that these statements are true and that I have not concealed anything. I am aware that making a false declaration under oath is punishable by a term of imprisonment of up to three years or by a fine.

Tübingen, den ....

Datum / Date Unterschrift /Signature

List of Contents

Abstract

Glioblastoma (GBM) is the most common malignant primary brain tumor in adults. Even with the current standard of care, including optimal surgical resection, radio- and chemotherapy, the median survival is limited to less than 20 months. Therefore, new therapeutic strategies are urgently needed. Reasons for the bad outcome are, belong others, the highly invasive growth and the strong immunosuppression of this tumor.

A promising approach to treat GBM is oncolytic virotherapy. It has been shown that oncolytic viruses (OV) provide, aside oncolysis, immunostimulatory effects. By the release of cytokines and damage associated molecular pattern (DAMP) proteins from OV infected tumor cells, OVs are able to initiate immunogenic cell death (ICD). Subsequently, tumor specific immune cells may be activated and attracted, leading to an anti-tumor response even towards those GBM cells, that have invaded in the healthy brain and that are located far away from the original tumor. In preclinical trials the oncolytic adenovirus (OAV) XVir-N-31 was already found to be effective in the therapy of experimental GBM as it significantly prolonged the survival of GBM bearing mice. The aim of this project was to examine the impact of XVir-N-31 on its capacity to induce ICD and to determine its immunostimulatory, anti-tumoral effects both *in vitro* and *in vivo* using an immuno-humanized GBM mouse model.

Besides others, one of the typical immunosuppressive features of GBM is the strong surface exposure of programmed cell death ligand 1 (PD-L1) on GBM cells, leading, by interaction with programmed cell death 1 (PD-1) expressed on immune cells, to the exhaustion of these cells. Therefore, the impact of an additional immune checkpoint inhibitory therapy was examined. In this regard, an XVir-N-31 based OVT in combination with a blockade of the PD-1/PD-L1 axis was conducted, either by the systemic application of Nivolumab in combination with an intra-tumoral injection of XVir-N-31, or by the local expression of an anti-PD-L1 neutralizing antibody that is coded by the XVir-N-31 derivate XVir-N-31-anti-PD-L1. For this, the functionality of XVir-N-31-anti-PD-L1 was confirmed *in vitro*.

In contrast to the wild type-like adenovirus dl309, which possesses higher cytotoxicity, XVir-N-31 and XVir-N-31-anti-PD-L1 induce ICD *in vitro* and *in vivo* as determined by the release of DAMPs and proinflammatory proteins. *In vivo*, a single intratumoral injection of XVir-N-31 increased the amount of tumor infiltrating T lymphocytes and natural killer cells even more than dl309. Furthermore, this effect was not only restricted to virus-injected tumors but was also visible in untreated tumors located in the contralateral hemisphere. The additional blockade of the PD-1/PD-L1 interaction by either multiple systemic applications of Nivolumab or by XVir-N-31-anti-PD-L1 further enhanced the DAMP concentration in the tumor, but also increased the number of tumor infiltrating lymphocytes (TILs). This was true for both, virus-injected as well as for contralateral located, untreated GBMs. Whereas a single, intratumoral injection of dl309 or XVir-N-31 led to massive tumor volume reduction of injected tumors, only the combination of an XVir-N-31 based OVT in combination with the blockade of the PD-1/PD-L1 interaction showed a significant growth reduction of contralateral tumors.

Overall, the obtained data provide strong evidence that XVir-N-31 is a promising therapeutic agent for a successful treatment of GBM and that its immune activating properties and the induction of ICD is of greater importance than its cell killing capacity. For the improvement of the therapy and an induction of strong abscopal effects on tumor cells that are located far away from the site of virus injection, an additional blockade of the PD-1/PD-L1 interaction, ideally by XVir-N-31-anti-PD-L1 expressed anti-PD-L1, seems to be highly beneficial.

Zusammenfassung

Das Glioblastom (GBM) ist der beim Menschen am häufigsten auftretende und bösartigste, primäre Hirntumor. Selbst mit der aktuell optimalen Therapie, bestehend aus operativer Resektion des Tumors, Bestrahlung und Chemotherapie, liegt die durchschnittliche Lebenserwartung bei weniger als 20 Monaten. Die Gründe für diese schlechte Prognose sind u.a. das hochinvasive Wachsen dieses Tumors in das gesunde Hirngewebe hinein, sowie dessen immunsuppressiven Eigenschaften.
Ein vielversprechender Ansatz um GBMs zu behandeln ist die onkolytische Virotherapie (OVT). Onkolytische Viren (OV) besitzen neben ihrer Fähigkeit Tumorzellen zu lysieren (Onkolyse) auch die Fähigkeit, das Immunsystem sowohl unspezifisch als auch gegen den Tumor gerichtet zu stimulieren, indem sie eine spezifische Art von Zelltod, den immunogenen Zelltod (ICD) induzieren. ICD ist gekennzeichnet durch die Freisetzung von Zytokinen und immunogenen Proteinen, den Damage-associated molecular patterns (DAMP). In Folge können Immunzellen angelockt und aktiviert werden, die dann Tumorzellen attackieren und abtöten. Diese Immunzellen können dabei nicht nur den Tumor, in den das OV injiziert wurde, sondern auch invasiv wachsende GBM-Zellen oder Metastasen, die sich weit weg vom Haupttumor befinden, angreifen. Aus Vorarbeiten war bekannt, dass das in dieser Studie verwendete onkolytische Adenovirus (OAV) XVir-N-31 effektiv GBM Zellen lysiert und dass die intratumorale Injektion von XVir-N-31 das Überleben GBM-tragender Mäuse signifikant verlängert. Das Ziel dieses Projekts war, die Effekte von XVir-N-31 auf seine Fähigkeit zur Induktion des ICD sowie hinsichtlich einer Aktivierung der tumorspezifischen Immunabwehr bei der Behandlung von GBM zu identifizieren. Die Untersuchungen erfolgte *in vitro* in Zellkulturen als auch *in vivo* unter Verwendung eines immun-humanisierten GBM Maus-Modells.
Neben vielen anderen Eigenschaften, die zur Immunsuppression beitragen, exprimieren GBM-Zellen oft das Protein programmed cell death ligand 1 (PD-L1) auf ihrer Oberfläche. PD-L1 kann an programmed cell death 1 (PD-1) binden, welches auf Immunzellen exprimiert ist. Diese Interaktion führt zur Inaktivierung (Exhaustion) der Immunzellen und verhindert dadurch eine aktive Immunzellantwort. Basierend auf diesen Kenntnissen wurde in der vorliegenden Studie die XVir-N-31-basierte OVT mit einer Blockade der PD-1/PD-L1 Interaktion kombiniert. Hierzu wurden GBM-tragende Mäuse, zusätzlich zur intratumoralen Injektion von XVir-N-31, Nivolumab appliziert. Alternativ wurde für die intratumorale Injektion XVir-N-31-anti-PD-L1 verwendet, welches für einen PD-L1 neutralisierenden Antikörper (anti-PD-L1) kodiert. Die Funktionalität von anti-PD-L1 wurde *in vitro* bestätigt.
Im Gegensatz zu dem Wildtyp-ähnlichen Adenovirus dl309, das Zellen effektiv lysiert, induzieren XVir-N-31 und XVir-N-31-anti-PD-L1 sowohl *in vitro* als auch *in vivo* ICD. *In vivo* resultierte eine einzelne, intratumorale Injektion von XVir-N-31 in einer, im Verglich zu dl309, signifikant erhöhten Infiltration von T Lymphozyten und natürlichen Killerzellen in das Tumorareal. Diese Beobachtung war nicht nur auf den Tumor beschränkt, in den das Virus injiziert wurde, sondern ebenfalls in unbehandelten, in der kontralateralen Hirnhemisphäre lokalisierten GMBs sichtbar. Die Kombination der XVir-N-31-basierten OVT mit einer Blockade der PD-1/PD-L1 Interaktion, entweder durch systemische Applikation von Nivolumab oder durch intratumorale Injektion von XVir-N-31-anti-PD-L1, resultierte in einer Erhöhung der Konzentration an DAMPs im Tumorareal und einer erhöhten Zahl tumor-infiltrierender Lymphozyten (TILs) in virus-injizierten als auch in kontralateral lokalisierten, unbehandelten GBMs. Während eine einzige intratumorale Injektion von dl309 oder XVir-N-31 zu einer massiven Reduktion des Tumorvolumens in virus-injizierten GBMs führte, war eine solche

Reduktion in kontralateral lokalisierten GBMs nur dann sichtbar, wenn zusätzlich zur OVT die Interaktion von PD-1/PD-L1 gehemmt wurde.
Zusammenfassend legen die von uns erhobenen Daten nahe, dass XVir-N-31 ein vielversprechendes Agens zur Behandlung des GBMs ist. Dabei wurde gezeigt, dass die Induktion von ICD und die anti-tumoralen, immun-aktivierenden Eigenschaften von XVir-N-31 wichtiger sind als seine Fähigkeit durch Onkolyse Tumorzellen direkt abzutöten. Um die XVir-N-31 basierte OVT des GBMs weiter zu optimieren und therapeutische Effekte auch in jenen GBM Zellen zu erzielen, die weit in das gesunde Hirngewebe infiltriert und somit weit vom Originaltumor lokalisiert sind, scheint die Blockade der PD-1/PD-L1 Interaktion als zusätzliche Immun-Checkpoint Inhibitionstherapie äußerst vielversprechend. Idealerweise sollte dieses durch eine intratumorale Injektion von XVir-N-31-anti-PD-L1 erfolgen, da dann der neutralisierende PD-L1 Antikörper nur lokal im Tumorberiech exprimiert wird. Derart können bekannte Nebenwirkungen (severe adverse effects) von Immun-Checkpoint-Inhibitor-basierten Therapieansätzen möglicherweise vermieden werden.

List of Figures

List of Abbreviations and Symbols

Ad/AdV	adenovirus
Ad-NULL	replication deficient adenovirus (E1 deleted)
Ad-WT	wild type adenovirus
ADP	adenovirus death protein
ADP	adenosine diphosphate
AED	anti-epileptic drugs
APC	antigen presenting cell
ATF	activating transcription factor
ATP	adenosine triphosphate
BBB	blood brain barrier
bFGF	basic fibroblast growth factor
bp	base pair
BSA	bovine serum albumin
CAR	chimeric antigen receptor
CAR	coxsackie adenovirus receptor
CD	cluster of differentiation
CDKN2B	cyclin-dependent kinase inhibitor 2B
cIMPACT-NOW	Consortium to Inform Molecular and Practical Approaches to CNS Tumor Taxonomy
CNS	central nervous system
COX2	cyclo-oxygenase 2
CPE	cytopathic effect
CR	conserved region
CRAd	conditionally replicative adenovirus
CSC	cancer stem cell
CTL	cytotoxic T lymphocyte
CTLA-4	cytotoxic T lymphocyte antigen 4
Ctrl	control
CRT	calreticulin
DAMP	damage-associated molecular pattern
DBP	DNA binding protein
DC	dendritic cell
DMEM	Dulbecco's Modified Eagle's Medium
DMSO	dimethylsufloxide
DNA	deoxyribonucleic acid
ds	double-stranded
EGFR	epidermal growth factor receptor
ELISA	Enzyme Linked Immunosorbent Assay
ER	endoplasmic reticulum
et al.	*et alii*
FACS	Fluorescence Activated Cell Sorting
FCS	fetal calf serum
FoxP3	forkhead box P3
g	gram

GABRA1	gamma-aminobutyric acid type A receptor subunit alpha1
GBM	glioblastoma
GM-CSF	granulocyte macrophage colony-stimulating factor
GSC	glioma stem like cell
GvHD	graft versus host disease
h	hour
hAdV	human adenoviruses
Her	human epidermal growth factor receptor
HIF	hypoxia-inducible factor
HLA	human leukocyte antigen
HMGB1	high mobility group B1
HSP70	heat shock protein 70
HSV	herpes simplex virus
IC	immune checkpoint
ICD	immunogenic cell death
ICI	immune checkpoint inhibitor
ICP	immune checkpoint protein
IDH	isocitrate dehydrogenase
IFN	interferon
Ig	immunoglobulin
IL	interleukin
ITR	inverted terminal repeat
IU	international unit
iNOS	inducible nitric oxide synthase
kg	kilogram
M	molar
m^2	square meter
MAPK	mitogen-activated protein kinase
MCP	monocyte chemoattractant protein
MDSC	myeloid-derived suppressor cell
MDR	multi-drug resistance
mg	milligram
MGMT	O^6-methylguanine-DNA methyltransferase
MHC	major histocompatibility complex
MIC	macrophage inhibitory cytokine
min	minute
ml	milliliter
MLP	major late promoter
mM	millimolar
MOI	moiety of infection
mOS	median overall survival
MRI	magnetic resonance imaging
mRNA	messenger RNA
MS	median survival
NEFL	neurofilament light chain
NF1	neurofibromin 1
NF-κB	nuclear factor 'kappa-light-chain-enhancer' of activated B-cells

ng	nanogram
NK cell	natural killer cell
NKG2D	natural killer group 2 member D
NKG2DL	natural killer group 2 member D ligand
NLR	NOD-like receptor
nm	nanometer
NO	nitric oxide
NOD	nucleotide-binding oligomerization domain
NPC	nuclear pore complex
NSG	NOD-scid IL2Rgamma^{null} (NOD.Cg-Prkdc^{scid} Il2rg^{tm1Wjl}/SzJ)
NSCLC	non-small cell lung cancer
OAV	oncolytic adenovirus
OS	overall survival
OV	oncolytic virus
OVT	oncolytic virotherapy
OVIT	oncoviro-immunotherapy
p53	tumor protein p53
PAMP	pathogen-associated molecular pattern
PBMC	peripheral blood mononuclear cell
PD-1	programmed cell death 1
PD-L1	programmed cell death ligand 1
PDGFRA	platelet-derived growth factor receptor A
PGE2	prostaglandin E2
PI3K	phosphoinositide 3-kinase
pH	*potentia hydrogenii*
PRR	pattern recognition receptor
P/S	Penicillin-Streptomycin
PTEN	phosphatase and tensin homolog
RAGE	receptor for advanced glycation end products
Rb	retinoblastoma pocket protein
RGD	arginine-glycine-aspartic acid
RNA	ribonucleic acid
ROS	reactive oxygen species
rpm	rounds per minute
RT	room temperature
scid	severe combined immune deficiency
SEM	standard error of the mean
SHP	SH2 domain-containing phosphatase
SLC12A5	solute carrier family 12 member 5
SNP	single nucleotide polymorphism
ss	single-stranded
STAT	signal transducer and activator of transcription
TAA	tumor associated antigen
TAM	tumor associated macrophage
TBP	TATA-Box binding protein
TCR	T cell receptor
TERT	telomerase reverse transcriptase

TF	transcription factor
TGF	transforming growth factor
Th cell	T helper cell
TIL	tumor infiltrating lymphocytes
TIM-3	T cell immunoglobulin and mucin domain 3
TLR	toll-like receptor
TME	tumor microenvironment
TMZ	temozolomide
TNF	tumor necrosis factor
TP	terminal protein
TRADD	tumor necrosis factor receptor type 1-associated DEATH domain protein
TRAIL	tumornecrosis factor-related apoptosis-inducing ligand
TSP	tumor-specific promoter
TTF	tumor treating field
T_{reg}	regulatory T cell
V	Volt
VEGF	vascular endothelial growth factor
VSV	vesicular stomatitis virus
VTE	venous thromboembolism
WHO	World Health Organization
WT	wild type
YB-1	Y-box binding protein 1
5-ALA	5-aminolevulinic acid
%	percent
°C	degree Celsius
$^{-/-}$	knockout
µg	microgram
µl	microliter
µM	micromolar
µm	micrometer

1. Introduction

1.1 Glioblastoma

Glioblastomas (GBM) are the most common primary brain tumors in adults accounting for over 80% of all malignant primary cerebral cancers (Ostrom, Gittleman et al. 2014). Although incidences can vary and did increase over the last decades (Dobes, Khurana et al. 2011, Leece, Xu et al. 2017), GBM is with less than 10 per 100000 person worldwide (Iacob and Dinca 2009) and approximately 3.22 per 100000 person in the U.S.A. (Wen, Weller et al. 2020) a relatively rare disease. It predominates in elderly patients (over 55 years of age) and in males with a sex ration of 1.5 : 1 (Ohgaki and Kleihues 2013, Louis, Perry et al. 2016, Sung, Ferlay et al. 2021). After diagnostics the prognosis is very poor, with a 5-year survival rate of approximately 5.1% (Ostrom, Gittleman et al. 2014) and a median survival of approximately 10 months (Zhu, Du et al. 2017). Besides age and sex, only ionizing radiation exposure to the head and neck as well as certain genetic factors are known risk factors (Ostrom, Fahmideh et al. 2019). Of note, certain atopic diseases as allergies or asthma as well as early life exposure to infections are associated with a decreased risk of glioblastoma (Ostrom, Fahmideh et al. 2019). While GBM patients usually do not have a family history of cancer (only 5% of all gliomas are familial) (Ranger, Patel et al. 2014), there are 11 specific single nucleotide polymorphisms (SNPs) known to be associated with increased risk for glioblastoma, including alterations in epidermal growth factor receptor (EGFR) (7p11.2), telomerase reverse transcriptase (TERT) (5p15.33) and cyclin-dependent kinase inhibitor 2B (CDKN2B) (9p21.3) (Melin, Barnholtz-Sloan et al. 2017). While the biological significance of these polymorphisms is not fully understood yet and they seem to account only for a small proportion of all cases, continued improvements in the analysis of potential risk factors for GBM will be essential for future diagnostics.

Typical characteristics of GBM are the locally destructive and highly invasive growth, enhanced microvascular proliferation and necrosis (D'Alessio, Proietti et al. 2019), resistance to apoptosis (Burster, Traut et al. 2021), as well as an extremely high immunosuppression (Nduom, Weller et al. 2015). Additionally, a subpopulation of cells, so called *glioma stem like cells* (GSC), are highly resistant to therapy and the foundation of recurrence after therapy (Yi, Hsieh et al. 2016).

1.1.1 Classification and molecular pathogenesis

Tumors of the central nervous system (CNS) have traditionally been classified by the World Health Organization (WHO) into different subtypes and severity grades, ranging from 1 to 4 according to their histology, mutation and dignity (Louis, Perry et al. 2021). GBM, belonging to the class of "Gliomas, Glioneuronal Tumors, and Neuronal Tumors" and the family of adult-type diffuse gliomas, corresponds with its high mortality and poor prognosis to the most malignant grade 4 CNS tumors (Louis, Perry et al. 2021). Overall, GBM classification is extremely difficult and heterogeneous and under constant change. Previously GBM classification was divided by the mutation status of isocitrate dehydrogenase (IDH), with IDH1/2 wildtype status called primary and IDH1/2 mutated GBM called secondary GBM. Secondary GBM was thought to originate from lower-grade gliomas and was overall found in

younger patients, while primary GBM, which accounts for the majority of all GBM, would arise *de novo* and mainly in older patients (Schwartzbaum, Fisher et al. 2006). State of the art classification by the WHO and the Consortium to Inform Molecular and Practical Approaches to CNS Tumor Taxonomy (cIMPACT-NOW), however, only grade IDH-wildtype tumors as GBM, while IDH mutant tumors are considered IDH-mutant astrocytoma WHO grade 4 due to their lower aggressiveness and better outcome of the patients (Yan, Parsons et al. 2009, Brat, Aldape et al. 2020, Louis, Perry et al. 2021).

GBM is now classically characterized by a *de novo* appearance of an IDH-wildtype WHO grade 4 tumor with diffuse and astrocytic features in adults with microvascular proliferation or necrosis (Brat, Aldape et al. 2018). Additionally, also gliomas with histological grade 2 or 3 features can be accounted as GBM if one or more of the three following genetic parameters are given: (i) EGFR gene amplification or (ii) TERT promoter mutation or (iii) the combined gain of the whole chromosome 7 and loss of chromosome 10 (+7/-10) (Tesileanu, Dirven et al. 2020).

Besides this “classical” appearance (I), GBM can be divided into several other subtypes on a molecular level: (II) mesenchymal (with characteristic deletions or mutations in the neurofibromin 1 (NF1) gene as well as high expression of genes in the tumor necrosis factor super family pathway and NF-κB pathway, such as TRADD, RELB, and TNFRSF1A); (III) proneural (with alterations in the platelet-derived growth factor receptor A (PDGFRA) and TP53 as well as loss of heterozygosity); and (IV) neural (typified by the expression of several neuronal markers such as GABRA1, NEFL or SLC12A5 (Verhaak, Hoadley et al. 2010). Nevertheless, this subdivision is only a rough classification since several other subgroups do also exist. Additionally, GBM can be mixed entities, where different cells contain multiple cell states and harbor different mutations. Also, many different mutations as for example PTEN loss overlap across the different subgroups. Taking all this together with the additional large number of rare mutations that can occur in all subclasses, GBM is a highly heterogeneous tumor which impedes the successful treatment (Omuro and DeAngelis 2013).

1.1.2 Diagnosis and conventional treatment

First diagnosis of GBM is usually after clinical presentation of the patient following first neurological symptoms. Rapid tumor growth and infiltrating destruction and displacing of healthy brain tissue with increased intracranial pressure leads to new onset of symptoms as epilepsy, progressive headaches or neurocognitive impairments (Weller, Van Den Bent et al. 2017). The most commonly diagnostic tool used is the contrast-enhanced magnetic resonance imaging (MRI), showing typically a necrotic tumor core mass which is surrounded by non-enhanced signal abnormalities which represent the infiltrative tumor cells as well as possible oedemas, haemorrhages or cystic changes (Ly, Wen et al. 2020, Wen, Weller et al. 2020). Diagnosed patient’s treatment focusses on two different pillars: the coping of the existing symptoms and the treatment of the underlying cause.

91 % of all GBM patients show cognitive deficits. The treatment of these symptoms is of fundamental importance to retain the quality of life and the patient’s will to fight this horrendous disease as well as supportive care for terminally ill patients. Anti-epileptic drugs (AED) can be administered to patients suffering from seizures. To relieve the intracranial pressure coming from the peritumoral vasogenic edemas and with this also the neurological deficits the corticosteroid Dexamethasone is used (Wen, Weller et al. 2020). This is currently under

discussion, since the side effects at high dosages over an extended period of time could worsen the patients outcome (Cenciarini, Valentino et al. 2019). Additionally to that and to further improve the patient's quality of life, including reduced sleep disturbance and fatigue, psychostimulants or acetylcholinesterase inhibitors might be given (Tucha, Smely et al. 2000). A high risk for GBM patients is also venous thromboembolism (VTE), indicating the usage of anticoagulants as beneficial. Nevertheless, frequently occurring haemorrhages following tumor resection as well as no significant improvement in overall survival (OS) leave doubts to the beneficial features (Le Rhun, Genbrugge et al. 2018, Muster and Gary 2020).

The treatment of the underlying cause for GBM has been the same since Stupp *et al.* showed in 2005 the beneficial use of the alkylating cytostatic drug temozolomide (TMZ) together with radiotherapy. Since then, standard therapy for primary GBM consists of maximal safe surgical resection, followed by radiotherapy and chemotherapy with TMZ.

With the help of 5-aminolevulinic acid (5-ALA), a typical compound used for photodynamic detection and surgery of cancer, a gross total resection of the tumor mass is performed (Ellingson, Abrey et al. 2018). Besides the intracranial reduction of the tumor volume, the taken biopsies are also used for histological analysis and tumor grading, as well as for genotyping. Special regard is thereby traditionally taken to IDH1/2 mutation status and the methylation status of the promotor region of O^6-methylguanine-DNA methyltransferase (MGMT), the so far only predictive biomarker for GBM (Eigenbrod, Trabold et al. 2014). Epigenetic silencing of MGMT due to enhanced promoter methylation is associated with a strong response to TMZ and thereby an improved outcome (Hegi, Diserens et al. 2005).

After resection, patients receive a combination of radiotherapy with concomitant TMZ treatment. Radiotherapy usually consists of a total of 60 Gray, given in 30 doses of 2 Gray over 6 weeks (Stupp, Mason et al. 2005). In patients with a certain medical history and in patients over 65 years of age a reduced dose of 40 Gray in 15 fractions can be applied since these patients show a higher vulnerability to toxic side effects and an overall impeded prognosis (Roa, Brasher et al. 2004). Concurrently, patients receive daily oral applications of TMZ (75 mg/m^2) over the course of these 6 weeks, followed by 6 cycles of maintenance TMZ over the next 6 months (150-200 mg/m^2 on days 1-5 every 28 days) (Stupp, Mason et al. 2005). Combined treatment of radiotherapy with TMZ application increased the median survival (MS) from 12,1 months (radiotherapy alone) to 14,6 months (radiotherapy plus TMZ) and the two-year survival from 10.4 % (radiotherapy alone) to 26.5 % (radiotherapy plus TMZ) while adding only minimal additional toxicity to the patient (Stupp, Mason et al. 2005). Recently, the addition of tumor treating fields (TTF) - low-intensity, electric fields applied to the scalp to impede cancer cell division and given during maintenance temozolomide - did further improve the median OS (mOS) to 20,9 months (Stupp, Taillibert et al. 2017). However, despite this multimodal best available therapy, the prognosis for patients remains poor and the recurrence rate is with over 90 % and a median recurrence time of 7 months extremely high and frequent (Stupp, Hegi et al. 2009). It was even shown that some of the current treatment options might have immunosuppressive effects, thereby hampering the optimal treatment for recurrent GBM (Chiocca, Yu et al. 2019, McGranahan, Therkelsen et al. 2019).

For recurrent GBM there is so far no standard therapy. Repeated resection and rechallenging with radio-chemotherapy might be applied depending on the individual patient's situation, otherwise best palliative supportive care is given (Tan, Ashley et al. 2020). Additional therapeutic approaches are under heavy investigation. Treatment with nitrosourea, such as carmustine or lomustine, as well as bevacizumab, an antibody targeting the vascular

endothelial growth factor (VEGF), a pro-angiogenic factor involved in tumor progression, or TTF were analysed, but failed to show statistically significant benefits in recurrent GBM (Nabors, Portnow et al. 2020). With an OS of 4-6 months, even after treatment, the prognosis remains extremely fatal. Therefore, new therapeutic strategies are urgently needed. A new approach is the specific targeted therapy, where new drugs or antibodies specifically target alterations of signalling pathways commonly dysregulated in GBM (Taylor, Brzozowski et al. 2019). Furthermore, several new methods as radiolabeled drugs, antiangiogenic agents, and gene therapy are in focus of research (Omuro and DeAngelis 2013). Another very promising approach to treat GBM might be immunotherapy. However, the typical characteristics of GBM (see 1.1) including immunosuppression and the poor understanding of the tumor microenvironment (Razavi, Lee et al. 2016) as well as its intracranial location, which prevents the tumor from the penetration of most conventionally applied drugs via the blood brain barrier (BBB) (Filley, Henriquez et al. 2017) are still major hurdles for the success of novel immunotherapies. Therefore, an enhanced understanding of the immune biology in the brain and especially in GBM is of fundamental importance.

1.1.3 The immune system in GBM

The CNS, and more specifically the brain, was long thought to be an “immune privileged” organ that is not in direct contact with the body’s immune system due to an intact BBB. This highly selective physical barrier, consisting of endothelial cells tightly connected through tight junctions and bolstered by astrocytes and pericytes, usually prevents the infiltration of large hydrophilic molecules and cells into the CNS (Bauer, Krizbai et al. 2014). This dogma changed, when Louveau *et. al.* proved in 2015 the existence of a functional lymphatic system in the brain, which is connected to the cervical lymph nodes and through which immune cells can access the brain parenchyma (Louveau, Smirnov et al. 2015). Nevertheless, in quiescent state, without infection or neoplasms, microglia cells, which account for approximately 10 % of all CNS cells, build the major primary resident immune cell fraction in the brain (Salter and Stevens 2017, Hutter, Theruvath et al. 2019). This changes under pathological stimuli, such as tumor growth. Thereby, interferon-inducible chemokines induce physiological changes to the blood vessels and lead to a selective permeability of the BBB allowing the recruitment and the invasion of peripheral immune cells, such as T cells, dendritic cells (DC), natural killer (NK) cells or macrophages, into the brain (Domingues, González-Tablas et al. 2016). Specifically GBM, with its highly immunosuppressive characteristics but also its high heterogeneity and specific microenvironment display a very complex relationship to immune surveillance. There are major differences of immune evasion mechanisms in all of the different subpopulations and subclasses of GBM and even intratumorally dependent on the relative location to blood vessels (Pombo Antunes, Scheyltjens et al. 2020). Nevertheless, certain mechanisms occur very frequent and are therefore discussed here in more detail. Typically, GBM immunosuppression is characterized by secretion of immunosuppressive cytokines, tissue hypoxia, downregulation of major histocompatibility complex (MHC) molecules and upregulation of immune checkpoint molecules, inhibition of T effector cell activation and proliferation and concurrent activation of regulatory T cells (T_{reg}) as well as repolarisation of macrophages and attraction and activation of myeloid-derived suppressor cells (MDSC) (see Figure 1). These mechanisms foster recurrence and are correlated with a poor prognosis for the patients (Gieryng, Pszczolkowska et al. 2017, Pereira, Barros et al. 2018).

Immunosuppressive cytokines frequently found in GBM microenvironment include interleukin (IL)-10, transforming growth factor-beta (TGF-β) and prostaglandin E2 (PGE2). IL-10 inhibits the production of interferon (IFN)-γ and tumor necrosis factor (TNF)-α by immune cells, induces anergy in T cells and can downregulate the expression of MHC in macrophages, while promoting tumor growth (Van Meir 1995, Huettner, Czub et al. 1997). TGF-β is a known suppressor of T and NK cell activity by the inhibition of IL-2 and the subsequent down-regulation of the activating receptor Natural Killer Group 2 Member D (NKG2D) (Fontana, Bodmer et al. 1991, Crane, Han et al. 2010) and can additionally modulate together with PGE2 the transformation of DCs into a regulatory phenotype, leading to the promotion of T_{regs} (Ghiringhelli, Puig et al. 2005). Furthermore, tumor-promoting cytokines as IL-1 or the basic fibroblast growth factor (bFGF) are also secreted and dampen the immune response (Jackson, Ruzevick et al. 2011).

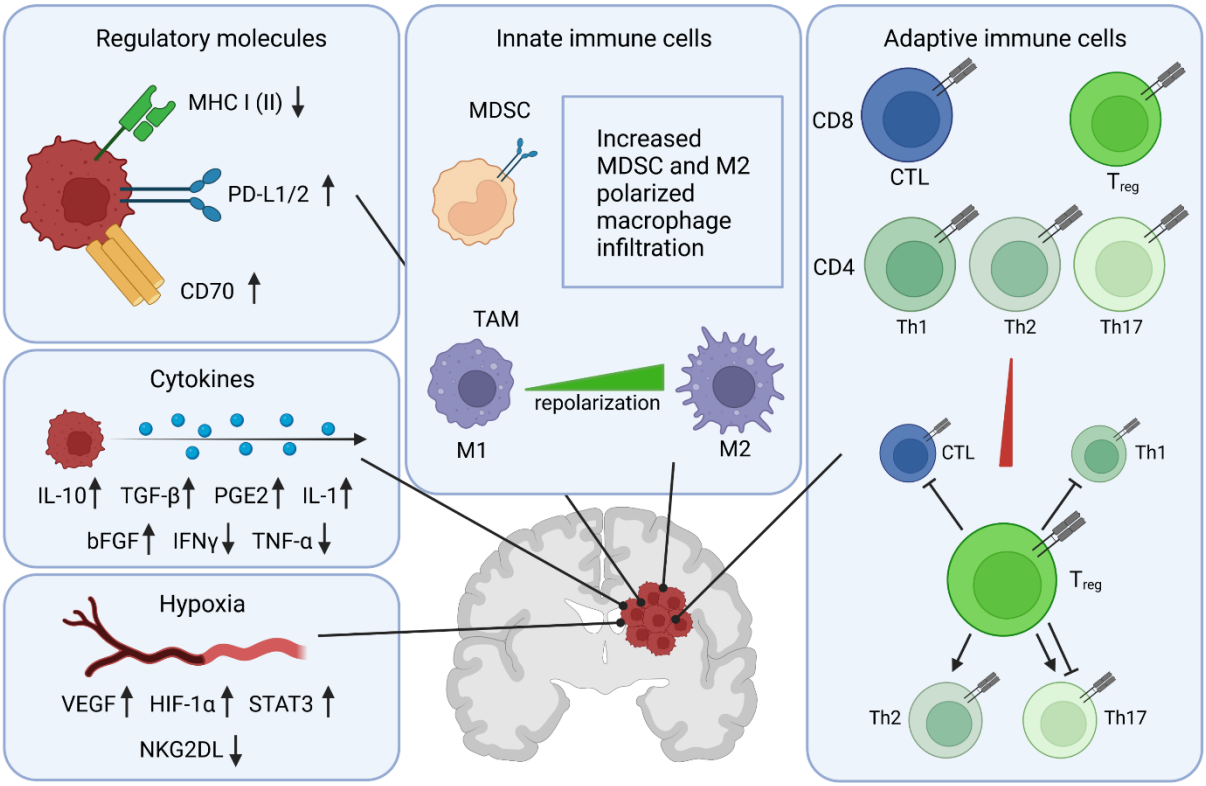

Figure 1. Immunosuppressive mechanisms in GBM. Immunosuppression in GBM occurs besides others via the upregulation of pro-tumorigenic as well as the downregulation of immunogenic genes caused by hypoxia. Additionally, gene expression of immunosuppressive cytokines as well as of immunosuppressive cell surface molecules is upregulated while pro-inflammatory cytokine and major histocompatibility complex (MHC) I and II expression are downregulated. Increased infiltration of myeloid-derived suppressor cells (MDSC), tumor associated macrophages (TAM) in an immunosuppressive M2 polarization and the immunosuppressive regulatory T cells (T_{reg}), which attenuate the T cell anti-tumor response of cytotoxic T lymphocytes (CTL) and T helper (Th) 1 cells but promote immunosuppressive Th2 cell fate, contribute further to the immunological cold tumor microenvironment. (Created with BioRender.com)

Tissue hypoxia, caused by excessive consumption of oxygen by rapidly proliferating GBM cells and insufficient neovascularisation, contributes also to immunosuppression. Hypoxia leads to the activation of genes involved in angiogenesis and tumor cell growth, such as signal transducer and activator of transcription 3 (STAT3) and hypoxia-inducible factor (HIF)-1α. This pathway induces the activation of T_{regs} as well as the production of vascular endothelial growth

factor (VEGF), which is highly involved in immunosuppression (Wei, Wu et al. 2011). Additionally, hypoxia also promotes immune escape from NK cells by downregulating the ligand of NKG2D (NKG2DL) on tumor cells (Burster, Traut et al. 2021).

Another method to evade immune cell response is the altered cell surface expression of immune regulatory molecules on GBM cells. It was shown that GBM cells downregulate the expression of MHC molecules, thereby escaping the recognition from T and NK cells (Zagzag, Salnikow et al. 2005). While in non-neoplastic cells antigens are usually presented on the cell surface via MHC I molecules, which are recognized via the T cell receptor (TCR) of $CD8^+$ T effector cells, GBM cells can lose this ability due to defects in the antigen-presentation pathway (Burster, Gärtner et al. 2021). On the other hand, the upregulation of immune checkpoint molecules such as programmed cell death ligand 1 (PD-L1) is highly common in GBM cells, thereby gaining adaptive resistance (for detail see 1.1.4) (Berghoff, Kiesel et al. 2015, Chen and Han 2015). Enhanced expression of CD70, a TNF family member that interacts with the TNF receptor family protein member CD27 on T cells, mediates additionally T cell apoptosis (Chahlavi, Rayman et al. 2005).

Besides the immediate characteristics of GBM cells causing immunosuppression, the interaction with the tumor microenvironment (TME) is also of fundamental importance. The TME usually consists of non-neoplastic cells, vascular, immune and other glial cells as well as of cytokines and other soluble molecules (Razavi, Lee et al. 2016). Although GBM is said to be an immunological “cold” tumor, meaning a tumor of low immunogenicity, immune cells display a rather big compartment of the total tumor mass. Nevertheless, these cells show heavy modifications concerning their function and phenotype due to the interaction with the tumor cells (Hambardzumyan, Gutmann et al. 2016). Typical immune cells found in the TME are tumor-associated macrophages (TAM) and microglia, MDSC and tumor-infiltrating lymphocytes (TIL), mainly T cells with only minor populations of NK and B cells or DCs.

TAMs are the predominant infiltrating immune cell population, accounting for 30-40 % of all cells (Chen and Hambardzumyan 2018). The TAM population is thereby subdivided into the population of bone marrow-derived infiltrating macrophages/monocytes, which infiltrate the tumor area early during GBM initiation and account for approximately 85% of all TAMs, and the activated resident microglia of the brain which are located mainly in the peritumoral regions and representing the remaining approximately 15 % (Chen, Feng et al. 2017). TAMs are recruited into the TME via the release of chemoattractants, such as the monocyte chemoattractant protein 1 (MCP-1) or the granulocyte macrophage colony-stimulating factor (GM-CSF) by the tumor cells (Hambardzumyan, Gutmann et al. 2016). Upon infiltration, high concentrations of TGF-β1, macrophage inhibitory cytokine-1 (MIC-1), and IL-10 lead to a repolarisation of the cells towards an immunosuppressive M2 phenotype. In this state the phagocytic abilities of TAMs are inhibited, while the capacity to inhibit cytotoxic T cell proliferation and to increase the effect of T_{regs} is enhanced (Wu, Wei et al. 2010). Therefore, an elevated level of M2 macrophages in the tumor area is shown to correlate with enhanced invasiveness and poor prognosis of the patients (Roesch, Rapp et al. 2018).

Another cell population prominently featured in GBM microenvironment are MDSCs. Typically defined by their myeloid linage and immature state, they suppress immune responses via several different mechanisms (Haile, Greten et al. 2012). Upon TGF-β activation they prevent the activation of NKG2D and the production of IFNγ by NK cells (Li, Han et al. 2009). Through the production and secretion of reactive oxygen species (ROS), inducible nitric oxide (NO) synthase 2 (iNOS2), cysteine depletion and the downregulation of CD62L, they favor the induction of T_{regs} and tumor-promoting $CD4^+$ Th2 T cells and induce $CD4^+$ Th1 T cell

suppression (Srivastava, Sinha et al. 2010). While promoting tumor growth and vasculogenesis, a high cell surface expression of PD-L1 leads to a general T cell exhaustion and an inhibition of the antitumoral immune response (Dubinski, Wölfer et al. 2016, Zhang, Ma et al. 2016).

T cells, the key players of adaptive immunity, do also infiltrate the tumor area of GBM and are therefore called TIL. However, with less than 0,25 % of all cells, they account only for a relatively small population in the TME (Han, Ma et al. 2016). Besides their limited quantity, especially the quality and the ratio of their subpopulations feature the immunosuppressive condition of the GBM. T cell subpopulations feature $CD8^+$ cytotoxic T lymphocytes (CTL), the typical immune effector cells essential for tumor cell eradication via the recognition of the MHC I molecule, as well as $CD4^+$ T helper (Th) cells, which recognize the MHC II molecule on antigen presenting cells (APC). Additionally, the $CD4^+$ Th cell population is subdivided into Th1 cells, which are responsible for the release of proinflammatory cytokines as IFNγ or TNFα and are capable of killing tumor cells and Th2 cells, which release multiple immunoregulatory cytokines as IL-4, IL-5, IL-10 and IL-13 and can therefore contribute to tumor growth. Two other subpopulations are $CD4^+$ Th17 cells and $CD4^+/FoxP3^+$ T_{regs} (Wang, Zhou et al. 2021). While Th17 cells, due to the release of IL-17, can have a dual role in tumor progression, favoring the Th1 cell fate, but also induce chronic inflammation favorable for tumor growth (Parajuli 2013), T_{regs} are typical suppressors of the cellular immune response by inhibiting the proliferation of effector T cells and their secretion of cytotoxic cytokines (Wang, Zhou et al. 2021). While $CD8^+$ CTLs, Th1, Th2 and T_{regs} are under normal conditions in a perfectly balanced equilibrium to encounter possible threats but also preventing autoimmune reactions, things change drastically in GBM. The overall CD8 to CD4 ratio within T cells shifts significantly, compared to the ratio in the peripheral blood, with approximately less than 23 % of all TILs being CTLs, depending on the GBM subtype (Han, Ma et al. 2016). Additionally, while infiltration of activated CTLs and Th1 cells is crucial for an effective antitumor immune response and are correlated positively with the survival rate of patients (Ueda, Kohanbash et al. 2009, Rosato, Wijeyesinghe et al. 2019), both subsets are frequently dysfunctional and in a state of exhaustion in GBM (Woroniecka, Rhodin et al. 2018). Multiple recent studies have shown that tumor progression can be decelerated in therapies using an enhanced activation of CTLs (Wang, Zhou et al. 2021). Besides the inactivation of Th1 cells, also the overall Th1/Th2 ratio is an important factor in tumor prognosis. While it was seen that in healthy controls a significantly higher Th1 cell population was found, GBM patients show a shift towards a stronger Th2 phenotype, especially under recurrence (Shimato, Maier et al. 2012). Several different treatments reversing this shift were found to be beneficial for an effective antitumoral response (Wang, Zhou et al. 2021). Although there are contradictory findings about the absolute amount, probably due to the use of different markers and methods, T_{regs} are known to infiltrate the TME in a relatively large number (Gieryng, Pszczolkowska et al. 2017, Tumangelova-Yuzeir, Naydenov et al. 2019). Under healthy conditions T_{regs} are important regulators of self-tolerance and in the maintenance of immune balance by inhibition of activation and proliferation of potential self-reactive T cells (Scheinecker, Göschl et al. 2020). In tumors such as the GBM these immunosuppressive characteristics lead to enhanced tumor progression by the downregulation of an appropriate immune response (Wang, Franco et al. 2017). Via the extensive secretion of TGF-β and IL-10, the subsequent downregulation of IL-2 and IFNγ leads to an exhaustion and even to cytolysis of effector T and NK cells (Woroniecka, Rhodin et al. 2018). It was shown in several studies that reduced numbers of T_{regs} in the TME led to relieved inhibition of the cellular immune response and a benefit in tumor treatment (Wang, Zhou et al. 2021).

Taken all this together, the activation of the immune system, either by depletion of T_{regs} in the TME or by overall stimulation of enhanced infiltration of activated immune cells might be a very promising approach for effective GBM management. The latter possibility would also benefit an increased infiltration of activated NK cells and B cells, which are usually only rarely found in the TME (Hussain, Yang et al. 2006, Poli, Wang et al. 2013).

1.1.4 The PD-1/PD-L1 axis

Programmed cell death 1 (PD-1; CD279), a transmembrane co-receptor, belongs to the family of immunoglobulins and is expressed predominantly by activated T lymphocytes as well as by pro B cells, myeloid cells and NK cells (Francisco, Sage et al. 2010). Activation of PD-1 occurs upon its interaction with its ligands PD-L1 or PD-L2, which are under normal conditions expressed by parenchymal cells, antigen presenting cells (APCs) and B lymphocytes (Flies and Chen 2007). As only recently awarded with the Nobel Prize in Physiology or Medicine to Tasuko Honjo, its interaction leads to negative regulation of T cells by inhibitory signals (Figure 2) (Ishida, Agata et al. 1992). TCR stimulation with concurrent PD-1/PD-L1 engagement leads to tyrosine phosphorylation on the intracellular part of the PD-1 molecule on high affinity sites of SH2 domain-containing phosphatase (SHP-1 and SHP-2) and a subsequent decreased T

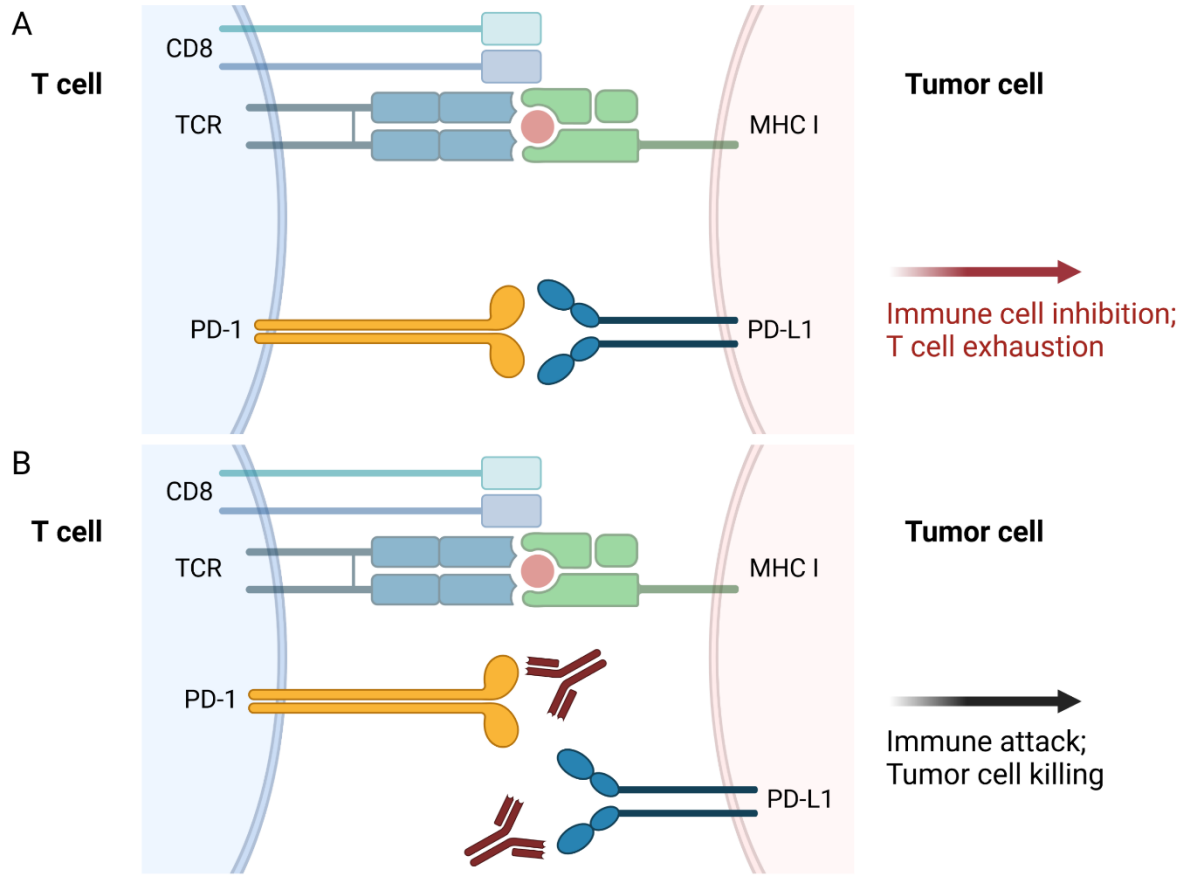

Figure 2. Schematic illustration of the PD-1/PD-L1 axis in the anti-tumor immune response. A. Activated CTL binds via its TCR and the co-stimulatory molecule CD8 to the MHC I molecule on the tumor cell surface. The interaction of PD-1 (T cell) with PD-L1 (tumor cell) leads to an inhibitory signal to the T cell and concurrent T cell exhaustion and no immune response. **B.** Blockade of the PD-1/PD-L1 interaction by neutralizing antibodies leads to no T cell exhaustion, and an efficient T cell mediated tumor cell killing. (Created with BioRender.com)

cell proliferation and survival signal via the PI3K and Akt pathways (Patsoukis, Wang et al. 2020). In contrary to this physiological expression important to prevent immune overreactions, GBM and its TME is also strongly correlated with PD-L1/PD-1 expression, making it the major negative regulation of CTLs and an important factor for tumor promotion. Whilst PD-L1 is strongly upregulated in GBM cells by several mechanisms (PTEN loss, hypoxia, oncogenic mutations and immunosuppressive cytokines induce PD-L1 expression) and over several activation pathways (via IFNγ receptor, EGFR, Toll-like receptor (TLR), IFNα receptor), also infiltrating cells as TAMs and T_{regs} are induced to express PD-1 as well as PD-L1 upon polarization to their immunosuppressive state, even feeding the loop and contributing to the extremely immunosuppressive microenvironment (Parsa, Waldron et al. 2007, Gianchecchi and Fierabracci 2018, Cai, Qi et al. 2019). Berghoff *et al.* showed in a study of 135 human GBM specimens, that 88 % of primary and also 72 % of recurrent GBM did express PD-L1 (Berghoff, Kiesel et al. 2015). Therefore, inhibition of this immune checkpoint (IC) molecule, as well as several others, has recently been under heavy investigation in several preclinical as well as in clinical trials, making it an interesting target for immunotherapy (Schalper, Rodriguez-Ruiz et al. 2019, Scheffel, Grave et al. 2021).

1.2 Immunotherapy

The idea that the immune system protects the body from frequently occurring cancer started in the early 1900s with Paul Ehrlich. This tenet became later on the foundation of Sir Macfarlane Burnet and Lewis Thomas' cancer immunosurveillance hypothesis, stating that in immunocompetent hosts the adaptive immunity is responsible for the prevention of cancer development. This hypothesis was adjusted and expanded over the years, leading to today's knowledge that the immune system exerts not only host-protective but also tumor-promoting functions. The so-called cancer immunoediting theory consists of 3 distinct phases: elimination, equilibrium and escape (the three "E" theory). The elimination phase is thereby an updated version of the immunosurveillance hypothesis, in which innate and adaptive immunity detect and eradicate developing cancer cells. In detail, neo-antigens from the tumor cells are taken up from APCs, processed and after homing to the lymph nodes, presented to naïve T cells. After T cell priming, Th and T effector cells migrate to and infiltrate the tumor where they recognize the antigens presented on the MHC I molecule of the cancer cells via the TCR. This leads to tumor cell killing and the release of tumor associated antigens (TAA), which even stimulates further immune responses. This mechanism is supported by other cells of the innate immune system like NK cells and macrophages. In the second phase, the equilibrium, this tumor cell elimination still occurs, but some rare tumor cells survive due to genetic modifications and immune evasion strategies. Nevertheless, they are kept in a dormant state by the immune system, thereby preventing tumor outgrowth. It was shown that this stage is mainly maintained by the adaptive immunity, while the innate immune system is only important for the first phase. In the escape phase tumor cells circumvent the immune surveillance then completely by several mechanisms, grow to a clinical relevance and induce active immunosuppression. This leads to the development of cancer entities as GBM (Schreiber, Old et al. 2011, Daniel and Mellman 2013).

The idea behind immunotherapy is to modulate the immune system, that is already suppressed and not functional against the cancer in the third phase, in a way that resembles the immune response of the first phase, including enhanced tumor cell killing and attenuation of the immunosuppressive mechanisms of the tumor (Daniel and Mellman 2013). The challenge in

the development of efficient immunotherapies is to broaden the understanding of the underlying mechanisms and to overcome the strong immunosuppression without harming the normal body's tissue and generating strong adverse side effects (Sharma, Hu-Lieskovan et al. 2017). Successful immunotherapy was already proven in several different solid tumor entities (Pham, Roth et al. 2018). In GBM, an immunologically cold tumor with extremely high immunosuppression by several mechanisms (see 1.1.3), the reactivation of the immune system might play a significant role for a successful treatment (Jackson, Choi et al. 2019). Besides immunosuppression, it should also be considered that the intracranial location of GBM, with the selective permeability of the BBB, can lead to limited access of the immunotherapeutics. Although there are many hurdles and even some results tend to be suboptimal (Filley, Henriquez et al. 2017, Tan, Ashley et al. 2020), several preclinical as well as clinical studies investigate the influence of different immunotherapies. Ongoing research in immunotherapy include: (i) therapeutic vaccines, (ii) adoptive cell therapies, (iii) immune checkpoint inhibitors (ICI) and (iv) oncolytic viruses (Huang, Li et al. 2021). Besides monotherapies, multidimensional combination therapies might also benefit an effective treatment regime (Bausart, Préat et al. 2022).

1.2.1 Therapeutic vaccines

The idea behind anti-tumor vaccination is to induce an effective anti-tumor immune response by the directed exposure to either tumor- specific or tumor-associated antigens in combination with adjuvants directly *in vivo* or by the stimulation of DC *ex vivo*. For the vaccination either specific peptides, whole tumor lysates or nucleic acids are used. While single peptide vaccinations against tumor-specific antigens (as Rindopepimut against EGFRvIII) have not reached clinical significant benefits in a phase III study (Malkki 2016), probably due to the low mutational burden and the immune evasion of GBM, the tackling of multiple homogenously expressed targets, as TAAs, or combinational therapies have shown encouraging results and are under further investigation (Ahluwalia, Reardon et al. 2018). Besides that, DC-based vaccines, generated by exposing dendritic cells extracted from the blood of GBM patients to specific peptides or whole tumor lysates, were also found to be extremely effective in phase I/II trials, with 33% of patients with glioblastoma having a mOS of 48 months and 27% even having a mOS of 72 months (Dunn-Pirio and Vlahovic 2017). Nevertheless, hurdles of vaccines, namely extremely high costs, long preparation time of individual antigens from patients, limited access to DCs from the blood of patients and the possible induction of autoimmune reactions also to healthy tissue, have to be considered upon treatment (Polyzoidis and Ashkan 2014, Huber, Dammeijer et al. 2018, Peng, Mo et al. 2019).

1.2.2 Adoptive cell therapies

Adoptive cell therapy consists of the treatment with chimeric antigen receptor (CAR) T cells or also NK cells. Therefore, T cells are isolated from the patient, mostly lentivirally transduced and thereby modified to express a chimeric T cell receptor, consisting of the antigen-recognition region of an immunoglobulin (Ig) specific for a TAA and the cytoplasmic domains of a T cell receptor. These cells are then transferred back into the patient to eradicate tumor cells (Salinas, Durgin et al. 2020). Being not dependent on MHC molecule recognition, which are often downregulated on tumor cells, CAR T cell therapy was found to be effective in B cell

lymphomas and leukaemia and is under investigation for GBM (Rodriguez, Brown et al. 2017). But although preclinical animal models showed significant benefits from the treatment (Pellegatta, Savoldo et al. 2018), clinical trials focussing mainly on IL-13Rα2, EGFRvIII or Human epidermal growth factor receptor 2 (Her2) showed only primary safety but limited success (McGranahan, Therkelsen et al. 2019). The reason for this, antigen escape, might be bypassed by CAR cells specific for multiple antigens, as it was seen to be effective for almost 100 % of all tumor cells in a heterogeneous animal tumor model (Bielamowicz, Fousek et al. 2018). The use of CAR-NK cells have so far not be conducted in clinical studies for GBM, although the isolation of primary NK cells from umbilical cord blood might benefit the treatment (Burster, Gärtner et al. 2021).

1.2.3 Immune checkpoint inhibitor therapy

Necessary for an effective T cell response are, besides TCR and MHC interaction, several co-stimulatory signals, which can be inhibited by engagement of immune checkpoint molecules. These molecules are coinhibitory proteins responsible for the attenuation of the duration and intensity of adaptive immune responses to prevent inflammatory overreactions and maintain self-tolerance. Besides this physiological function they also play a significant role in tumor progression and concurrent immunosuppression. Typical molecules that play a role in GBM and are under current investigation are cytotoxic T-lymphocyte antigen 4 (CTLA-4), PD-1 and PD-L1 and T-cell immunoglobulin and mucin domain 3 (TIM-3). Immune checkpoint inhibitors (ICI) are usually monoclonal antibodies targeting these molecules to block their inhibitory effects and increase immune activation (Preusser, Lim et al. 2015). In contrast to other immunotherapeutics, which can stimulate immune cells in the periphery before they enter the CNS, the usage of ICIs can be hindered by the BBB. As quite large molecules, ICIs should generally be excluded from the brain when applied systemically. Nevertheless, it was found in several preclinical as well as in clinical trials, that ICI therapy showed significant effects in brain cancers, probably due to the cancer induced leakiness of the BBB (Van Bussel, Beijnen et al. 2019).

TIM-3, an immunosuppressive receptor expressed on DCs, NK cells, macrophages, T effector cells and T_{regs}, can promote T-cell exhaustion upon its interaction with its ligands, such as galectin-9 or phosphatidylserine and is upregulated in TILs. Ongoing clinical trials will elucidate the clinical relevance of its blockade with ICIs in solid tumors (NCT02608268, NCT02817633).

CTLA-4, which is expressed on T-cells, competes with the co-stimulatory receptor CD28 for binding its ligands CD80 and CD86, thereby stimulating T_{reg} cell fate and reducing the activation of Th cells and CTLs. The first approved ICI targeting CTLA-4, Ipilimumab, showed its clinical benefit for the treatment of metastatic melanoma and several solid tumors in different clinical studies (Li and Gu 2019). For GBM, CTLA-4 blockade as monotherapy promoted long-term-survival as well as complete cure in a combination with PD-1 blockade in different animal models (Fecci, Ochiai et al. 2007, Reardon, Gokhale et al. 2016). Nevertheless, clinical trials couldn't reflect these encouraging findings so far. Therefore, combination therapy with several different therapeutic options, such as TTFs or radiation therapy, are under current investigation (Desai, Hubben et al. 2019).

The physiological function and expression of PD-1 and PD-L1 as well as its pathophysiological involvement in GBM is in detail already discussed in 1.1.3 and 1.1.4. Monoclonal antibodies

against PD-1 (namely Pembrolizumab and Nivolumab) showed significant benefits in clinical trials and are approved for the treatment of non-small cell lung cancer (NSCLC), melanoma and other tumors (Ansell, Lesokhin et al. 2015, Ferris, Blumenschein et al. 2016, Bellmunt, De Wit et al. 2017). Nevertheless, for GBM the effect of anti-PD-1/PD-L1 treatment shows only limited success so far. While in preclinical studies combination therapy of PD-1 blockade and radiotherapy increased medium survival significantly (Zeng, See et al. 2013) and combination with DC vaccines led to long-term survival in animal models (Antonios, Soto et al. 2016), larger clinical trials show more reluctant results. Although good tolerably and promising results were found in humans in early clinical trials (Omuro, Vlahovic et al. 2018, Cloughesy, Mochizuki et al. 2019), a large phase III clinical study, CheckMate-143, showed no increased mOS in recurrent GBM after treatment with Nivolumab compared to treatment with anti-VEGF antibody Bevacizumab (Reardon, Brandes et al. 2020). With a lesser overall response rate of Nivolumab (8 %) compared to Bevacizumab (23 %), it should nevertheless be mentioned, that for those patients that did respond to treatment, those responses were more effective for Nivolumab (11,1 months vs. 5,3 months Bev), leaving hope for a subpopulation of GBM patients. Additionally, the humanized PD-L1 neutralizing antibody Durvalumab showed in a phase II study promising results in combination with radiation and Bevacizumab, with an impressive long-term OS of 86 weeks in one patient (Reardon, Kaley et al. 2017). While monotherapy with ICIs targeting PD-1/PD-L1 might only have limited success due to the diverse immune evasion strategies of GBM, combination with other therapeutic options as radiotherapy, CAR T cell therapy or especially oncolytic virotherapy might bring several benefits.

1.2.4 Oncolytic virotherapy

Oncolytic viruses (OV) are either wild-type or genetically modified viruses which selectively replicate in and therefore lyse cancer cells while leaving non-neoplastic cells unharmed. Via the tumor cell lysis viral particles as well as pathogen-associated molecular pattern (PAMP), damage-associated molecular pattern (DAMP), pro-inflammatory cytokines and chemokines and TAAs are released, thereby triggering inflammation and an effective immune response to the viral particles but also to the tumor cells (Figure 3) (Russell, Peng et al. 2012, Hardcastle, Mills et al. 2017). Because the immune response is also directed against the viral particles themselves and to prevent viral clearance before reaching the tumor cells, OV are often applied directly intratumorally or post-surgically into the resection cavity. The following activation of an adaptive immune response, with increased infiltration of immune cells in the tumor area and induced immunogenic cell death (ICD) can alter the TME, “heating up” the “cold” tumor and is therefore considered an immunotherapy (Larocca and Warner 2018). Additionally, the activated immune cells can target invaded cancer cells far away from the main tumor side, which are not directly affected by viral lysis. While already noted in the early 1900s that viral infections can lead to tumor remission, Alice Moore pioneered the idea in 1952 that viruses could be actively used to treat cancer (Choi, O’Leary et al. 2016). After several clinical trials, the first and so far only OVs approved were in 2005 the genetically modified adenovirus H101 for the treatment of head and neck squamous cell carcinoma in China (Garber 2006) and in the western world in 2015 the genetically modified herpes simplex virus T-Vec for the treatment of advanced melanoma (Rehman, Silk et al. 2016). Today, multiple different virus species, including DNA and RNA viruses, are under investigation as platforms for oncolytic virotherapy (OVT) also in glioma, including adenovirus, herpes simplex virus (HSV), vaccinia virus, measles virus, poliovirus and reovirus (Chaurasiya, Fong et al. 2021). After several very promising results in preclinical models (Rius-Rocabert, García-Romero et al. 2020), many

different OVs are already in clinical trials. For example, DNX-2401 (Ad5-Delta-24-RGD), a modified replication-competent adenovirus, led in a phase I study in patients with recurrent GBM to an at least 3 year long-term survival in 20 % of all cases, with significantly reduced tumor volume, no toxicity and only minor side effects and showed even enhanced CTL and Th cell infiltration in the tumor area (Lang, Conrad et al. 2018). Currently, a combination therapy of DNX-2401 with pembrolizumab is investigated in a phase II trial for recurrent GBM patients, where first interim results showed 100 % 9-months survival rate for the first 7 patients (Gea 2018). Also, other phase I/II trials with different OVs showed promising results in OS, although often only a subset of patients seem to benefit from the treatment (Markert, Liechty et al. 2009, Kicielinski, Chiocca et al. 2014, Geletneky, Hajda et al. 2017). Although some phase III trials failed to show significant benefits (Cloughesy, Brenner et al. 2020), the findings that OVT also improves anti-PD-1 immunotherapy suggests an advantageous effect for the combination with other immunotherapies and makes it an interesting strategy of treatment (Ribas, Dummer et al. 2017).

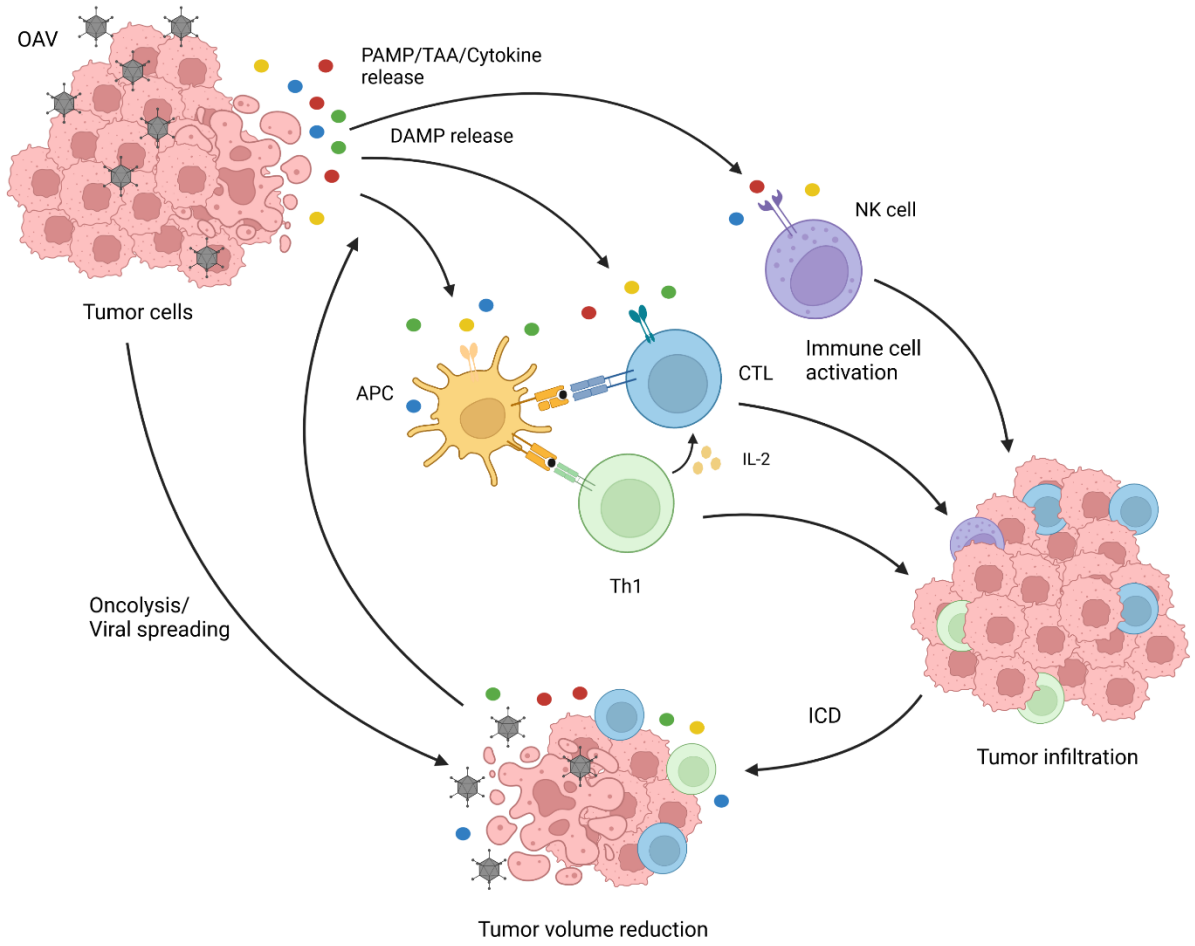

Figure 3. Induction of antitumor immunity by oncolytic viruses. Selective infection of tumor cells with oncolytic viruses (here, oncolytic adenovirus – OAV) leads to lysis of these cells but also to the release of immunogenic PAMPs, TAAs, proinflammatory cytokines as well as DAMPs. These molecules cause local and systemic immune responses by the attraction and activation of innate (e.g. NK cells) and adaptive immune cells. Antigen presenting cells (APC) process and present immunogenic peptides to T cells, thereby activating a strong Th1 and CTL immune response. Attracted immune cells infiltrate the tumor area and benefit further immunogenic cell death (ICD). Oncolysis and ICD lead to the reduction of the tumor volume with subsequent release of new virus and DAMPs. IL-2, Interleukin 2. Created with BioRender.com

In the following, special focus will be led on oncolytic virotherapy with adenoviruses, the Y-box binding protein 1 (YB-1) specific oncolytic adenovirus (OAV) XVir-N-31 and the combination therapy with a blockade of the PD-1/PD-L1 axis.

1.3 Adenovirus and oncolytic adenoviral therapy

Adenoviruses are a group of medium-sized, non-enveloped, double-stranded DNA viruses, which belong to the family of adenoviridae and the genus of mastadenovirus (Kajon and Lynch 2016). While the family of adenoviridae currently consists of 6 genera, including mastadenovirus, and a total of 88 species, mastadenoviruses are subdivided in at least 51 different species, found in different mammals like bats, mice, sheep, pigs, apes, and humans (human adenoviruses). In all these species adenoviral infection leads in general to inflammatory diseases as pneumonia, gastroenteritis or conjunctivitis (inflammation of the outermost layer of the white part of the eye) (Russell 2009, Jhanji, Chan et al. 2015).

Human adenoviruses (HAdV) are classified into seven different species (A – G) and are historically subdivided into serotypes based on their agglutination capability and absence of serological cross-neutralization (Hoeben and Uil 2013, Dhingra, Hage et al. 2019). While with this method up to 51 different types where accounted, recent genotype sequencing defined up to 112 HAdV types (hadvwg.gmu.edu; Update April 2022). Depending on the species tropism different diseases with clinical manifestations can occur: B1 and C type infection mainly cause respiratory diseases, B2 infection leads to inflammation of the urinary tract, D and E types infect mainly the eye and F types are responsible for gastrointestinal infections (Russell 2009). Some types are even known to have oncogenic properties (Ghebremedhin 2014). For virotherapeutic approaches usually HAdV species C type 2 and 5 are used which have been proven to be non-oncogenic and safe even in higher doses (Braithwaite and Russell 2001, Toth and Wold 2010).

1.3.1 Human adenovirus biology and lifecycle

The non-enveloped HAdV viral particle (virion) has a diameter of 65 to 80 nm and consists of an icosahedral protein capsid and a nucleoprotein core. The capsid consists of minor proteins important for the structural integrity (VI, VIII, IX, IIIa) and the three major proteins: hexon, penton base and a knobbed fibre, of which the latter two form a penton capsomere essential for viral infection. Inside the capsid there is the linear dsDNA genome which is associated with the core proteins IVa2, V, VII, and Mu(μ) and attached to the terminal protein (TP) at its 5´ termini and the viral protease, important for the virion assembly (see Fig. 4 A) (Russell 2009). The DNA is 26-46 kbp long (34-36 kbp for most HAdV) and harbours 23-46 protein coding genes, which are divided into the three major groups of early, intermediate and late genes. The early genes E1A, E1B, E2, E3 and E4 are mainly involved in DNA replication, the regulation of viral gene expression and the regulation of apoptosis. While the intermediate genes are expressed with increasing intensity over the infection period and contain only the minor proteins of the capsid and the core (IX and IVa2), the five late genes L1, L2, L3, L4 and L5 are all under control of the major late promoter (MLP) and encode for the remaining minor and the major viral capsid proteins (Figure 4 B) (Braithwaite and Russell 2001).

The viral lifecycle starts with the interaction of a capsid fibre protein with a receptor on the host cell. Depending on the viral type and tropism the host cell receptor as well as the tissue can differ, including oropharynx, conjunctiva or cells of the respiratory or gastrointestinal tract. Nevertheless, the most important receptor for HAdV of the type A, C, E and F is the cell adhesion molecule coxsackie adenovirus receptor (CAR), which is expressed on epithelial and endothelial cells as well as on brain and heart tissue. CAR belongs to the immunoglobulin superfamily and is involved in the formation of tight junctions. After the binding of the viral fibre protein to CAR, the highly conserved viral arginine-glycine-aspartic acid (RGD) motif of the penton base protein located below the fibre spike binds to cellular αvβ3/αvβ5 integrins, leading to rapid viral internalization via clathrin-coated vesicles and endosomes (Russell 2009). To prevent degradation, the virion escapes the endosome via an acidic pH shift (Blumenthal, Seth et al. 1986) and is transported along the microtubules to the nucleus. There the hexon protein of the virion docks to a nuclear pore complex (NPC) and the viral DNA as well as the DNA associated proteins are released into the nucleus and the viral replication starts. The residual capsid proteins remain at the nuclear membrane and get subsequently degraded (Cassany, Ragues et al. 2015).

The first gene that is transcribed is the E1A gene. Via alternative splicing the gene accounts for five different proteins (9S, 10S, 11S, 12S and 13S), which are responsible for the stimulation of the transcription of the other early genes via the recruitment of cellular transcription factors and the optimization of the viral replication conditions (Braithwaite and Russell 2001). Within the E1A transcripts there are four conserved regions (CR), which allow the binding of transcription factors and of which only E1A13S has all of them (CR1/2/3/4) (Avvakumov, Kajon et al. 2004). Via the CR2 domain E1A proteins can bind to the tumor suppressor retinoblastoma pocket protein (Rb), leading to the release of the transcription factors E2Fs and the subsequent promotion of cell cycle progression and S-phase induction as well as increased E2 protein expression (Bandara and La Thangue 1991, Ben-Israel 2002). Also the CR3 region of the E1A protein plays an important role for the recruitment of transcription factors to the other early gene loci (Ablack, Pelka et al. 2010). Upon that activation, E1B is expressed. Both its proteins, E1B19k and E1B55k, inhibit apoptosis via binding to p53 and other cell death proteins and their subsequent degradation (Braithwaite and Russell 2001). Furthermore, E1B55k builds a complex with the viral protein E4orf6, leading to the translocation of cytosolic YB-1 to the nucleus, which is an important transcription factor for the E2-late promoter and correct viral replication. The E2 gene has thereby an early and a late promoter, of which the first is activated upon the binding of a transcription complex consisting of TATA-Box binding protein (TBP), activating transcription factor (ATF) and E2F1 and the second upon YB-1 binding to its 3 YB-1 binding sites (Holm, Bergmann et al. 2002, Seifried, Talluri et al. 2008). E2 proteins contain of DNA polymerase, primase and the DNA binding protein (DBP.E2A) and are therefore of essential importance for the viral replication. On the contrary, the seven proteins of the E3 region are responsible for the modulation and reduction of anti-viral immune response of the host, leading to the downregulation of immunogenic antigens and the reduced MHC I exposure on the cell surface. Additionally, the E3 adenovirus death protein (ADP) is transcribed quite late during replication, allowing the host cell lysis and the release of the freshly assembled virions (Braithwaite and Russell 2001, Lichtenstein, Toth et al. 2004). The E4 proteins are in general regulators and modulators of many of the previous processes, involved in DNA and protein synthesis, mRNA shuttling but also cell death (Braithwaite and Russell 2001).

The intermediate genes are activated only after viral DNA replication has started. Both proteins, IX and IVa2, although later on located in the capsid and serving structural purposes, act also as transcription factors of the MLP and play a role in DNA packaging (Berk 1986, Lutz, Rosa-Calatrava et al. 1997, Zhang and Imperiale 2003).

After the activation of the MLP via the intermediate proteins, all 5 late proteins are expressed. L2-L5 are only transcribed after replication of the viral DNA is completed and encode for the capsid proteins (L3 = hexon; L5 = fibre protein). After successful expression the viral capsid can be assembled and the new virion is released from the dying cell (Braithwaite and Russell 2001).

The whole adenovirus life cycle takes thereby approximately 24-36 h. E1A mRNAs are already detectable as soon as 30 min after infection, with an induction of all early genes within 8 h. Activation of the MLP and therefore transcription of the structural proteins is seen within 10 h after infection, followed by assembly and virion release (Giberson, Davidson et al. 2012).

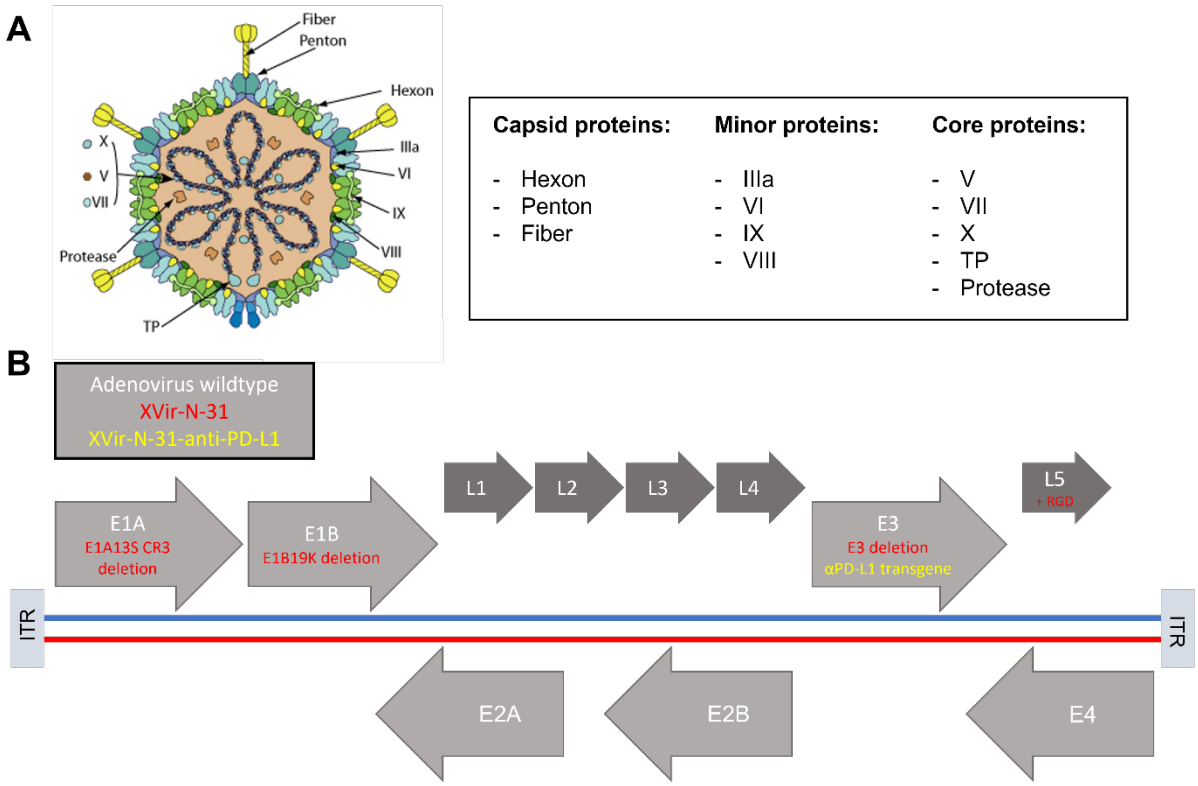

Figure 4. Structure and genome organization of an adenovirus. A. Graphical representation of an adenoviral structure, including its capsid, minor and core proteins (adapted from https://viralzone.expasy.org; Adenoviridae). **B.** Schematic adenovirus genome map, including early genes E1-E4 and late genes L1-L5. Additionally to wild type adenovirus genes (given in white), also the genetic modifications of the oncolytic adenovirus XVir-N-31 (red) as well as its offspring XVir-N-31-anti-PD-L1 are shown here (yellow; harbours the same modifications as XVir-N-31 in the E1A, E1B and L5 regions, but is only E319K deleted in the E3 region). ITR, inverted terminal repeat.

1.3.2 Oncolytic adenovirus therapy and its improvements

Adenovirus is a perfect virus family for oncolytic virotherapy. Besides their strong oncolytic capacity, they can infect dividing and non-dividing cells, have a well-known infection route and a large packaging capacity, do not integrate into the host's genome and can stimulate strong immune responses (Robert-Guroff 2007, Gonzalez-Pastor, Goedegebuure et al. 2021). The perfect oncolytic adenovirus (OAV) has enhanced tumor selectivity, improved tumor tropism and an increased induction of antitumoral immune responses. In contrast to wild type adenovirus (Ad-WT), which can replicate in almost all cells, OAVs are usually modified to replicate selectively in tumor cells by the generation of conditionally replicative adenoviruses (CRAd). To gain this tumor selectivity, in general two different strategies are used: either (i) tumor-specific promoter (TSP) or (ii) the partial deletion of the E1A or E1B genes, which are essential for replication in non-neoplastic cells but can be restored in tumor cells (Gonzalez-Pastor, Goedegebuure et al. 2021). The insertion of TSPs in the viral genome, for example as the promoter of the transactivator E1A, couples the expression of its proteins to the expression of the selected tumor protein that is usually not highly expressed or activated in healthy cells. The insertion of the human telomerase reverse transcriptase (hTERT) promoter in front of E1A in a serotype 3 adenovirus (Ad3) led to selective replication in and lysis of cells with high hTERT activity – typical for cancer (Hemminki, Diaconu et al. 2012). Also different other TSPs, as for example the cyclo-oxygenase 2 (COX2) promoter, were successfully inserted in the adenovirus genome, creating thereby OAVs (Bauerschmitz, Guse et al. 2006). On the contrary, partial deletion of viral genes necessary for replication leads to the generation of an OAV that can selectively replicate under certain conditions given only in tumor cells. For example, a deletion of only 24 bp in the CR2 region of E1A (dl922-947 or delta24) inhibits the efficient binding of E1A proteins to the Rb protein. Only in cells with mutated Rb and defects in the Rb pathway, as it is seen in many cancers, E2F can be released and replication can proceed, while in non-neoplastic cells the replication and therefore the lysis is stalled (Heise, Hermiston et al. 2000, Kitajima, Li et al. 2020). Furthermore, Bischoff *et al.* described already in 1996 the selective viral replication of an E1B55K gene deleted OAV to p53 deficient tumor cells (Bischoff, Kirn et al. 1996). Since a lot of tumors have defects in the p53 or the Rb pathways, a benefit of these OAVs is that they can be used in several different tumor entities. To improve the tumor tropism of adenoviruses usually the generation of chimeric fibre proteins or the insertion of an RGD motive in the fibre knob is used to address other receptors for cell entry. While the replacement of the Ad5 fibre knob with Ad3 fibre knob (5/3 chimerism) was found to increase the infectivity for cancer cells due to the interaction with the adenovirus type 3 receptor on the cell surface (Koodie, Robertson et al. 2019), most designed OAVs carry an RGD motive. This insertion in the knob fibre allows the interaction and the cell entry via the αvβ3 or αvβ5 integrins in a CAR-independent manner, especially important for GBM cells, which frequently downregulate CAR cell surface expression (Fueyo, Alemany et al. 2003, Lang, Conrad et al. 2018). The third category of modifications for OAVs include all modifications leading to an enhanced immune response. Partial deletion of immunosuppressive AdV genes or the insertion of immunostimulatory transgenes or additionally ICIs are typical alterations and are addressed in a plethora of different studies (Zhao, Liu et al. 2021).

1.3.3 The YB-1 dependent oncolytic adenovirus XVir-N-31

The YB-1 dependent OAV XVir-N-31, a modified HAdV species C subtype 5 previously termed Ad-Delo3-RGD, was first described in 2009 by Rognoni *et. al.* and features several gene deletions as well as one insertion (see Fig. 4 B), making the virus highly infectious, cancer cell specific and even more immunogenic (Rognoni, Widmaier et al. 2009). A deletion of 10 bp in the CR3 domain of the E1A gene leads to no functional expression of the E1A13S protein. Since this protein is the main transactivator of the viral early gene expression via the E2-early promoter, viral replication depends on the activation via the E2-late promoter bearing three YB-1 binding sites. Due to the missing E1A13S, no E1B55k expression occurs, which results in the lack of E1B55k/E4orf6 complex formation and subsequently no YB-1 translocation from the cytosol to the nucleus. Therefore, E2-late promotion and with this the whole viral replication is dependent on already pre-existing nuclear YB-1, which was found to be highly upregulated in cancers and especially in recurrent GBM but not in normal brain tissue (Figure 5) (Holm, Bergmann et al. 2002, Holm, Lage et al. 2004, Czolk, Schwarz et al. 2019). Due to this, XVir-N-31 selectively replicates in and lyses tumor cells, but leaves non-neoplastic cells unaffected. Additionally, the E1B19k gene of XVir-N-31 is partially deleted, allowing the increased induction of immunogenic cell death, and a deletion of 2681 bp in the E3 region leads to enhanced immune responses to the tumor cell. While also E1A13S was proven to have immunosuppressive functions, for example by antagonizing the cGas-Sting pathway (Anghelina, Lam et al. 2016), proteins of the E3 region are known for their function as immunomodulatory proteins by interfering with the MHC I antigen presentation pathway (Oliveira and Bouvier 2019). Besides, the latter, big deletion allows the integration of additional transgene expression like an anti-PD-L1 antibody (XVir-N-31-anti-PD-L1), further improving the immunostimulatory characteristics (Lichtenegger, 2018)(Lichtenegger, Koll et al. 2019). Finally, XVir-N-31 contains an insertion for an integrin-binding RGD motive in the knob fibre domain for a CAR-independent cell infection (Rognoni, Widmaier et al. 2009).

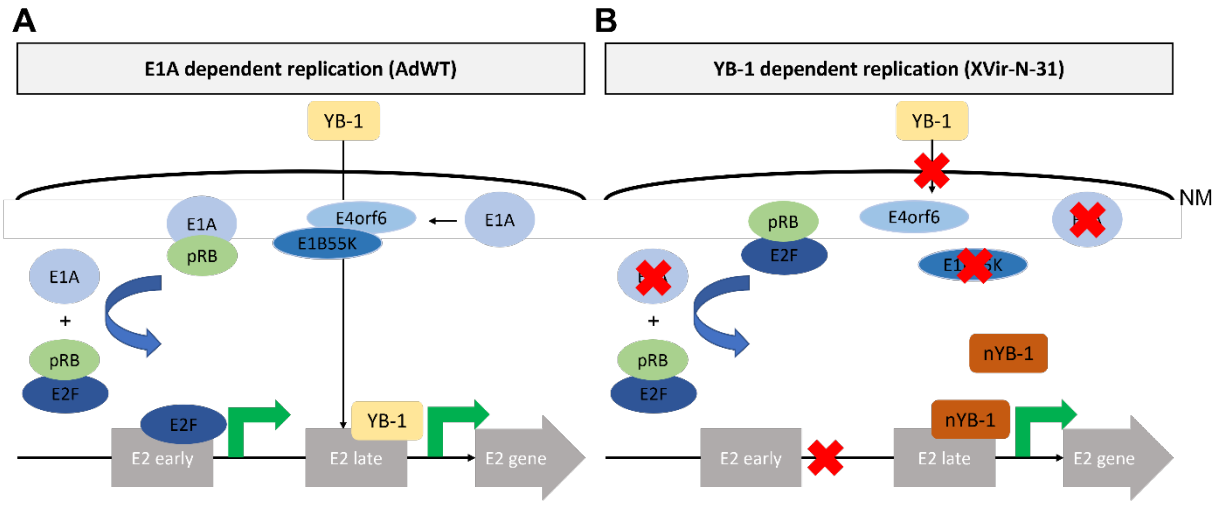

Figure 5. Replication process of Ad-WT and XVir-N-31. A. Replication of Ad-WT depends on the functional integrity and presence of the E1A proteins (especially E1A13S). E1A13S leads to E2 gene activation via E2F binding on the E2 early and via translocated YB-1 binding on the E2 late promoter. **B.** In XVir-N-31 E1A13S is partially deleted and not functional, leading to no E2F release from pRB and no activation of the E2 early promoter. Subsequently no E1B55K expression occurs and no E1B55k/E4orf6 complex can translocate YB-1 to the nucleus. Replication depends only on E2 late promoter activation via pre-existing nuclear YB-1 (nYB-1), which is given in cancer, but not in non-neoplastic cells. NM, nuclear membrane; E1A = E1A13S.

1.3.4 Immune response to Ad-WT and OAV

Upon Ad-WT infection the body has several different strategies to eliminate the virus. Pre-existing immunity is already given in the majority of all humans since many infections, especially during childhood, are caused by Ad-WT. About 2–5 % of respiratory infections, 5–10 % of gastrointestinal infections and 10 % of febrile illnesses are caused by adenoviruses, leading to pre-existing immunity in approximately 65-100 % of African, 61 % in European and 37-70 % in American population only against the HAdV serotype 5 (Fausther-Bovendo and Kobinger 2014). Chirmule *et. al.* even showed in a study that 96 % of all individuals had previous immunity to adenoviruses (Chirmule, Propert et al. 1999). This immunity is usually driven by neutralizing antibodies and memory T cells mainly of Th1 property, with a rapid re-induction of a CTL immune response and is accompanied by antiviral innate immune factors as the complement system and activated macrophages and NK cells (Chirmule, Propert et al. 1999, Atasheva and Shayakhmetov 2016). To escape this immune response the virus aims for rapid cell infection and internalization, thereby “stealthing” from the immune system and the subsequent upregulation of its immunosuppressive genes and interference with the cellular homeostasis. Besides the already mentioned suppression of MHC I expression on the cell surface (see 1.3.1), also several other proteins of the E3 region have immunosuppressive functions. The E3 proteins RIDα, RIDβ, 6.7K, 14.7K and 49K cause a downregulation of Fas/CD95 and tumornecrosis factor-(TNF)-related apoptosis-inducing ligand (TRAIL) receptors on the cell surface and interfere with the IFN and TNF signalling pathways (Lichtenstein, Toth et al. 2004, Ghebremedhin 2014). An additional very important mechanism is the virus-mediated induction of the regulated cell death, apoptosis. Thereby, caspase proteases and DNA fragmentation as well as cell shrinkage and the formation of apoptotic bodies mark and prepare the cells for elimination mainly by macrophage phagocytosis. While this cell death is immunologically completely asymptomatic, without any release of TAAs, PAMPs or DAMPs, it promotes even the secretion of anti-inflammatory cytokines, “stealthing” the virus for the time of replication from the immune system (Green 2017, Laevskaya, Borovjagin et al. 2021). Nevertheless, there are also several mechanisms of the infected cells to direct the immune system and prevent virus spreading. Infected cells enhance the secretion of type I IFNs, IFNα and IFNβ, attracting immune cells and activating different anti-viral genes in proximate, non-infected cells, putting them in an anti-viral state (Randall and Goodbourn 2008). Furthermore, macrophages infected with virus after apoptotic cell digestion release several cytokines and chemokines thereby attracting and activating immune effector cells mainly over the IL-1α/IL-1R1 pathway (Kolaczkowska and Kubes 2013). With these mechanisms the host’s body can usually clear adenoviral infections pretty fast.

On the contrary, OAVs, with all their usual modifications show a different interaction with the immune system. Although pre-existing immunity also occurs, receptor modification and enhanced tumor tropism (see 1.3.2) but especially also the often-used direct application into the tumor area lead to escape from the rapid viral neutralization in the blood stream. Selectively replicating virus in cancer cells then face different challenges than Ad-WT in normal cells due to the immunosuppressive microenvironment of many cancers. Therefore, the activation of the immune system and the redirection of the immune answer against the tumor cells are the main tasks of OAVs concerning the immune modulation. While the immunosuppressive characteristics of the adenoviral vector are often reduced by E3 deletions, the shift of apoptotic cell death to the unsterile immunogenic cell death by OAV is the strongest activator of the immune system. ICD, which shows features of necrosis, necroptosis, inflammasome activation and autophagy and a subsequent rupture of the plasma membrane is characterized by the

release of immunogenic molecules even prior to lysis and a strong induction of the immune response (Green 2017, Ma, Ramachandran et al. 2020). Besides PAMPs, also pro-inflammatory cytokines, TAAs and DAMPs are expressed and released from the cells, which can be recognized by pattern recognition receptors (PRR), such as Toll-like receptors (TLR) or NOD-like receptors (NLR), expressed on DCs, macrophages, monocytes, neutrophils but also cells of the adaptive immune system. With this, DAMPs induce (i) opsonisation and direct killing by the acute phase proteins of the complement system, (ii) direct killing and antigen processing by phagocytosis and (iii) the activation of pro-inflammatory signalling pathways with local inflammation and the attraction of effector cells (Land 2015).

Typical molecules functioning as DAMPs are extracellular released adenosine triphosphate (ATP), High Mobility Group B1 (HMGB1) and heat shock protein 70 (HSP70) as well as the cell surface expression of calreticulin (CRT). In the following a few of these proteins will be described further, together with the immunogenic features of released YB-1.

1.3.4.1 DAMPs induced by ICD

HMGB1 is a non-histone chromatin-associated nucleoprotein, that is involved in many different processes in the nucleus such as DNA replication, transcription, V(D)J recombination and chromatin remodelling. The multifunctional protein acts as a DNA chaperone and is thereby regulating DNA damage repair and the maintenance of the genomic stability (Wang and Zhang 2020). Upon posttranslational modifications, including acetylation, methylation or phosphorylation, HMGB1 can translocate to the cytoplasm and regulate mitochondrial functions and inhibit apoptosis (Huebener, Gwak et al. 2014). Besides these intracellular functions, HMGB1 can also be released into the extracellular space and act there as a typical DAMP. It is either released actively from immunocompetent cells or passively from dying and necrotic cells. A third possibility is the secretion during the ICD of cancer cells after treatment with chemotherapeutic drugs or oncolytic viruses (Ahmed and Tait 2020). Extracellular molecules can interact with receptors as the TLR-2/4/9 or the receptor for advanced glycation end products (RAGE) and are thereby involved in many different immune responses such as proinflammatory cytokine production and the promotion of immune cell maturation and activation (Rivera Vargas and Apetoh 2017, Paudel, Angelopoulou et al. 2019). Also in GBM it was found that the release of HMGB1 has immunostimulatory functions using adenoviral vectors (Candolfi, Yagiz et al. 2009). Apetoh *et al.* even showed that the processing and presentation of tumor antigens via DCs is dependent on the HMGB1 release from dying tumor cells (Apetoh, Ghiringhelli et al. 2007).

Heat shock proteins, including HSP70, are highly conserved proteins that form as chaperones for other proteins and have strong cell-protective and antiapoptotic properties. HSP70 facilitates the refolding of proteins and prevents misfolded protein aggregation and is upregulated in cells with high stress, e.g. after cellular injuries or infections (Hulina, Grdić Rajković et al. 2018). Also, various cancer cells have been shown to have an elevated level of HSP70 (Chanteloup, Cordonnier et al. 2020). When HSP70 is released from the cells, for example due to ICD after OV infection or chemotherapy, it acts as a DAMP and induces inflammation and a competent immune response (Pouwels, Heijink et al. 2014). Via the binding to TLR2 and TLR4, it activates NF-κB and MAPK and promotes therefore the release of proinflammatory cytokines (Piccinini and Midwood 2010). Melcher *et al.* showed already in

1998 that increased HSP70 release of tumor cells upon cell death led to increased immunogenicity and enhanced eradication of the tumor. Furthermore, it was shown that increased expression of HSP70 after chemotherapy correlated with a stronger immune response and DC activation (Melcher, Todryk et al. 1998, Cirone, Di Renzo et al. 2012).

Another very important molecule implicated in ICD is calreticulin. Under normal conditions, CRT is a protein mainly located in the endoplasmic reticulum (ER) with several different functions. It is responsible for the Ca^{2+} homeostasis, the loading of cellular antigens on MHC I molecules and involved in correct protein folding (Kielbik, Szulc-Kielbik et al. 2021). Upon cellular stress leading to ICD or apoptosis, CRT is re-localized to the cell surface and acts there as a co-stimulatory “eat-me” signal to different immune cells, especially to APCs as macrophages, thereby activating the innate as well as the adaptive immune system. The upregulation on the cell surface of cancer cells due to different anti-cancer therapies was also shown in several entities (Radogna and Diederich 2018, Fucikova, Spisek et al. 2021).

YB-1 belongs to the highly conserved superfamily of cold-shock domain proteins and is involved in several different processes in the cell dependent on its localization. In the cytoplasm, where YB-1 is usually located largely unmodified in healthy cells, it acts as a regulator for mRNA translation, splicing and localization and serves as a packaging protein for mRNPs. Upon phosphorylation and/or acetylation it translocates to the nucleus, where it functions as a transcription factor, regulates the upregulation of oncogenes and is involved in DNA repair. It is also involved in the activation of multi-drug resistance 1 (MDR1) gene transcription as well as in the expression of other detoxification factors, leading to the resistance of these cells to chemotherapy. Enhanced expression of nuclear YB-1 was found in fast proliferating cells and several different cancers, especially also in cancer stem cells (CSC) like GSCs (Kuwano, Uchiumi et al. 2003, Eliseeva, Kim et al. 2011, Czolk, Schwarz et al. 2019). Besides these cellular functions, extracellular YB-1 was shown to be an immunogenic factor, that can form as an inflammatory mediator and was identified as a TAA in neuroblastoma, that is capable of eliciting a potent T cell immune response against the tumor (Zheng, Jing et al. 2009, Hanssen, Alidousty et al. 2013).

1.4 Aims and objectives

OVT is a promising approach to treat GBM and was proven to be effective in different preclinical models (Fueyo, Gomez-Manzano et al. 2000, Geoerger, Grill et al. 2002). Besides direct oncolysis, the strong immunostimulatory effects of OVs with an induction of a long-lasting immune response are important for the successful treatment (Zamarin, Holmgaard et al. 2014, Andtbacka, Kaufman et al. 2015). Nevertheless, a fundamental understanding of the virus-mediated processes leading to a potent anti-tumor immune response is still missing.

The YB-1 dependent OAV XVir-N-31 has been proven to be effective against GBM cells *in vitro* and *in vivo* (Holzmüller, Mantwill et al. 2011, Mantwill, Naumann et al. 2013). Additionally, it showed strong immunostimulatory effects in the treatment of bladder cancer (Lichtenegger, Koll et al. 2019). Its derivate, XVir-N-31-anti-PD-L1, was so far never analyzed for its immunogenic effects. XVir-N-31-anti-PD-L1 harbours the same modifications as XVir-N-31 in the E1A, E1B and L5 regions but is only deleted in the E319K gene in the E3 region, instead of the deletion of the whole region. Therefore, it encodes for a PD-L1 blocking single chain

antibody, inserted in that region. The aim of this thesis was to elucidate the impact of XVir-N-31 and XVir-N-31-anti-PD-L1 in the treatment of GBM, with a special focus on its immunostimulatory effects *in vitro* and *in vivo*. Furthermore, these effects were compared to the treatment of GBM with a wild type adenovirus-like virus.

To analyze the effects of the viruses *in vitro*, typical molecules related to ICD were analysed after viral infection of GBM cells by ELISA and flow cytometry. Furthermore, the induction of a proinflammatory boost after viral infection was evaluated in virus-infected GBM/HLA A/B matched PBMC cocultures via ELISA.

The immunostimulatory effects of the viruses were analyzed *in vivo* in an immuno-humanized GBM mouse model. The benefits of a local anti-PD-L1 expression after XVir-N-31-anti-PD-L1 treatment were furthermore compared to treatment with XVir-N-31 plus multiple concurrent systemic applications of Nivolumab. The expression of the DAMPs HMGB1 and HSP70 and the infiltration of different immune cell subsets in the tumor area were investigated by immunofluorescence staining. Viral spreading was examined by fluorescence staining of the viral hexon protein. Finally, tumor growth after treatment was analyzed by H&E staining. All analyses were performed in tumors directly injected with virus and in tumors far away from the injection side, to investigate possible abscopal effects.

2. Material and methods

2.1 Material

2.1.1 Viruses

Virus	Titer (IFU/µl)	Source	Cat. No.
XVir-N-31	$1x10^8$	P.S. Holm (TU Munich) preparation by M. Klawitter	-
XVir-N-31-anti-PD-L1	$2x10^9$	P.S. Holm (TU Munich) preparation by M. Klawitter	-
dl309	$1x10^8$	P.S. Holm (TU Munich)	-
Ad-NULL	$1x10^8$	SignaGen Laboratories, Frederick, MA, USA	SL100705

2.1.2 Cells

Cells	Supplier	Cat. No.
HEK293	Microbix (Mississauga, Kanada)	-
Human PBMCs	Buffy Coats Institute for Transfusion Medicine (University Hospital Tübingen, Germany)	-
U87MG	ATCC (Manassas, U.S.A.)	CRL-2611
LN-229	ATCC (Manassas, U.S.A.)	HTB-14

2.1.3 Chemicals, agents and reagents

Material	Supplier
0,1% hematoxylin solution	Sigma-Aldrich (Darmstadt, Germany)
2-Mecaptoethanol	Sigma-Aldrich (Darmstadt, Germany)
100% Ethanol	Sigma-Aldrich (Darmstadt, Germany)
Accutase solution	Sigma-Aldrich (Darmstadt, Germany)
Acetic acid 100 %	Merck (Darmstadt, Germany)

ACK Lysing Buffer	Thermo Scientific, (Waltham, MA, U.S.A.)
Acrylamide/Bis Solution 37.5:1	Serva Electrophoresis (Heidelberg, Germany)
Ammonium persulfate (APS)	Thermo Scientific, (Waltham, MA, U.S.A.)
Bovine serum albumin (BSA)	Sigma-Aldrich (Darmstadt, Germany)
Bromophenol blue	Serva Electrophoresis (Heidelberg, Germany)
Cesium chloride (CsCl)	Sigma-Aldrich (Darmstadt, Germany)
Clarity Western ECL Substrate	Bio-Rad Laboratories (Feldkirchen, Germany)
Dimethyl sulfoxide (DMSO)	Carl Roth (Karlsruhe, Germany)
Dulbecco´s Modified Eagle´s Medium (DMEM)	Sigma-Aldrich (Darmstadt, Germany)
Eosin Y	Sigma-Aldrich (Darmstadt, Germany)
Ethylenediaminetetraacetic acid (EDTA, 0.5M)	Sigma-Aldrich (Darmstadt, Germany)
Fetal calf serum (FCS)	Sigma-Aldrich (Darmstadt, Germany)
Ficoll-Paque PLUS	GE Healthcare (Chalfont St Giles, UK)
Glucose	Sigma-Aldrich (Darmstadt, Germany)
Glycerol	Sigma-Aldrich (Darmstadt, Germany)
Glycerin	Carl Roth (Karlsruhe, Germany)
Hydrochloric acid fuming 37 %	Carl Roth (Karlsruhe, Germany)
Hydrogen chloride (HCl)	Merck (Darmstadt, Germany)
Hydrogen peroxide	VWR lifescience (Darmstadt, Germany)
Interleukin-2 (Rh IL-2)	Immuno Tools (Friesoythe, Germany)
Isofluran CP	CP-pharma (Burgdorf, Germany)
Isopropanol	Sigma-Aldrich (Darmstadt, Germany)
L-Glutamine	SAFC/ Sigma-Aldrich (Darmstadt, Germany)
Magnesium chloride ($MgCl_2$)	Sigma-Aldrich (Darmstadt, Germany)
Methanol	Honeywell (Charlotte, NC, U.S.A.)
MTT stock solution	Merck (Darmstadt, Germany)
Non-essential amino acids (NEA)	Sigma-Aldrich (Darmstadt, Germany)
NP-40	Thermo Scientific, (Waltham, MA, U.S.A.)
Penicilin/Streptomycin (P/S; 10.000 U/mL penicillin, 10 mg/mL streptomycin)	Sigma-Aldrich (Darmstadt, Germany)

Paraformaldehyde (PFA) powder	Sigma-Aldrich (Darmstadt, Germany)
Permount mounting media	Thermo Scientific, (Waltham, MA, U.S.A.)
Phosphate buffered saline (PBS, 1x, 10x)	VWR lifescience (Darmstadt, Germany)
Potassium chloride (KCl)	Merck (Darmstadt, Germany)
Potassium hydrogen carbonate ($KHCO_3$)	Sigma-Aldrich (Darmstadt, Germany)
Potassium dihydrogen phosphate (KH_2PO_4)	Carl Roth (Karlsruhe, Germany)
Protease Arrest, 1x	GBiosciences (St. Louis, MO, U.S.A.)
RPMI Medium 1640	Thermo Scientific, (Waltham, MA, U.S.A.)
Skimmed milk powder	Carl Roth (Karlsruhe, Germany)
Sodium chloride (NaCl)	Merck (Darmstadt, Germany)
Sodium hydroxide (NaOH)	VWR lifescience (Darmstadt, Germany)
Sodium dodecyl sulfate (SDS)	Carl Roth (Karlsruhe, Germany)
Spectra Multicolor Protein Ladder	Thermo Scientific, (Waltham, MA, U.S.A.)
Sucrose	Sigma-Aldrich (Darmstadt, Germany)
Tetramethylethylenediamine (TEMED)	Carl Roth (Karlsruhe, Germany)
Tissue Tek O.C.T. compound	Thermo Scientific, (Waltham, MA, U.S.A.)
Trichloroacetic acid (TCA)	Sigma-Aldrich (Darmstadt, Germany)
Tris-HCl	Carl Roth (Karlsruhe, Germany)
Trizma base	Carl Roth (Karlsruhe, Germany)
Triton X-100	Sigma-Aldrich (Darmstadt, Germany)
Trypan blue (0.5%)	Biochrom/Merck-Millipore (Darmstadt, Germany)
Trypsin/EDTA	Thermo Scientific, (Waltham, MA, U.S.A.)
Tween-20	Carl Roth (Karlsruhe, Germany)
Vectashield antifade mounting media containing DAPI	Biolegend/Biozol (Eching, Germany)
Xylene	Sigma-Aldrich (Darmstadt, Germany)

2.1.4 Mediums, buffers and solutions

Buffer	Composition
Cell culture media (HEK293 cells, glioma cells)	DMEM, 10 % FCS, 1 % P/S
Cell culture media (PBMCs)	RPMI 1640, 10 % FCS, 1 % P/S, 1 % NEA

Dialysis Buffer	H_2O, 10mM Tris pH7.5, 10 % glycerol, and 1mM $MgCl_2$
FACS buffer	PBS, 0,02 % NaAzid, 2 mM EDTA, 2 % FCS
Immunoblotting antibody dilution buffer	2,5 % non-fat milk powder in TBS-T
Immunoblotting blocking solution	5 % non-fat milk powder in TBS-T
Laemmli Buffer	4 % SDS; 0.2 % bromophenol blue; 20 % glycerol, 10 % β-mercaptoethanol
Lysis Buffer P	50 mM Tris-HCl, pH=8; 120 mM NaCl; 5 mM EDTA; 0.5 % NP-40; 1X Protease Arrest
PBS-Tween (PBS-T)	PBS + 0.2 % Tween 20
Running Buffer (10x; 1 L)	30.6 g Trizma base, 144 g glycin
Separating gel buffer	1.5 M Tris/HCl pH 8.8
Stacking gel buffer	0.5 M Tris/HCl pH 6.8
Tris buffered saline (TBS) solution	Tris: 20 mM, NaCl: 150 mM
TBS-T	TBS + Tween 20: 0.1 % (w/v)
Transfer buffer (10x)	H_2O; 25 mM Tris, 190 mM Glycine
Transfer buffer (1x)	H_2O; 10 % Transfer buffer (10x), 20 % Methanol

2.1.5 Antibodies

Name	Dilution	Supplier	Cat. No
GAPDH	1:1000	Santa Cruz, Heidelberg, Germany	sc-25778
HA-tag	1:500	Thermo Scientific, (Waltham, MA, U.S.A.)	14-6756-81
Anti-rabbit IgG, HRP-linked Antibody	1:5000	Cell Signaling (Leiden, Netherlands)	7074S
Human PD-L1 (CD274)	1:20	Invitrogen (Walham, MA, USA)	16-5983-82
Human PD-L1-AF488	1:20	Thermo Scientific, (Waltham, MA, U.S.A.)	53-5983-42

Calreticulin-AF488	1:20	Novus Bio (Littleton, U.S.A.)	B-4-120621
Isotype Control IgG1, κ; unconjugated	1:20	BioLegend (San Diego, CA, U.S.A.)	400150
Human CD3-PB	1:10	BioLegend (San Diego, CA, U.S.A.)	300431
Human CD4-FITC	1:10	Invitrogen (Walham, MA, USA)	11-0049-42
Human CD8-APC	1:10	BioLegend (San Diego, CA, U.S.A.)	344722
Human CD19-PE-Cy7	1:10	BioLegend (San Diego, CA, U.S.A.)	302215
Human CD45-APC	1:10	BioLegend (San Diego, CA, U.S.A.)	304012
Mouse CD45-FITC	1:10	BioLegend (San Diego, CA, U.S.A.)	103108
Isotype Control IgG1, κ; PB	1:10	BioLegend (San Diego, CA, U.S.A.)	400131
Isotype Control IgG1, κ; FITC	1:10	BioLegend (San Diego, CA, U.S.A.)	400107
Isotype Control IgG1, κ; APC	1:10	BioLegend (San Diego, CA, U.S.A.)	400120
Isotype Control IgG1, κ; PE-Cy7	1:10	BioLegend (San Diego, CA, U.S.A.)	400125
Human nuclei-Cy3	1:50	Merck-Millipore (Darmstadt, Germany)	MAB1281C3
Human CD45	1:100	Invitrogen (Walham, MA, USA)	14-0459-82
Human CD3	1:100	Invitrogen (Walham, MA, USA)	14-0038-82
Human CD4	1:100	Invitrogen (Walham, MA, USA)	14-0459-82
Human CD8	1:100	Invitrogen (Walham, MA, USA)	14-0089-82
Human FoxP3	1:100	Invitrogen (Walham, MA, USA)	14-4777-80

Human CD56	1:100	BioLegend (San Diego, CA, U.S.A.)	304602
Human CD134	1:100	eBioscience (San Diego, CA, U.S.A.)	14-1347-82
Hexon	1:100	Santa Cruz, Heidelberg, Germany	F0517
HMGB1	1:100	Invitrogen (Walham, MA, USA)	MA5-17278
HSP70	1:100	Invitrogen (Walham, MA, USA)	MA3-007
Goat anti-Mouse IgG (H+L), Superclonal™ Recombinant Secondary Antibody, Alexa Fluor 488	1:1000	Invitrogen (Walham, MA, USA)	2208228
Donkey anti-Mouse IgG (H+L), Superclonal™ Recombinant Secondary Antibody, Alexa Fluor 680	1:1000	Invitrogen (Walham, MA, USA)	A32788
Human PD-1 (CD279; Nivolumab)	200 µg / mouse	BioXCell (Lebanon, NH, U.S.A.)	BE0188

2.1.6 Kits

Kit	Supplier	Cat. No.
Adeno-Rapid-X-Titration Kit	Takara Bio Europe SAS, Saint-Germain-en-Laye, France	632250
Bradford Assay (Roti Quant)	Carl Roth (Karlsruhe, Germany)	K015.1
ELISA MAX™ Deluxe Set Human IFN-γ Kit	Biolegend/Biozol (Eching, Germany)	430804
ELISA Kit for Heat Shock Protein 70 (hsp-70)	Hölzel Diagnostics (Köln, Germany)	SEA873Hu
ELISA Kit for High Mobility Group Protein 1 (HMGB1)	Hölzel Diagnostics (Köln, Germany)	SEA399Hu
ELISA Kit for Y-Box Binding Protein 1 (YBX1)	Hölzel Diagnostics (Köln, Germany)	SEC609Hu

MTT Cell Proliferation Kit	Merck (Darmstadt, Germany)	CT02
MycoAlert mycoplasm detection Kit	Lonza (Basel, Switzerland)	LT07-118
PD-1/PD-L1 Blockade Assay Kit	Promega (Walldorf, Germany)	J1250

2.1.7 Disposables

Name	Supplier
A-PAP Pen slide marker	Daido Sangyo Co. (Kawasaki, Japan)
Cell culture plates (96-well, 24-well, 12-well, 6-well, 10cm, 15cm) flat bottom	Greiner Bio-One (Frickenhausen, Germany)
Cell culture plates (96-well) round bottom	Cellstar/Sigma-Aldrich (Darmstadt, Germany)
Cell culture plate white (96 well) flat bottom	Thermo Scientific, (Waltham, MA, U.S.A.)
Cell culture flask 25 mm3, 75mm3, 175mm3	Greiner Bio-One (Frickenhausen, Germany)
Cell lifter	Sigma-Aldrich (Darmstadt, Germany)
Centricon Plus Centrifugal filter Concentrators	Merck-Millipore (Darmstadt, Germany)
Combitips advanced 0,5 ml	Eppendorf (Hamburg, Germany)
Disposable bags	Brand (Hamburg, Germany)
Gauze balls, sterile	Fuhrmann (Much, Germany)
Glass coverslips 25 x 50 mm	R. Langenbrinck (Emmendingen, Germany)
Gloves Gentle Skin sensitive; M, L	Arnova (Salzkotten, Germany)
Histoacryl tissue glue	Braun (Kronberg im Taunus, Germany)
Medical applicator	Heinz Herenz Hamburg (Hamburg, Germany)
Microlance 3	BD Biosciences (Heidelberg, Germany)
Microplate, 96-well, Microlon®, high binding	Greiner Bio-One (Frickenhausen, Germany)
Microtome blade, steel	VWR lifescience (Darmstadt, Germany)
Pasteur Capillary Pipettes 150 mm; 230 mm	WU Mainz (Mainz, Germany)
Pasteur Plast pipets 2,5 ml	Ratiolab (Dreieich, Germany)
Parafilm M	Sigma-Aldrich (Darmstadt, Germany)
PD tips 1,25 ml	Thermo Scientific, (Waltham, MA, U.S.A.)
Perma-hand Silk, stitches	Ethicon (New Jersey, U.S.A.)
Petri Dishes	Carl Roth (Karlsruhe, Germany)

Pipet tips 20 µl, 200 µl, 1000 µl	Greiner Bio-One (Frickenhausen, Germany)
PVDF0.45 transfer membrane	Serva (Heidelberg, Germany)
Raucodrape OR Drape System	R. Langenbrinck (Emmendingen, Germany)
Reaction Tube 0,5 ml, 1,5 ml, 2 ml	Greiner Bio-One (Frickenhausen, Germany)
Sample vial 7 ml	Kartell (Noviglio, Italy)
Serological Pipettes (5 ml, 10 ml, 25 ml, 50 ml)	Greiner Bio-One (Frickenhausen, Germany)
Slide-A-Lyzer™ Dialysis Cassette	Thermo Scientific, (Waltham, MA, U.S.A.)
Surgical Blades, steel	VWR lifescience (Darmstadt, Germany)
SuperFrost Plus microscope slides	R. Langenbrinck (Emmendingen, Germany)
Syringes (1 ml, 2 ml, 5 ml, 10 ml, 20 ml)	Braun (Kronberg im Taunus, Germany)
Syringe filter Aerodisk 0,2 µm	Pall Corporation (New York, U.S.A.)
Tube 5 ml 75x12 mm Flow cytometry	SARSTEDT (Newton, U.S.A.)
Tube 15 ml, 120 x 17 mm, PP, sterile	SARSTEDT (Newton, U.S.A.)
Tube 50 ml, 114 x 28 mm, PP, sterile	SARSTEDT (Newton, U.S.A.)
Whatman 3MM-CHR	GE Healthcare (Chalfont St Giles, UK)

2.1.8 Devices

Name	Supplier
Accu-jet Pipettboy	Brand (Wertheim, Germany)
Autoclave VX-150	Systec (Linden, Germany)
Axiovert 200M fluorescent microscope	Zeiss (Wetzlar, Germany)
Axiovert 200M confocal microscope	Zeiss (Wetzlar, Germany)
Biofuge pico	Heraeus (Hanau, Germany)
Centrifuge 5417 R	Eppendorf (Hamburg, Germany)
Centrifuge wX + Ultra Series	Thermo Scientific, (Waltham, MA, U.S.A.)
Chemidoc MP Imaging System	Bio-Rad Laboratories (Feldkirchen, Germany)
Cryomicrotome CM3050S	Leica Mikrosystems GmbH (Wetzlar, Germany)
Digital Heatblock	VWR lifescience (Darmstadt, Germany)
Digital Clock Timer	Cole-Parmer (St. Neots, UK)
DMi8 flourescent microscope	Leica Mikrosystems GmbH (Wetzlar, Germany)

Drill, for operation	Foredom (Bethel, CT, U.S.A.)
Eclipse TS100 microscope	Nikon (Tokio, Japan)
Finnpipette Mulipipette 50-300 µl	Labsystems (Vantaa, Finnland)
Freezer (-20°C)	Liebherr (Kirchdorf an der Iller, Germany)
Syringe 10 µl glass	Hamilton (Nevada, U.S.A.)
Heating Block QBT	Grant (Saint Joseph, U.S.A.)
Heating warm pad	ConductScience (Skokie, U.S.A.)
HeraSafe steril bench	Heraeus (Hanau, Germany)
HeraFreeze Freezer (-80°C)	Heraeus (Hanau, Germany)
Ice donor machine	Ziegra Eismaschinen (Isernhagen, Germany)
Incubator CO_2	Sanyo (Osaka, Japan)
Lenovo ThinkPad, PC	Lenovo (Quarry Bay, Hongkong)
LSM 710, confocal microscope	Zeiss (Wetzlar, Germany)
MACSQuant Analyser 10 Flow Cytometer	Miltenyi Biotec (Bergisch-Gladbach, Germany)
Megafuge 1.0 R	Heraeus (Hanau, Germany)
Microwave exquisit	Amica (Wronki, Poland)
Mini-Protean Tetra System	Bio-Rad Laboratories (Feldkirchen, Germany)
MS 1 Minishaker	IKA Works (Staufen, Germany)
MR 3000 Magnetic stirrer	Heidolph (Schwabach, Germany)
Mr. Frosty freezing container	Sigma-Aldrich (Darmstadt, Germany)
Multifuge 3 S-R	Heraeus (Hanau, Germany)
Multiskan Ex absorbance reader	Thermo Electron, (Langenselbold, Germany)
NanoDrop ND-1000 Specrophotometer	PeqLab (Erlangen, Germany)
pH meter	Schott (Mainz, Germany)
Pipetman Pipet 10 µl, 50 µl, 200 µl, 1 ml	Gilson (Middleton, U.S.A.)
Pipetus Pipettboy	Hirschmann Laborgeräte (Eberstadt, Germany)
Power Pac basic	Bio-Rad Laboratories (Feldkirchen, Germany)
SteREO lamp	Zeiss (Wetzlar, Germany)
Stereotactic device, mouse	ConductScience (Skokie, U.S.A.)
Stripettor Plus Pipettboy	Corning (Corning, U.S.A.)
Thermomixer comfort	Eppendorf (Hamburg, Germany)
TriStar2 S LB 942 Multimode Reader	Berthold Technologies (Bad Wildbad, Germany)
VIP plus, ultra low freezer (-150°C)	Sanyo (Osaka, Japan)
Vortex Genie 2	Scientific Industries (Bohemia, U.S.A.)

Waterbath WB 12	Medingen (Dresden, Germany)

2.1.9 Programs and Software

Program	Supplier
Adobe Illustrator	Adobe Inc. (San Jose, U.S.A.)
Biorender Online Tool	Free on www.biorender.com
FlowJo, Version 10	FlowJo, LLC (Ashland, OR, U.S.A.)
GraphPad Prism, Version 7	GraphPad Software, Inc. (CA, U.S.A.)
ImageJ	Freely available
ImageLab 5.1 Software	Bio-Rad Laboratories (Feldkirchen, Germany)
Inkscape	Freely available under GNU General Public License
MACSQuantify Software 2.11	Miltenyi Biotec (Bergisch-Gladbach, Germany)
Microsoft Office	Microsoft (Redmond, U.S.A.)
Quantity One	Bio-Rad Laboratories (Feldkirchen, Germany)
Zen lite (blue edition) 3.0	Zeiss (Wetzlar, Germany)

2.2 Methods

2.2.1 Cells and cell cultures

HEK293 cells were provided by Microbix. Human GBM cell lines LN-229 and U87MG were provided by N. Tribolet and have been described in detail before (Ishii, Maier et al. 1999). Phenotyping of LN-229 and U87MG cells was performed routinely at the Institute for Immunopathology (University Hospital Tübingen, Germany), while both cell lines showed an HLA A*02:01, B*13:02, *27:05; C*06:02, *01:02; DRB1*07:01, *11:03; DQB1*02:02, *03:01 phenotype. If not described differently, all cells were maintained in Dulbecco's Modified Eagle's Medium (DMEM) supplemented with 10 % fetal calf serum (FCS) and 1 % Penicillin-Streptomycin (P/S). Human HLA A/B matched peripheral blood mononuclear cells (PBMC) were isolated from buffy coats as described in 2.2.1.2 and obtained from the Institute for Transfusion Medicine (University Hospital Tübingen, Germany). The use of PBMCs was covered by the ethics votum 972/201BO2 from the ethics committee of the University of Tübingen. All donors have given written consent that their cells can be used for research. If not mentioned otherwise, human PBMCs were cultured in RPMI Medium 1640 supplemented with 10 % FCS, 1 % non-essential amino acids and 1 % P/S. If not mentioned otherwise, all cells were cultured and incubated at 37°C in a humidified atmosphere containing 5 % CO_2 and were regularly tested to be free of mycoplasm with a MycoAlert mycoplasm detection kit.

2.2.1.1 Freezing and thawing of cells

Cells were frozen slowly (approximately 1°C/min in a Mr. Frosty freezing container) in freezing medium (the respective, cooled medium containing 5-10 % Dimethylsufloxid (DMSO)). For short term storage, all cells were frozen and kept at -80°C, for longer storage cells were transferred to -145°C. Human PBMCs were stored at -145°C. For thawing, cells were rapidly and under constant shaking defrosted in a 37°C water bath and diluted in 37°C warm growth media. On the day after the thawing, all media were always changed.

2.2.1.2 Purification of human PBMCs from blood

Blood samples were collected as buffy coats. The blood was distributed carefully under sterile conditions into 50 ml Falcon tubes on top of 15 ml Ficoll-Paque™ PLUS solution and then centrifuged for 20 min at 20°C with 2000 rpm (acc. 1; breaking 1). PBMCs were concentrated in a ring layer on top of the Ficoll solution but below the plasma. Collected PBMCs were washed three times with PBS, with 2 mM EDTA and centrifuged for 5 min at 1200 rpm. After the subsequent centrifugation step 3 ml ACK buffer were added to the cell pellet to remove red blood cells. Following 5 min of incubation under constant shaking, the suspension was washed, centrifuged and cells were counted. After a last centrifugation step, the cells were taken up in the appropriate amount of freezing medium ($5x10^7$ cells per ml) and frozen as described before for later usage.

2.2.2 Adenoviral vectors and infection

XVir-N-31 has been described before (see 1.3.3 and (Rognoni, Widmaier et al. 2009, Mantwill, Naumann et al. 2013)). Both, XVir-N-31 and XVir-N-31-anti-PD-L1 have been kindly gifted from P.S. Holm (TU Munich, Germany). XVir-N-31-anti-PD-L1 was generated in the Holm lab by Eva Lichtenegger using the AdEasy Adenoviral Vector System. The entire transgene containing the PD-L1 binding Fab fragment (Kozak – Ig kappa leader – HA-tag - light chain - linker - heavy chain) was synthesized and ligated to the Fc part from the human IgG1 (kindly provided by Dr. Laschinger, TU Munich, Germany) (Lichtenegger, 2018). The Ig kappa (Igκ) leader sequence (ATG-GAGACAGACACACTCCTGCTATGGGTACTGCTGCTCTGGGT-TCCAGGTTCCACTGGTAC) was used to enhance protein secretion while the sequence encoding the HA tag was included for detection. The sequence of the variable light chain and the variable heavy chain connected by a glycine-serine linker originates from the patent US20100203056 A1. The transgene is inserted into the adenoviral E3-region via the two *DraI* sites (nt28706 and nt29308 with respect to AY339865.1), thereby replacing the E319K protein and is expressed under the control of the natural adenoviral E3 promoter. A stop codon generated during the cloning in the hinge region results in the expression of the PD-L1 blocking single chain antibody (hereafter referred to as anti-PD-L1) of a size of 32 kD. Additionally to these two OAVs, the wild type adenovirus-like virus dl309 was used in several experiments. dl309 is similar to subtype 5 wild type adenovirus (Ad-5), but contains, in contrast to Ad-5, a small deletion in the E3 region leading to enhanced cytopathogenicity but lesser viral replication and has been described before (Hibma, Real et al. 2009). As a control, the replication deficient adenovirus Ad-NULL (SignaGen), which lacks the E1 gene, was included in the experiments. All viruses were prepared, purified and titrated as described in the next chapter. For *in vitro* experiments cells were infected with the aforementioned viruses by adding virus particles counting for the indicated moiety of infection (MOI) to the culture medium.

2.2.2.1 Preparation, purification and titration of viruses

All viruses were produced in HEK293X cells using 15 cm cell culture dishes. Cells were split the day before infection and were 90 % confluent at the day of infection. Between 20 and 60 dishes were infected with the amount of virus that was evaluated before to be optimal to lyse cells in a period of 48 h. Approximately 48h (+/- 6h) later the cells showed strong visible signs of oncolysis. Subsequently, the cells were harvested by scraping, collected, centrifuged and the pellet taken up in PBS (with approx. 5 ml PBS for cells from 20 plates). The cells were lysed with three freeze/thaw cycles and centrifuged for 10 min at 3000 rpm. The supernatant, containing the virus, was collected and overlaid onto a CsCl step gradient. For this, 3 ml of 1,41 g/ml CsCl overlaid with 4,5 ml of 1,27 g/ml CsCl overlaid with 4 ml of the freeze/thaw supernatant was added into a centrifugation tube for ultracentrifugation. 500 µl of mineral oil was added on top. The tubes were ultra-centrifuged for 2h at 32000 rpm and 5°C, whereafter the living virus could be detected as a white band. This band was collected and transferred into a new centrifugation tube, which was filled up with 1,34 g/ml CsCl solution and overlaid with 500 µl of mineral oil. The tubes were ultra-centrifuged again at 32000 rpm and 5°C for 20h. Purified virus particles were detected as a sharp white band, which was taken up in as little volume as possible and injected into a previously prepared Thermo Scientific™ Slide-A-Lyzer™ dialysis cassette. After extracting the remaining air, the cassette was placed in dialysis buffer and kept in the fridge at 4°C with mild stirring. The buffer was exchanged after 1h, 2h,

4h, 6h and on the next morning. Two hours after the final change, the virus was extracted from the cassette, mixed with 10 % glycerol and frozen at -80°C. Viral titers were determined in HEK293 cells using the Adeno-Rapid-X-Titration kit (Takara Bio Europe SAS) following the manufacturer's protocol. Briefly, cells were seeded, allowed to attach and infected with serial dilutions of the virus. After 48 h the cells were fixed with 100 % methanol at -20°C, washed, incubated for one hour with the anti-hexon primary antibody and after washing steps incubated for one hour with a secondary HRP conjugated antibody. After subsequent washing, incubation with a 3,3′-Diaminobenzidine (DAB) solution and a final washing step, infected cells appeared as brown dots, were counted and the titer was evaluated.

2.2.3 Cell viability assay after viral infection

$1x10^4$ glioma cells were plated in 96 well flat bottom plates and allowed to attach overnight. On the next day, cells were infected with different viruses at increasing MOI (0-100 MOI). 48 h later photos were taken and subsequently cell viability was measured using a MTT Cell Proliferation Kit (Merck, Germany). Briefly, MTT stock solution (5 mg/ml in PBS) was added 1:10 directly into the media and incubated for 2 h again. Next, the medium was discarded and 100µl DMSO was added into each well. Following 2 min of shaking the cells were analyzed on their absorbance at 570 nm with an absorbance reader (Multiskan EX).

2.2.4 Immunoblot analysis

To determine the expression of the HA-tagged PD-L1 blocking single chain antibody coded by XVir-N-31-anti-PD-L1, lysates and supernatants of infected HEK293 cells were taken, protein concentration was determined and protein expression was analyzed via Sodium dodecyl sulfate polyacrylamide gel electrophoresis (SDS-PAGE) and western blot analysis.

2.2.4.1 Generation of cell lysates and supernatants for protein detection

Cells were infected with 30 MOI of XVir-N-31, XVir-N-31-anti-PD-L1 or were left untreated. For lysates, cells were harvested after 48 h, washed, centrifuged, resuspended in 50-500 µl of lysis buffer (according to the size of the cell pellet) and incubated on ice for 20 min. Finally, the suspension was centrifuged for 15 min at 12800 rpm at 4°C and the supernatant, containing the proteins, was stored. For the detection of the release of anti-PD-L1 from infected cells, cells were infected as described above, but the medium was exchanged to serum-free medium 4 h after infection. After 48 and 72 h, supernatants were collected, cleared by centrifugation and concentrated by acetone precipitation after determination of the protein concentration using the Bradford protein assay. For precipitation the supernatant was mixed with three volumes of ice-cold acetone and centrifuged for 20 min at 4000 rpm. The protein pellets were air dried and resuspended in Laemmli buffer and stored at -20°C.

2.2.4.2 Bradford protein assay

Bradford protein assay was used for the detection of total protein concentrations in lysates and in supernatants and is described before. Briefly, eight increasing protein standard solutions of bovine serum albumin (BSA; 0 – 12 mg/ml) in lysis buffer were prepared and 1 µl of each were pipetted in triplicates into a 96-well flat bottom plate containing 50 µl water. Additionally, for the lysates 1 µl of the analysed samples were pipetted in triplicates into the plate and filled up with ddH_2O to 50 µl. For the supernatants 50 µl of the supernatant was taken directly while the standard solutions were filled up to 50 µl with serum free medium. 150 µl of Bradford reagent was added to each well. Color turnover was visible immediately and absorbance was measured at 595 nm using an absorbance reader (Multiskan EX). By creating a standard curve with the values from the standard solutions with Microsoft Excel, the protein concentration of the lysates and supernatants could be evaluated.

2.2.4.3 SDS-PAGE and western blot analysis

Gel composition:

10 % separation gel (for 10 ml)	**Stacking gel (for 3 ml)**
4.0 ml H_2O	2.1 ml H_2O
3.4 ml 30 % acrylamide mix	0.5 ml 30 % acrylamide mix
2.6 ml 1.5 M Tris (ph 8.8)	0.38 ml 1.0 M Tris (ph 6.8)
0.1 ml 10 % SDS	0.03 ml 10 % SDS
0.1 ml 10 % ammonium persulfate	0.03 ml 10 % ammonium persulfate
0.004 ml TEMED	0.003 ml TEMED

SDS-PAGE was performed to separate and detect proteins from different lysates or supernatants according to their molecular weight and has been described before. Briefly, 10 % separation gel, overlayed with stacking gel, was transferred into a running chamber and the chamber was filled with running buffer. Samples from lysates (mixed 3:1 with Laemmli buffer) or supernatants (already taken up in Laemmli buffer) were heated for 5 min at 95°C and loaded onto the gel. For molecular weight detection 5 µl of Spectra™ Multicolor Protein Ladder (Thermo Scientific) was added in a separate well. The gel was run for 30 min at 50 V and 80 min at 111 V. Proteins were blotted for 1 h at 100 V onto methanol-activated PVDF membranes, blocked (30 min at RT with 5 % non-fat milk powder in TBST) washed and incubated overnight at 4°C with the respective primary antibody (anti-HA: 1:500; anti-GAPDH: 1:1000) in 2,5 % milk powder in TBST. After another 3 washing steps with TBST, the membrane was incubated for 2 h with the secondary antibody, subsequently washed again and the immunoreactive proteins were detected using Clarity ECL substrates on a ChemiDoc™ MP Imaging System and ImageLab 5.1 software.

2.2.5 PD-1/PD-L1 binding assay

For the analysis of the functionality of the anti-PD-L1 blocking single chain antibody HEK293 cells were either infected with 50 MOI of XVir-N-31 or XVir-N-31-anti-PD-L1 or left untreated. After 48 h supernatants were collected, cleared by centrifugation and concentrated with Centricon Plus Centrifugal filter devices according to the manufacturer's protocol (concentration spin with 3500 x g for 45 min and recovery spin for 1000 x g for 2 min). 40 µl of the concentrated supernatants were used in a commercial PD-1/PD-L1 Blockade Assay Kit (Promega) according to the manufacturer's protocol. Briefly, the day before the supernatant collection PD-L1 aAPC/CHO-K1 cells were seeded in a 96 well white flat bottom plate ($4x10^4$ cells/well). After overnight incubation, 40 µl of concentrated supernatant and $5x10^4$ PD-1 effector cells in assay buffer were added to each well and were incubated for another 6 h. As a negative control PBS and as a positive control 10 µg/ml anti-PD-L1 antibody was added to the cells. Finally, 80 µl of Bio-Glo™ reagent per well was added and after 30 min of incubation at room temperature luminescence was measured using a TriStar2 S LB 942 Multimode Reader.

2.2.6 Enzyme Linked Immunosorbent Assay (ELISA)

HSP70, HMGB1, YB-1 and IFNγ concentrations in supernatants of infected cells were analyzed by ELISA. For HSP70, HMGB1 and YB-1 release, $0,6x10^6$ U87MG or LN-229 cells were seeded and infected 24 h later with different MOI (XVir-N-31 and XVir-N-31-anti-PD-L1: 50 MOI; dl309: 20 MOI). The supernatants of the cells were collected at the time point the cells showed 50 % oncolysis (time points were analyzed before; dl309: 48,5 h, XVir-N-31: 72 h and XVir-N-31-anti-PD-L1: 82,5 h), cleared by centrifugation (14000rpm, 15 min) and used in the respective ELISA kit (hsp-70, HMGB1, YBX1; Cloud-Clone Corp, Hölzel Diagnostics) according to the manufacturer's protocols. For IFNγ $5x10^4$ glioma cells (U87MG; LN-229) were seeded and infected 24 h later with 30 MOI of XVir-N-31, XVir-N-31-anti-PD-L1, dl309, Ad-NULL or were left untreated. 48 h later the cells were washed with PBS and then cocultured with $1x10^6$ "glioma cell HLA A/B-matched" human PBMCs that have been previously stimulated over 6 days by the addition of IL-2 (100 IU/ml; 3 days with IL-2, 3 days without IL-2). After another 48 h of cocultivation supernatants were taken, cleared by centrifugation and the amount of IFNγ was analyzed using the ELISA MAX™ Deluxe Set Human IFNγ Kit according to the manufacturer's protocol. Absorbance was measured at 450 nm using a TriStar2 S LB 942 Multimode Reader.

2.2.7 Flow cytometry analysis

For the determination of PD-L1 expression on glioma cells (U87MG or LN-229), cells were harvested, and single cell suspensions were stained with a PD-L1 specific antibody (1:20 in FACS buffer). For the surface exposure of CRT, glioma cells (U87MG or LN-229) were infected with different MOI of the respective virus (XVir-N-31 and XVir-N-31-anti-PD-L1: 50 MOI; dl309: 20 MOI) or were left untreated. At time points the cells showed 50 % cell oncolysis (dl309: 48,5 h, XVir-N-31: 72 h and XVir-N-31-anti-PD-L1: 82,5 h), cells were harvested and single cell

suspensions were stained using a CRT specific antibody (1:20 in FACS buffer). For the analysis of human immune cells from whole murine blood, blood was taken from the murine tail vein, mixed 1:1 with a 10 µM EDTA solution, distributed to several samples and incubated with the following antibodies: anti-mouse CD45-FITC, anti-human CD45-APC, anti-human CD19-PE-Cy7, anti-human CD3-PB, anti-human CD4-FITC, anti-human CD8-APC (all 1:10). For all antibodies mouse IgG1κ isotype control antibodies (with their respective fluorochromes) served as negative controls. All samples were incubated for 30 min on ice in the dark, washed 2 times with FACS buffer and taken up finally in 200 µl of FACS buffer. Samples of murine blood were additionally incubated two times for 3 min with 1 ml of ACK lysis buffer and subsequent washed to remove erythrocytes before taking up in the final FACS buffer. All analyses were performed on a MACSQuant Analyser 10 Flow Cytometer and the data was analyzed using FlowJo v10 Software.

2.2.8 Immuno-humanized pseudo-syngeneic mouse model

NOD.Cg-Prkdc^{scid} Il2rg^{tm1Wjl}/SzJ (NSG) mice (Jackson Laboratory, Maine, USA) were bread in the animal facility of the Hertie Institute, housed in IVC cages under standard pathogen-free conditions and used for all experiments at an age between 2 - 6 months (TVA number N02/19G). NSG mice harbor a *scid* mutation in the DNA repair complex protein *Prkdc*, rendering them B and T cell deficient, and a complete null allele of the IL-2 receptor common gamma chain, leadings also to a deficiency of functional NK cells. For surgery, mice were narcotized using peritoneally applied anesthesia (0.05 mg/kg Fentanyl, 5 mg/ml Midazolam and 0.5 mg/kg Medetomin) with Carprofen (5 mg/kg) subcutaneously injected as an analgesic. Subsequently, the mice were orthotopically inoculated using a mouse stereotactic device and 1 × 10^5 U87MG or LN-229 glioma cells were injected into both the striata of the right and the left hemisphere of the brain with an automated infusion pump and a 10 µl Hamilton syringe (2 µl cells in total, 1 µl/min). The drill hole was closed using histoacryl tissue glue (Braun, Germany) and the skin wound was closed by suture. Anesthesia was antagonized by a subcutaneous injection of antidote (Naloxon (1.2 mg/kg), Flumazenil (0.5 mg/kg) and Atipamezol (2.5 mg/kg)). 10 days post glioma cell implantation, 2 x 10^6 human PBMCs, HLA-A/B identic to the implanted GBM cells, were injected in 50 µl NaCl in the tail vein of the mice to establish a humanized immune system. Four days later, mice were narcotized and inoculated as mentioned before and either PBS (sham) or 3x10^8 infectious particles (IFU) of dl309, XVir-N-31 or XVir-N-31-anti-PD-L1 were injected in a total of 3 µl into the tumor of the right hemisphere. The contralaterally growing tumor was left untreated and should mimic into the healthy brain invaded glioma cells, which are not directly effected by viral cell lysis. Mice of the respective groups (Nivolumab; XVir-N-31 plus Nivolumab) were injected intraperitoneally with Nivolumab (200 µg/injection/mouse) on day 4, 7, 10 and day 14 after virus injection. All mice were monitored constantly and examined on pathological symptoms (either by tumor growth or graft versus host disease (GvHD) symptoms as weight loss, scruffy fur, hunched posture etc. Murine blood was taken multiple times from the tail vein and analyzed by flow cytometry as described above to follow the onset of the human immune cell engraftment as well as to analyze the composition of the immune cell populations. All mice were sacrificed at the same time point, namely 35 days after intratumoral injections. At that time point, blood was taken for a final immune cell analysis and brains were extracted and preserved for further analyses.

2.2.8.1 Histology and immunofluorescent staining

Whole mouse brains were fixed overnight in 4% PFA and in the following dehydrated with 20 % and 30 % sucrose solutions for two days each. After embedding the tumor containing parts of the brain in Tissue-Tek O.C.T., samples were cryosectioned for further histological analysis using a Leica Cryomicrotome CM3050S at 10 µm thick sections and stored on glass slides until usage at -20°C. For immunofluorescent staining, slides were washed and warmed up for 10 min in PBS, pretreated for antigen retrieval by boiling in Tris-EDTA buffer pH 9 for 15 min, washed with TBS-T and treated with 3 % H_2O_2 in methanol for 10 min to block endogenous peroxidase activity. After another three washing steps, slides were blocked with 3 % animal serum of the respective secondary antibody in TBS-T for 1 h and finally stained overnight with the following primary antibodies: anti-human nuclei (1:50), anti-human CD45, CD3, CD4, CD8, FoxP3, CD56, CD134, hexon, HMGB1, or HSP70 (all 1:100 in TBS-T). The next day, after three washing steps the slides were incubated with fluorochrome conjugated secondary antibodies (AF488 or AF680; 1:1000 in TBS-T) for two hours and after final washing steps mounted with Vectashield mounting media containing DAPI or Permount mounting media. Images were taken using a Zeiss LSM 710 confocal microscope with different magnifications and analysed with the ZEN 3.0 software. Tumor infiltrating lymphocytes were counted using ImageJ software.

2.2.8.2 Hematoxylin and Eosin (H&E) staining and tumor volumetry analysis

Slides of mouse brain tissue were generated and stored as described in chapter 2.2.8.1. For H&E staining, slides were warmed up for 10 min with PBS, stained for 10 min with 0,1 % hematoxylin solution, washed for 7 min under running tab water until the pH shift was visible and stained subsequently for 90 seconds with eosin Y solution. Afterwards, the slides were washed under running tab water until no streaking was seen. Following dehydration, using alcohol dilution series (70 %, 95 %, 100 % EtOH for 1 min each) and xylene (100 %, 1 min), the slides were mounted with Permount mounting media and images were taken using a Leica DMi8 microscope. To determine the tumor volume, the start and the end of the tumors were determined and the area of the hematoxylin positive tumor was measured throughout the whole tumor every 100 µm using ImageJ. The surface area multiplied with the thickness of each section (100 µm – until the next section) gave the partial volume and the sum of all partial volumes approximated the volume of the whole tumor. All these measurements were performed independently for tumors of the ipsilateral as well as of the contralateral hemisphere.

2.2.9 Statistical analysis

All *in vitro* experiments were performed at least thrice if not mentioned otherwise. For all *in vivo* experiments, the group and sample size are indicated in each figure legend, with a maximum of 8 animals per group. To assume a gaussian distribution, all data received from *in vitro* experiments passed a normality test (Shapiro-Wilk and the Tukeys multiple comparison test). Further statistical analyses were done with one-way ANOVA or two-tailed Student's t-test using GraphPad Prism 7.0 software. The results are represented as mean ± standard error

of the mean (SEM). p-values of < 0.05 are considered as statistically significant (ns: not significant; * $p < 0.05$; ** $p < 0.01$; *** $p < 0.001$; **** $p < 0.0001$).

3. Results

3.1 Lytic activity of XVir-N-31 and XVir-N-31-anti-PD-L1 in GBM

The lytic activity and the effectivity of XVir-N-31 has been shown already in several different cancer entities, including GBM (Mantwill, Naumann et al. 2013, Czolk, Schwarz et al. 2019, Hindupur, Schmid et al. 2020). However, comparison of its lytic efficacy to Ad-WT in combination with the characterization of XVir-N-31-anti-PD-L1 was never performed in GBM cells before. As seen in Figure 6A, both U87MG and LN-229 GBM cell lines showed typical lytic morphology 48 h after infection with 50 MOI of both OAVs XVir-N-31 and XVir-N-31-anti-PD-L1, as well as with the wild type adenovirus-like virus (from here on always referred to as dl309, for exact characterization see 2.2.2) compared to untreated control. To analyze and quantify the lytic potential of these viruses, U87MG and LN-229 cells were infected with increasing MOI and viability was analyzed 48 h after infection by MTT assay. As a control the replication deficient adenovirus Ad-NULL was included in the experiments (Figure 6B). As expected, dl309 showed an extremely strong lytic activity in both cell lines, being slightly more

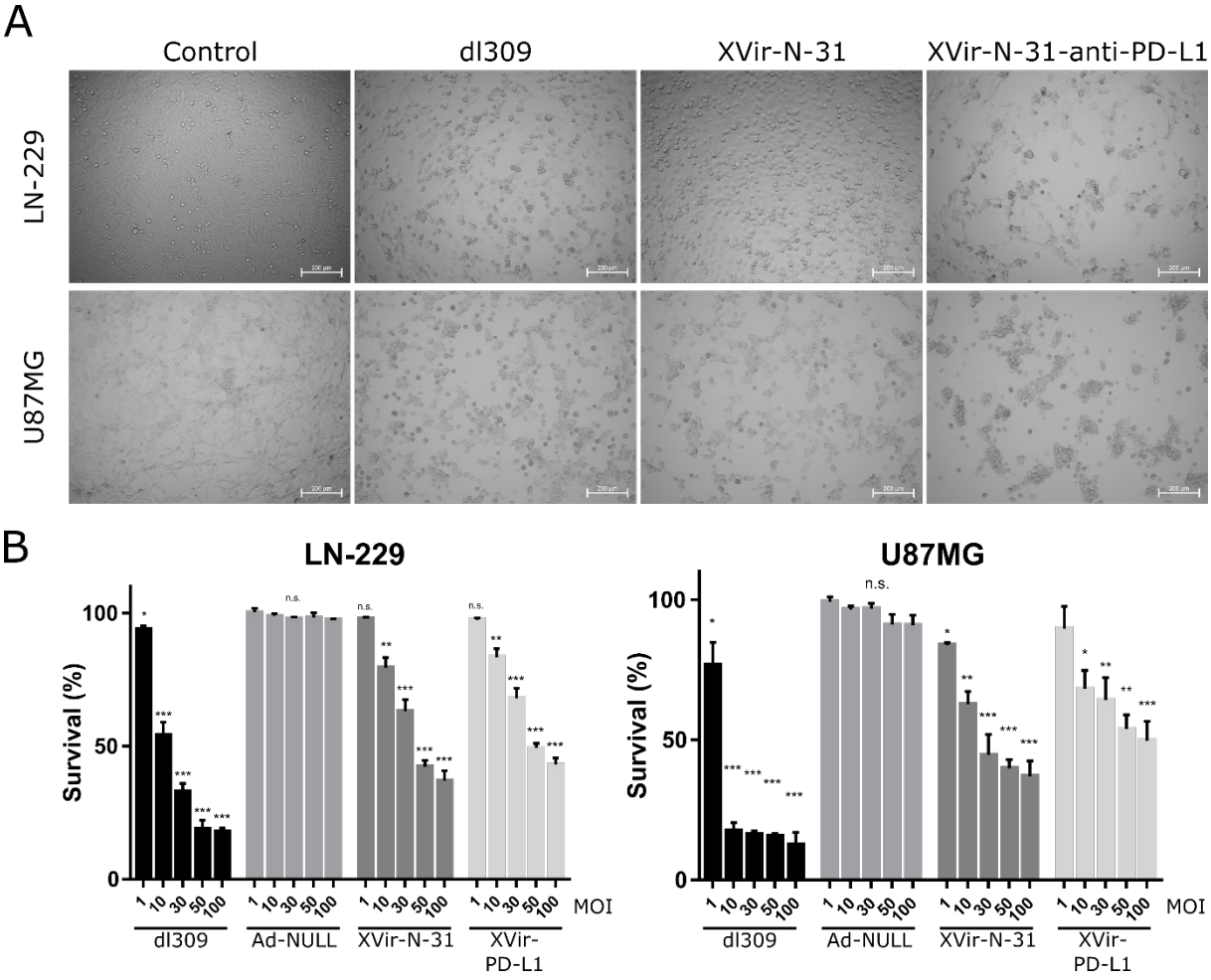

Figure 6. Properties of OAVs XVir-N-31 and XVir-N-31-anti-PD-L1. A. LN-229 or U87MG cells were infected with 50 MOI of dl309, XVir-N-31, XVir-N-31-anti-PD-L1 or were left untreated (control). Pictures were taken 48 h after infection. **B.** LN-229 or U87MG cells were infected with increasing MOI of the indicated viruses. Cell lysis was determined 48 h after infection by MTT assay (XVir-PD-L1: XVir-N-31-anti-PD-L1; n = 3; SEM; ns: not significant; * $p < 0.05$, ** $p < 0.01$, *** $p < 0.001$).

potent in U87MG cells. Nevertheless, an IC_{50} was reached with approximately only 10 MOI after 48 h in both cell lines. On the contrary, Ad-NULL infection did not lead to any significant decrease in cell survival in both cell lines even with higher MOI, proving that successful replication is essential for cell lysis. XVir-N-31 and XVir-N-31-anti-PD-L1 (in Figures hereafter often referred to as XVir-PD-L1) showed a comparable lytic activity, with XVir-N-31 only slightly more potent in U87MG cells. In both cell lines the IC_{50} was reached with approximately 30-50 MOI for both viruses, demonstrating a good oncolytic activity in GBM, even though the cell lysis is diminished compared to dl309.

3.2 XVir-N-31-anti-PD-L1 expresses a functionally active PD-L1 neutralizing antibody

After proving the lytic activity of XVir-N-31-anti-PD-L1, we tested the expression and secretion of the PD-L1 blocking single chain antibody (anti-PD-L1) coded by this virus. Therefore, HEK293 cells were infected with 30 MOI of XVir-N-31-anti-PD-L1, XVir-N-31 or left uninfected, lysates and supernatants were taken (lysates: 48 h; supernatants: 48 h and 72 h) and anti-PD-L1 expression was determined by western blot via the HA-tag of anti-PD-L1 (Figure 7A). As expected, in lysates as well as in supernatants of uninfected cells, but also of cells infected with XVir-N-31, no anti-PD-L1 was detected. On the contrary, anti-PD-L1 was found in the lysates of cells infected with XVir-N-31-anti-PD-L1, but also in supernatants after 48 h and stronger after 72 h, proving a correct expression but also secretion of the antibody. To examine the functional activity of this antibody, a PD-1/PD-L1 blockade assay was performed. Supernatants of untreated, XVir-N-31 or XVir-N-31-anti-PD-L1 infected HEK293 cells were

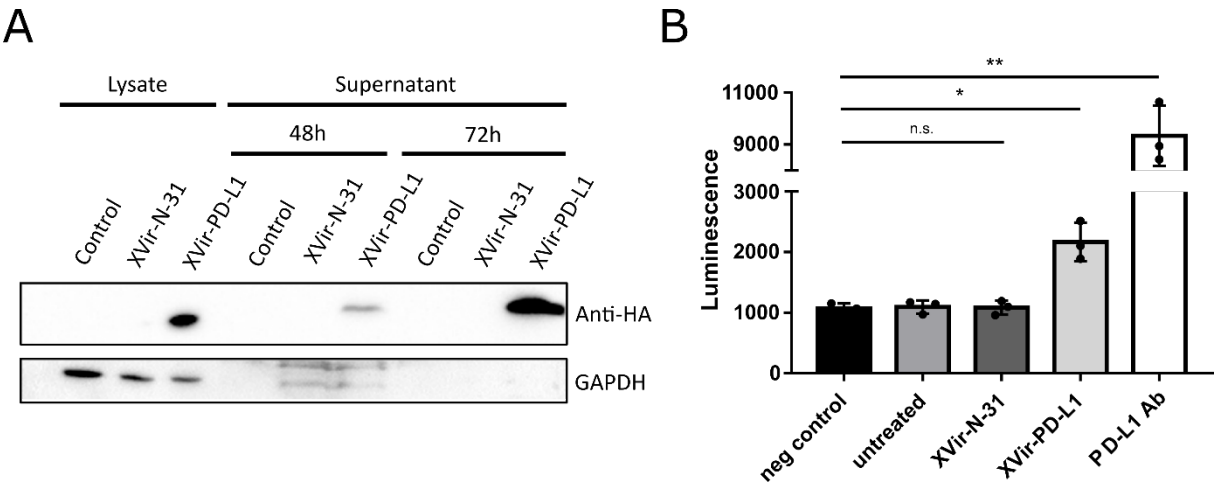

Figure 7. Expression, secretion and functional activity of anti-PD-L1 coded by XVir-N-31-anti-PD-L1. A. HEK293 cells were infected with 30 MOI of XVir-N-31 or XVir-N-31-anti-PD-L1, or were left untreated (control). Lysates or supernatants were collected at the indicated time points. Production and secretion of anti-PD-L1 was analysed by immunoblot using an anti-HA antibody, GAPDH served as loading control. **B.** Cells were infected with 50 MOI of XVir-N-31, XVir-N-31-anti-PD-L1 or were left untreated. Supernatants were collected 48h after infection and were subsequently used in an PD-1/PD-L1 blocking assay. Increased luminescence indicates an interrupted PD-1/PD-L1 binding. PBS served as negative control, 10 µg/ml anti-PD-L1 antibody for a positive control (XVir-PD-L1: XVir-N-31-anti-PD-L1; n = 3; SEM; ns: not significant; * $p < 0.05$, ** $p < 0.01$).

used in this assay that displays the blockade of the PD-1/PD-L1 interaction by enhanced luminescence (Figure 7B). While the positive control with a commercially available anti-PD-L1 antibody showed a strong blockade of PD-1/PD-L1 binding, supernatants of untreated cells or cells infected with XVir-N-31 did not increase background luminescence compared to PBS negative controls. On the contrary, supernatants from cells infected with XVir-N-31-anti-PD-L1 led to a significant increase of luminescence, showing that the secreted anti-PD-L1 antibody is also functionally active and capable to block the interaction of PD-1 and PD-L1.

3.3 Immunogenic effects of XVir-N-31 and XVir-N-31-anti-PD-L1 in GBM *in vitro*

The immunogenic properties of XVir-N-31 have already been analyzed in a bladder cancer model (Lichtenegger, Koll et al. 2019), but have never been addressed in GBM. Additionally, XVir-N-31-anti-PD-L1, a derivate of XVir-N-31, has never been properly characterized due to its immunogenic effects in GBM or even other entities. Therefore, certain immunostimulatory

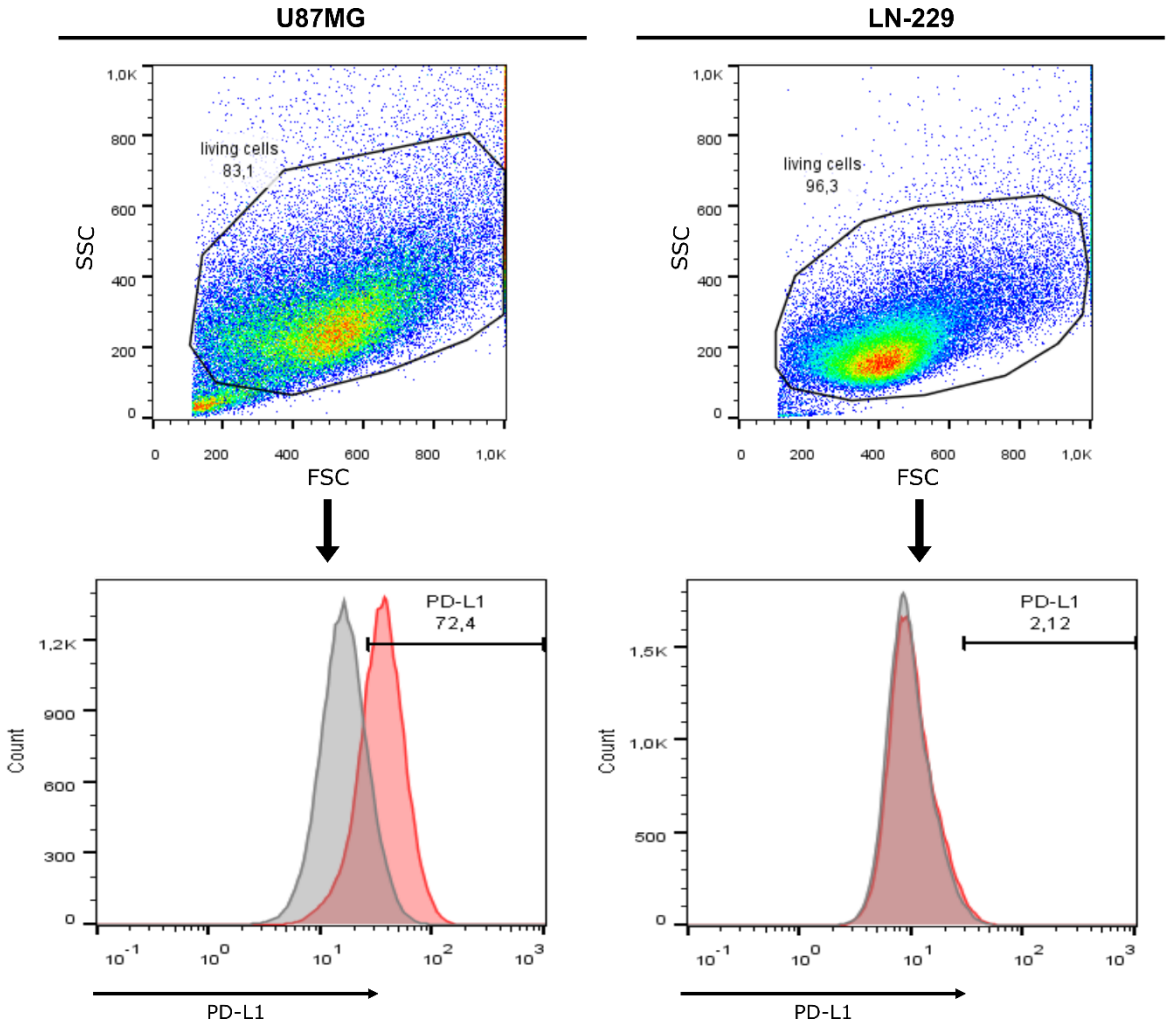

Figure 8. PD-L1 status of glioma cells as determined by FACS analysis. U87MG and LN-229 cells were detected as living, single cells by flow cytometry via the forward (FSC) and side scatter (SSC) and were analyzed on their PD-L1 cell surface expression (red: PD-L1; grey: isotype control).

effects typical for ICD and additional immune responses were analyzed after infection of two different GBM cell lines with XVir-N-31 and XVir-N-31-anti-PD-L1 and were compared to dl309. Since anti-PD-L1 secreted from XVir-N-31-anti-PD-L1 infected cells will only show an effect on cells expressing PD-L1 on their cell surface, the used cell lines, U87MG and LN-229, were in a first step examined on PD-L1 expression by flow cytometry (Figure 8). When focusing on the isolated, viable cells, cultured LN-229 cells show barely any PD-L1 expression (in red; grey as the isotype control), whereas U87MG cells express PD-L1 strongly on their cell surface, making these cells an interesting target to determine the immunostimulatory effects of XVir-N-31-anti-PD-L1.

3.3.1 XVir-N-31 and XVir-N-31-anti-PD-L1 induce immunogenic cell death in GBM cells

Unlike wild type adenoviruses, OVs used for OVT induce ICD in tumor cells and an anti-tumoral immune response, thereby probably increasing their therapeutic effects (for detail see 1.3.4). One typical feature of ICD is the release of DAMPs. Consequently, the release of the DAMPs HSP70 and HMGB1 as well as the release of the immunogenic protein YB-1 was examined upon viral infection in two different cell lines via ELISA (Figure 9A, performed under my direct supervision by Jasmin Buch; Figure 9C). Additionally, cell surface expression of CRT, which is typically upregulated in ICD and serves as an “eat me” signal to immune cells, was analysed by flow cytometry (Figure 9B, D). To ensure an equal lysis and a comparable relative DAMP release, glioma cells were infected with the appropriate viruses and, depending on the virus, were harvested at those time points the cultures showed 50 % oncolysis. In U87MG and LN-229 cells, dl309 infection led to a minor release of HMGB1 and YB-1, whereas no HSP70 release was detected. On the contrary, compared to dl309, infection of the cells with either XVir-N-31 or XVir-N-31-anti-PD-L1 resulted in a significantly stronger release of all three molecules in both cell lines (Figure 9A, C). Interestingly, in LN-229 cells, compared to cells infected with XVir-N-31, XVir-N-31-anti-PD-L1 induced a significantly stronger release of HSP70 and YB-1. For the cell surface expression of CRT (in red; grey as the isotype control), dl309 infection resulted in hardly any (Figure 9B) or only a very moderate increase (Figure 9D) compared to uninfected cells. In both cell lines, CRT expression was increased after infection with XVir-N-31 and even stronger upregulated by XVir-N-31-anti-PD-L1. Taken all together, XVir-N-31 and XVir-N-31-anti-PD-L1 seem to be potent inducers of ICD in GBM and therefore also potent inducers of an effective anti-tumor immune response.

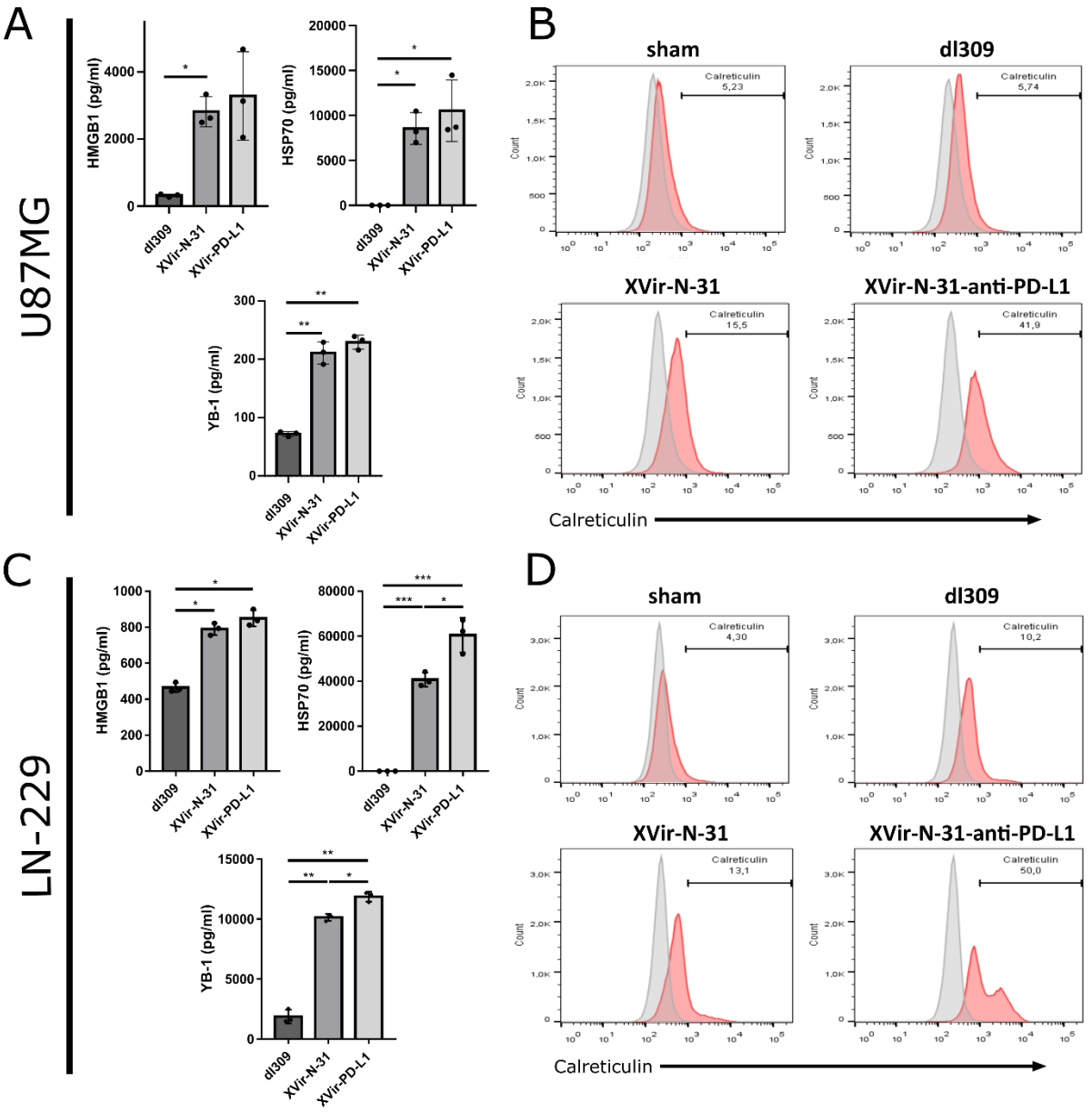

Figure 9. Induction of immunogenic cell death by XVir-N-31 and XVir-N-31-anti-PD-L1. U87MG **(A)** and LN-229 cells **(C)** were infected with 50 MOI XVir-N-31 or XVir-N-31-anti-PD-L1, or with 20 MOI dl309. Supernatants were taken at the timepoint the cultures showed 50% cell viability, and were analysed for HMGB1, HSP70 or YB-1 release via ELISA (XVir-PD-L1: XVir-N-31-anti-PD-L1). CRT cell surface expression was analysed in U87MG **(B)** and LN-229 cells **(D)** via flow cytometry at the same conditions as indicated in A (red: CRT; grey: isotype control) (n=3; SEM; ns: not significant; * $p < 0.05$; ** $p < 0.01$; *** $p < 0.001$).

3.3.2 Lytic adenoviruses induce the release of IFNγ from infected cells

While DAMPs were efficiently released from tumor cells upon XVir-N-31 and XVir-N-31-anti-PD-L1 infection, but not by dl309, a general induction of a pro-inflammatory immune boost might generally occur after viral infection, independent of its replication status. It is already known that wild type adenoviruses induce a subsequent immune reaction (see 1.3.4). A first line defence mechanism is thereby the release of the pro-inflammatory cytokine IFNγ from infected cells. IFNγ can be secreted by either virus infected cancer cells as well as by activated

immune cells. To investigate whether an adenoviral infection or a specifically by ICD mediated release of DAMPs is responsible for the primary immunostimulatory boost, virus-infected GBM cells were co-cultured with previously stimulated, “glioma cell HLA A/B matched” human PBMCs and the IFNγ release by these co-cultures was measured via ELISA. Of note, it was shown before in the group of our collaborator P.S. Holm (TU Munich), that in contrary to wild type adenovirus XVir-N-31 can’t replicate in PBMCs (Koll, 2018). As shown in Figure 10, no increased induction of IFNγ release was observed in U87MG and LN-229 cell cultures after infection with Ad-NULL compared to uninfected cells. On the contrary, infection of the cells with a replication-competent virus induced a significantly elevated level of IFNγ in the supernatants of GBM cell / PBMC co-cultures. Compared to dl309 there was no significant difference in concentration of IFNγ by XVir-N-31 infection of both co-cultures models. This indicates that a general, unspecific immunostimulatory effect might be provoked by the infection of GBM cells with lytic adenoviruses, whereas the release of DAMPs is only induced by the infection with OAVs. Interestingly, in co-cultures of XVir-N-31-anti-PD-L1 infected U87MG PD-L1^{pos} cells and matched PBMCs, the IFNγ concentration was significantly elevated compared to XVir-N-31 or dl309 infected GBM cell / PBMC co-cultures. These findings indicate an additional immunostimulatory effect for XVir-N-31-anti-PD-L1 if the OVT-targeted tumor cells express PD-L1.

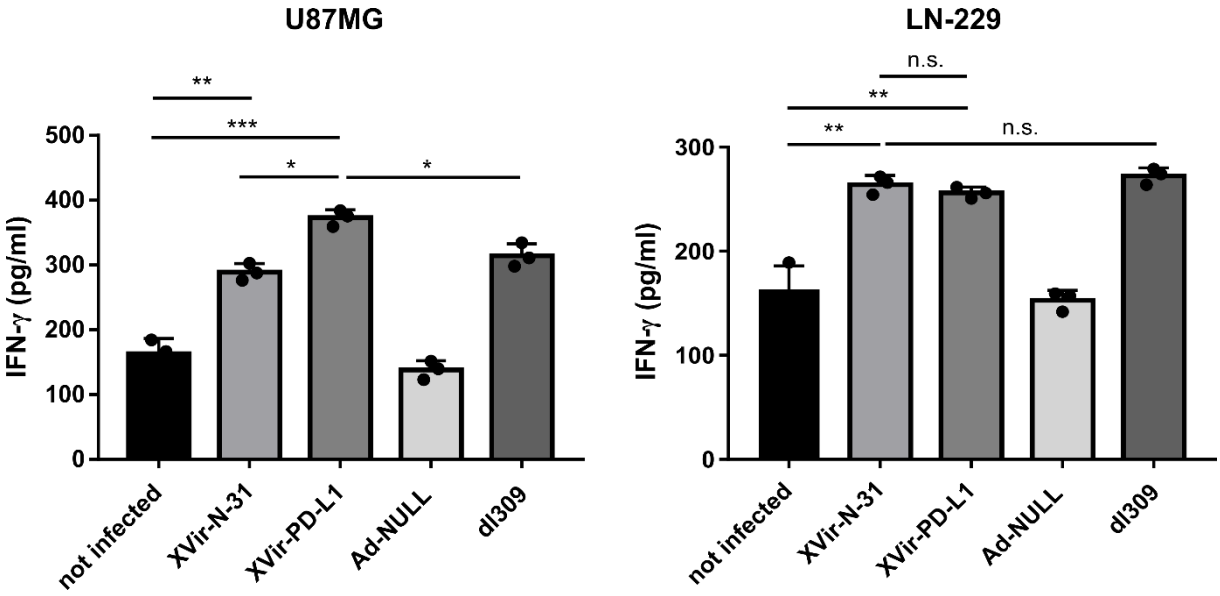

Figure 10. IFNγ release induced by XVir-N-31 and XVir-N-31-anti-PD-L1. IFNγ release from co-cultures of “GBM cell HLA A/B matched” human PBMCs with virus infected U87MG or LN-229 cells was measured by ELISA. Prior to co-cultivation, GBM cells were infected for 48 h with 30 MOI of the indicated virus and PBMCs were stimulated with IL-2 for 6 days (3d with IL-2; 3d without). Supernatants were collected 48 h after co-cultivation (XVir-PD-L1: XVir-N-31-anti-PD-L1; n=3; SEM; ns: not significant; * $p < 0.05$, ** $p < 0.01$, *** $p < 0.001$).

3.4 Immuno-stimulatory and therapeutic effects of XVir-N-31 and XVir-N-31-anti-PD-L1 *in vivo*

Following the promising data obtained *in vitro*, we were interested in investigating the impact of an OVT using XVir-N-31 and XVir-N-31-anti-PD-L1 also *in vivo* using an orthotopic mouse GBM model. Since the murine one only partially reflects the human immune system, but mainly because subtype 5 adenoviruses (dl309 and XVir-N-31 or XVir-N-31-anti-PD-L1) do not replicate in murine cells, a syngeneic mouse model was not feasible for our purposes. Therefore, we decided to establish a glioma model with human glioma cells in immuno-deficient mice that allow the growth of human tumors as well as an engraftment with human PBMCs. This model is described in the following chapter.

3.4.1 The immuno-humanized "pseudo-syngeneic" glioma mouse model

In the following experiments NOD.Cg-Prkdc^{scid} Il2rg^{tm1Wjl}/SzJ (NSG) mice, that do not develop either functional T cells or NK cells, were used (for detail, see 2.2.8). In these mice a human immune system can be established by an intravenous injection of human PBMCs. A disadvantage of this model is the development of GvHD over time, which might influence immune responses evoked by OVT, but which also makes survival analysis impossible. The timepoint of GvHD onset becomes visible by a massive, sudden burst of CD45$^+$ cells in the murine blood. In former animal experiments of our group, we observed this burst at the earliest 80 days after PBMC injection (Suppl. Figure 1A, unpublished data by Yana Parfyonova) which was slightly later than described by Ehx *et al*. (Ehx, Somja et al. 2018). Other signs typical for GvHD, as weight loss or scrubby fur, were not detected over this period of time (Suppl. Figure 1B; and data not shown). Nevertheless, to avoid analyzing effects related to GvHD, we decided to finalize all animal experiments to a considerably earlier timepoint.

As depicted in Figure 11, either U87MG or LN-229 glioma cells were implanted in both striata of the mice's brains. Ten days later a humanized immune system was established in these mice by an intravenous injection of - to the GBM cells HLA A/B matched - human PBMCs. Four days after engraftment the tumor in the right striatum was treated, leaving the contralaterally located tumor unaffected. This allows to analyze the impact of oncolysis plus OVT-mediated immune responses in the ipsilateral located tumors (right hemisphere) as well as of abscopal effects in the untreated, contralaterally located tumors (left hemisphere). In this study the contralateral tumor should mimic those GBM cells that in patients have been invaded into the healthy brain and that are located far away from the original tumor and therefore from the side of virus injection. The ipsilateral tumors were treated by either single intratumoral injections of PBS (sham cohort), dl309, XVir-N-31 or XVir-N-31-anti-PD-L1. Two additional cohorts (after either intratumoral PBS or XVir-N-31 injection) received subsequently repeated systemic applications of Nivolumab to demonstrate the effects of an (additional concomitant) immune checkpoint inhibition. Over the following course, the murine blood was analyzed several times by flow cytometry on the presence and quantity of human immune cells (data not shown). To avoid to analyze immune effects associated with the onset of GvHD, and since the median survival of U87MG or LN-229 bearing mice is approximately 40 days (Roth, Isenmann et al. 1999, Armento, Ilina et al. 2017), all mice were sacrificed 35 days after treatment, which was also the time point the first mouse developed neurological symptoms associated with an

advanced tumor growth. The brains were fixed and tumor containing tissues were analyzed on immune cell infiltration, DAMPs and tumor growth.

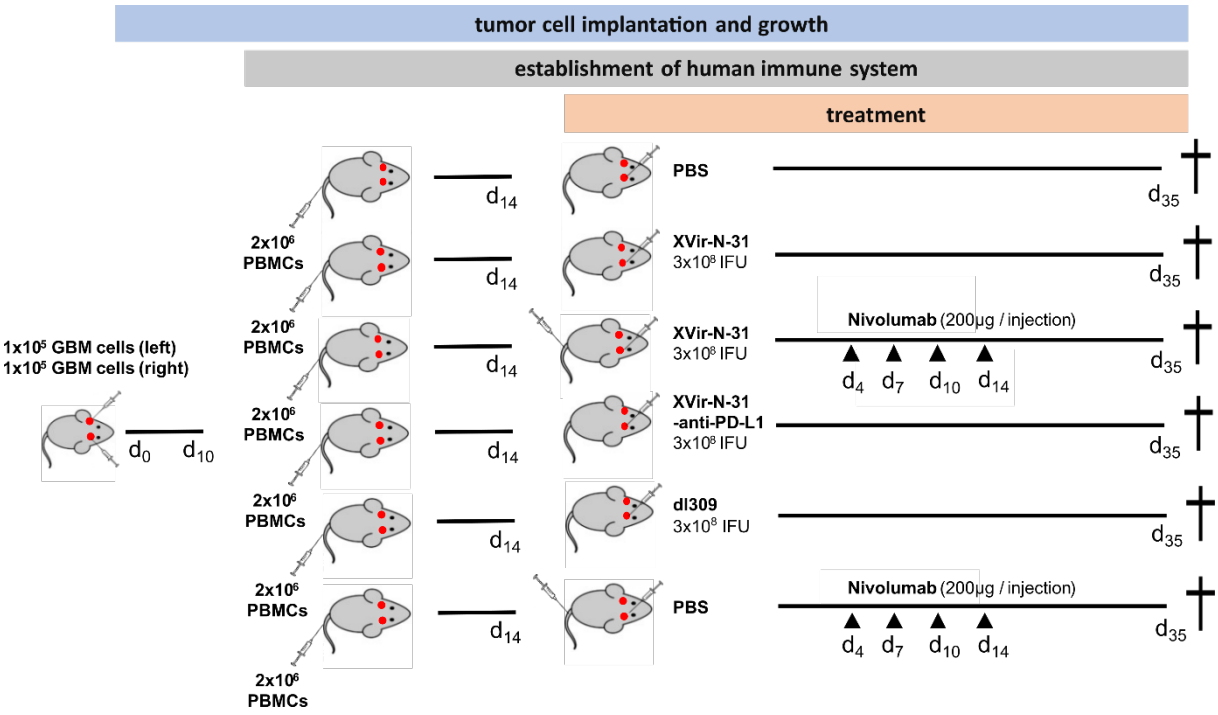

Figure 11. Immuno-humanized mouse GBM model. Treatment scheme. For details, see 2.2.8

3.4.2 In GBM bearing mice Nivolumab monotherapy provides no beneficial effects

Brains harvested from sacrificed mice harboring tumors were analyzed on tumor growth by H&E staining and on immune cell infiltration (using a human CD45 specific antibody) as well as on the induction of ICD by staining for HSP70 and HMGB1. First and to prove that the examined effects were located in the tumor area and not in the healthy brain adjacent to the tumor, nuclear staining with DAPI that, by a dense package of nuclei, indicates the tumor area, was also confirmed using an antibody specific for human nuclei. As demonstrated in Figure 12 for the group of XVir-N-31 treated mice (refer to Figure 11), in the tumor area the nuclei of U87MG glioma cells as well as those of human CD45$^+$ cells were clearly detectable by staining for human nuclei as well as by DAPI, whereas in the healthy mouse tissue adjacent to the tumor only nuclei of human CD45$^+$ immune cells were detected (red staining for human nuclei and green staining for human CD45). This allows us to clearly identify the tumor area and to distinguish it from the healthy adjacent brain.

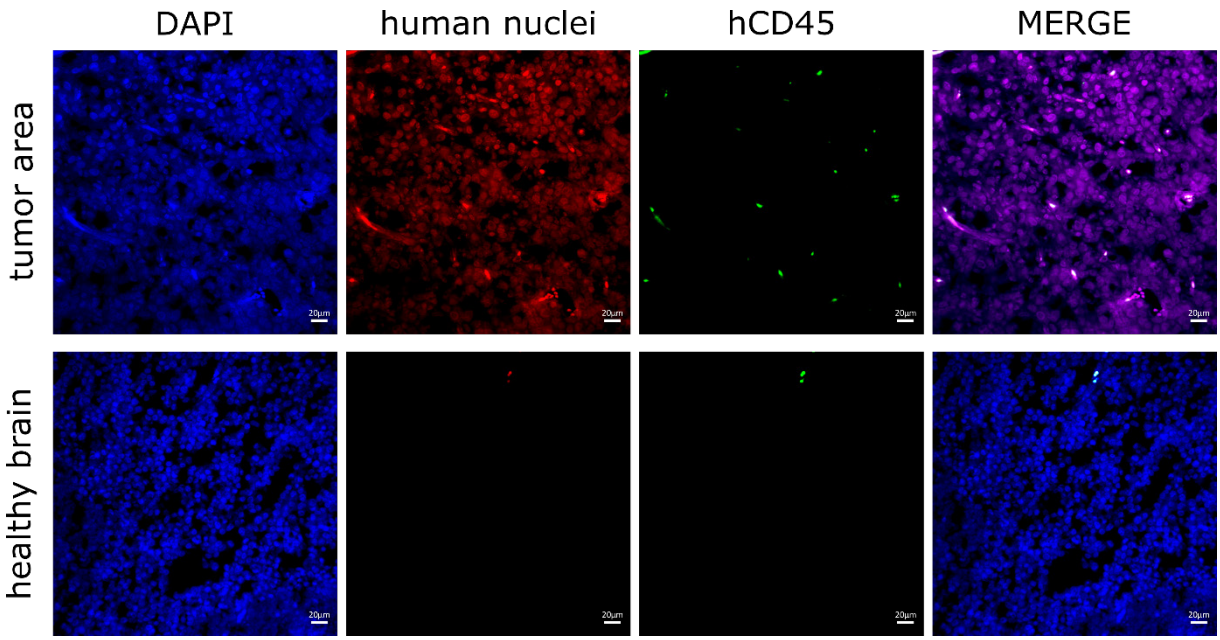

Figure 12. Representative fluorescence staining of human cells in the mouse brain. After implantation of U87MG tumors into the striata of NSG mice, PBMC engraftment and intratumoral injection of XVir-N-31, human CD45$^+$ immune cells (green) were detected predominantly in the tumor area (indicated by human nuclei staining (red) and human CD45 (green); ipsilateral tumors are shown). Only very few human nuclei positive cells were detected in the adjacent healthy brain, and in this area human nuclei staining co-localized with the hCD45 staining. The number of hCD45$^+$ cells in the healthy brain was not further analyzed (representative pictures depicted from the XVir-N-31 group of animals).

In GBM patients the concomitant treatment with Nivolumab additional to standard therapy was already shown to be not effective (Reardon, Brandes et al. 2020). To confirm this and to investigate the impact of Nivolumab in our animal model, a preliminary experiment was performed in an immuno-humanized mouse cohort harboring U87MG glioma. These mice received systemic applications of Nivolumab whereas two additional control cohorts were intratumorally injected with either XVir-N-31 or PBS (for treatment scheme refer to Figure 11). ICD in the tumor area was determined by staining for HSP70 and HMGB1. After Nivolumab monotherapy no HSP70 staining was found and only weak HMGB1 staining was observed (Figure 13A, B; stainings were performed by Jakob Rüttinger under my direct supervision). Besides that, immune cell infiltration in the tumor areas was determined by fluorescence staining. While XVir-N-31 treated mice showed significantly more human CD45$^+$ immune cell infiltration in ipsilateral virus-injected as well as in contralateral untreated tumors, like PBS also Nivolumab monotherapy failed to increase the number of human CD45$^+$ TILs (Figure 13C). Consistently with the minor induction of ICD and the low number of TILs by Nivolumab, in the Nivolumab cohort of mice large tumors of the same size as in the sham cohort were detected, whilst in XVir-N-31 treated animals the tumor size was significantly smaller, at least that of ipsilateral tumors (Figure 13D). Taken together, at least in the mouse model used in this study the systemic application of Nivolumab as a monotherapy does not have a significant influence on the induction of ICD and on lymphocyte infiltration into the tumor area.

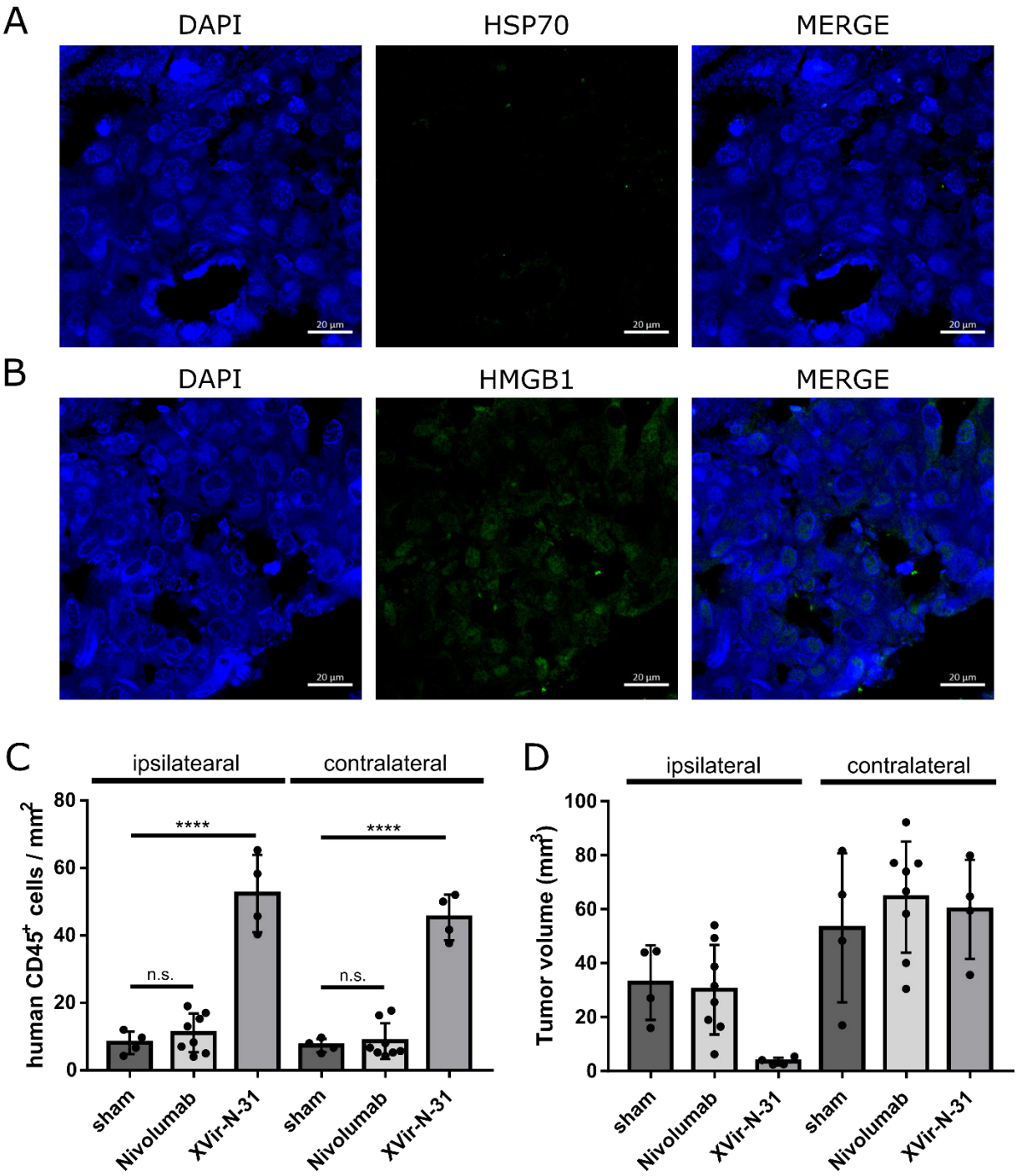

Figure 13. Nivolumab monotherapy has no therapeutic effect in an immuno-humanized glioma mouse model. U87MG bearing mice received four intraperitoneal injections of Nivolumab (200µg/injection) as indicated in the methods part and in Figure 11. Immunofluorescence staining for HSP70 (**A**), and HMGB1 (**B**), representative pictures are shown. Number of human CD45$^+$ TILs in ipsi- and contralateral tumors (**C**) as well as the tumor volume (**D**) were measured (n= 8 mice in the Nivolumab group, n= 4 mice in control groups, SEM; **** p<0.0001).

3.4.3 XVir-N-31 and XVir-N-31-anti-PD-L1 based OVT induce DAMPs *in vivo*

On the one hand Nivolumab monotherapy resulted in a very low presence of DAMPs in the tumor area, suggesting an insufficient induction of ICD. On the other hand, it was shown before by several other groups and for different OVs like vesicular stomatitis virus (VSV) or herpes simplex virus (HSV), that OVs mainly induce ICD rather than immunogenic silent apoptosis (Takasu, Masui et al. 2016, Melzer, Lopez-Martinez et al. 2017). Since our *in vitro* results demonstrated that XVir-N-31 induced ICD, we were further interested whether this is the case also *in vivo*. To evaluate if there is only locally restricted ICD in virus-injected tumors or whether signs of ICD will be observed also in contralateral tumors located far away from the virus injection side, we performed the experimental setup and treatment regime presented in Figure 11, using mice harboring ipsilateral virus- or sham-injected and contralateral untreated PD-L1-expressing U87MG glioma.

After harvesting the brains 35 days after treatment, we stained the tumors of all cohorts for the presence of the DAMPs HMGB1 (Figure 14) and HSP70 (Figure 15; stainings performed by Jakob Rüttinger under my direct supervision). No HMGB1 was found in tumors of sham treated controls (Figure 14A), not even after enlightment of the original photographs (Figure 14B). Interestingly, although HMGB1 release was found *in vitro* after the infection with dl309, this was not the case in the dl309 treated cohort of mice both in ipsilateral injected as well as in contralateral tumors. On the contrary, in all cohorts of mice that received an intratumoral injection with XVir-N-31 or XVir-N-31-anti-PD-L1, HMGB1 staining was visible and was even enhanced in those cohorts that received an additional ICI (XVir-N-31 + Nivolumab and XVir-N-31-anti-PD-L1). Remarkably, the positive staining for HMGB1 in these cohorts of mice was not restricted to injected, but was also found in contralateral tumors. Comparable results were found for HSP70 (Figure 15A), although only weaker staining was detected. Nevertheless, especially after enlightment of the original photographs (Figure 15B), HSP70 staining was observed not only in all XVir-N-31 or XVir-N-31-anti-PD-L1 injected but also in contralateral tumors. Together, this indicates both OAVs induced the expression of HMGB1 and HSP70 not only locally in virus-injected tumors, but also in the contralateral tumors that are located far away from the injection site, while dl309 does not. Additionally, the amount of detectable DAMPs was elevated by the combination of OVT with the blockade of the PD-1/PD-L1 axis.

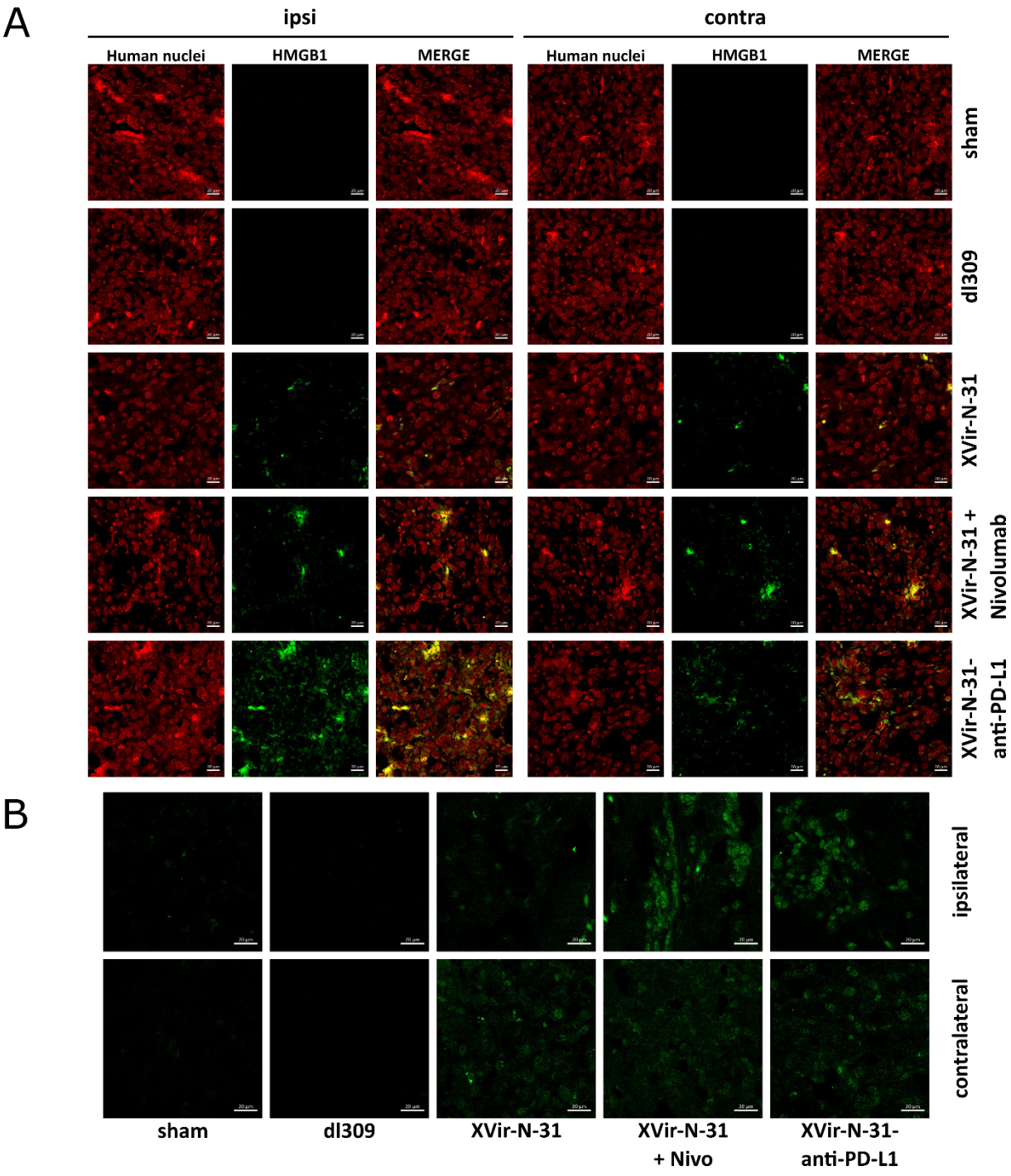

Figure 14. Induction of HMGB1 by XVir-N-31 and XVir-N-31-anti-PD-L1 *in vivo*. A. Detection of HMGB1 (green) in ipsilateral virus-injected and contralateral non-treated U87MG tumors in immuno-humanized NSG mice 35 days after a single intratumoral injection of either PBS (sham), 3 x 10^8 IFU of either dl309, of XVir-N-31 alone or in combination with multiple intraperitoneal injections of Nivolumab, or of XVir-N-31-anti-PD-L1 (n = 8 mice per group; representative pictures are shown). The staining of human nuclei (red) indicates the tumor area. **B.** Enlightment of HMGB1 staining as indicated in A.

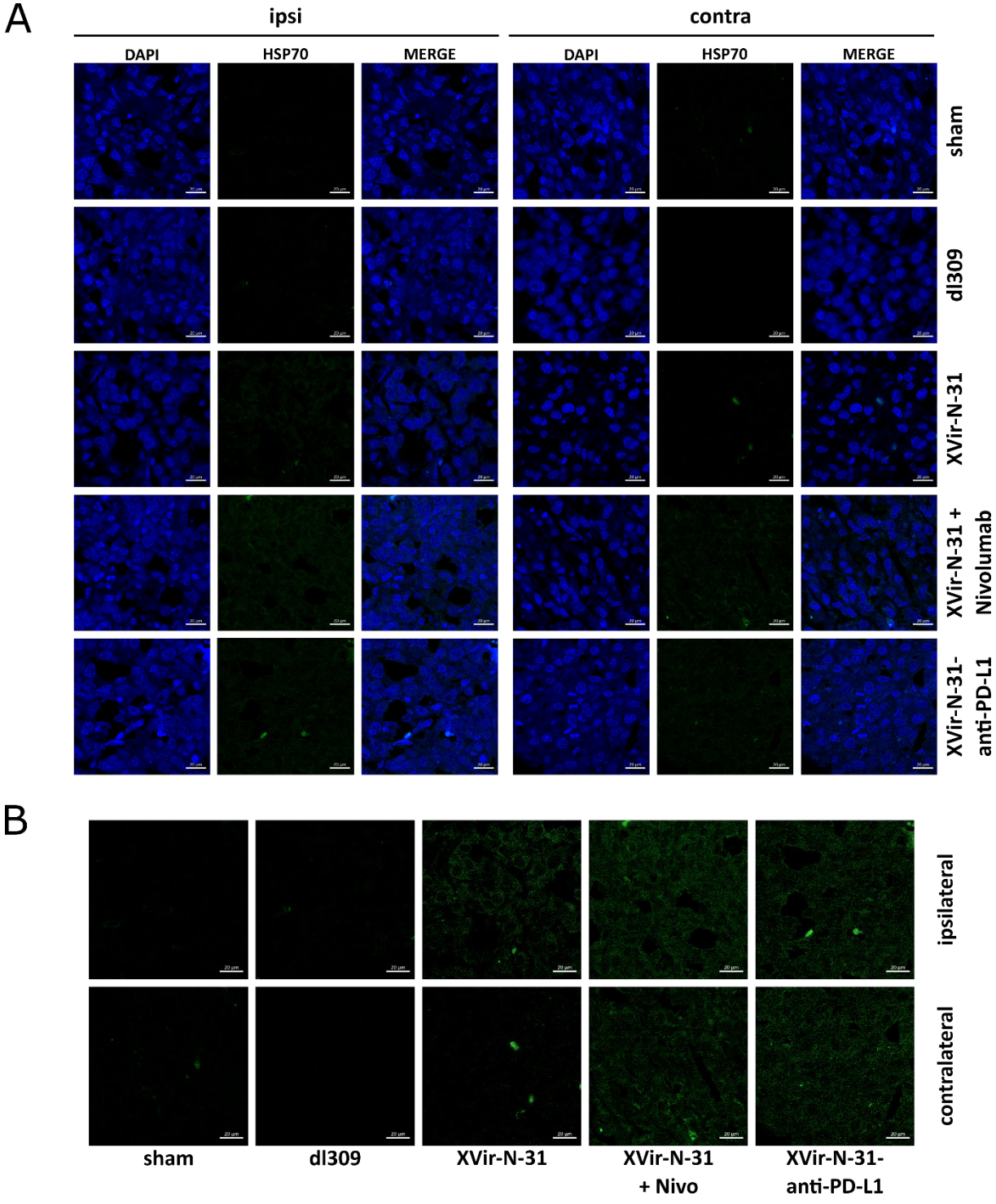

Figure 15. Induction of HSP70 by XVir-N-31 and XVir-N-31-anti-PD-L1 *in vivo*. A. Detection of HSP70 (green) in ipsilateral virus-injected and contralateral non-treated U87MG tumors in immuno-humanized NSG mice 35 days after a single intratumoral injection of either PBS (sham), 3 x 10^8 IFU of either dl309, of XVir-N-31 alone or in combination with multiple intraperitoneal injections of Nivolumab, or of XVir-N-31-anti-PD-L1 (n = 8 mice per group; representative pictures are shown). **B.** Enlightment of HSP70 staining as indicated in A.

3.4.4 Determination of virus replication in ipsi- and contralateral tumors

An elevated level of DAMPs was not exclusively found in virus-injected tumors, but also in contralateral untreated tumors. Viral replication is restricted only to the injected tumor area and can't occur in the adjacent tissue around. Nevertheless, a spreading of infectious virus particles over the brain during virus injection, or later on from infected tumor cells around the injection site via the cerebrospinal fluid, might occur. This spreading might subsequently lead to virus replication also in contralateral tumors which then might induce the above described observed immunostimulatory, abscopal effects in these non-virus-injected tumors. To examine this, both ipsi- and contralateral U87MG tumors were analyzed on the presence of adenovirus particles by staining for the adenoviral hexon protein. While in the sham treated cohort of mice no hexon was found in any tumor area (ipsi- and contralateral), all virus-injected cohorts clearly showed hexon staining in virus-injected (ipsilateral) tumors at day 35, the time point we finalized the experiment (Figure 16). In contrast, in contralaterally located, untreated tumors, no hexon staining was observed, neither in the dl309, XVir-N-31 nor XVir-N-31-anti-PD-L1 injected cohorts of mice.

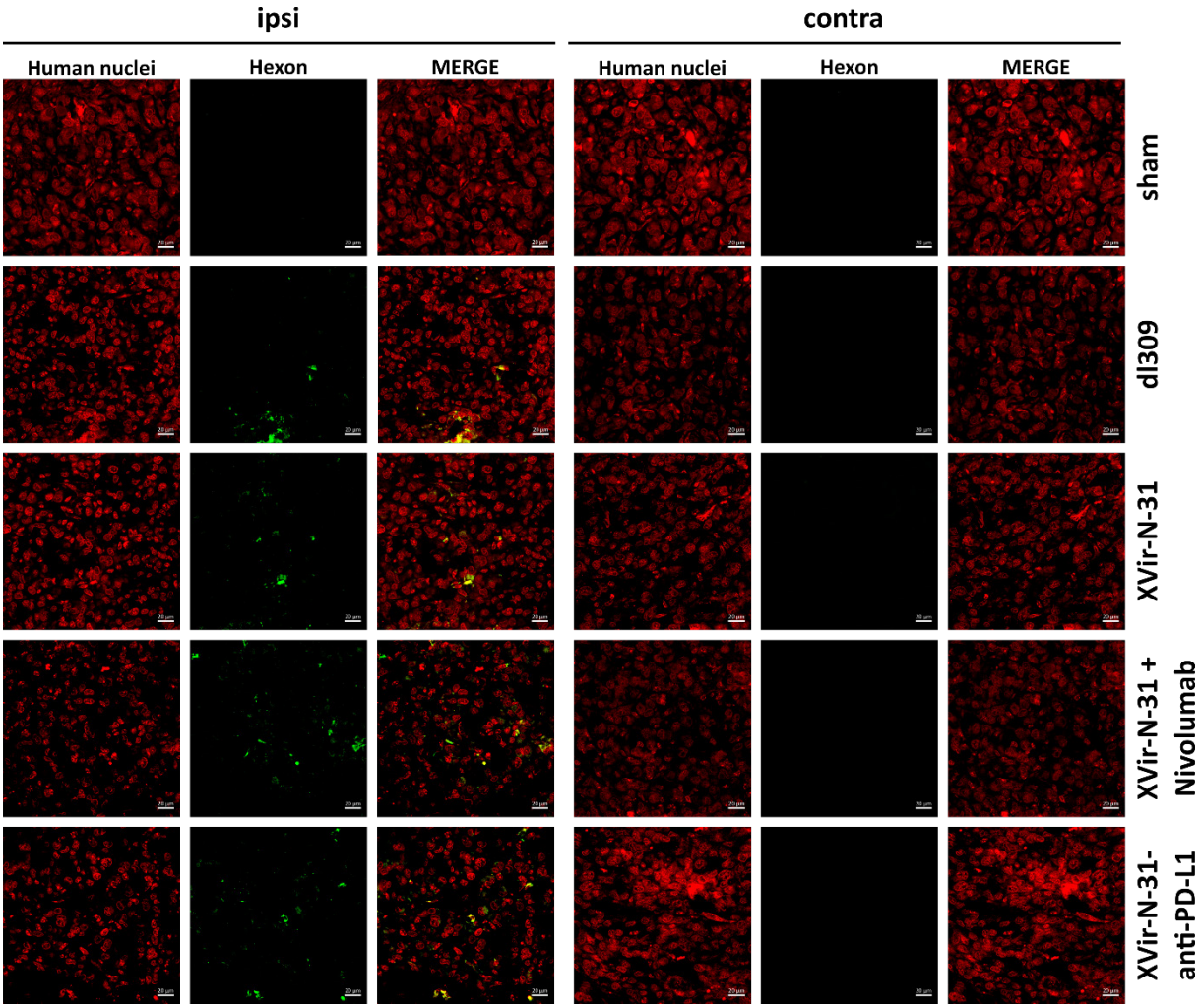

Figure 16. Hexon staining of ipsilateral virus-injected and contralateral untreated tumors. Detection of the adenoviral hexon protein (green) in ipsilateral virus-injected and contralateral non-treated U87MG tumors in immuno-humanized NSG mice 35 days after a single intratumoral injection of either PBS (sham), 3 x 10^8 IFU of either dl309, of XVir-N-31 alone or in combination with multiple intraperitoneal injections of Nivolumab, or of XVir-N-31-anti-PD-L1 (n = 8 mice per group; representative pictures are shown). The staining of human nuclei (red) indicates the tumor area.

3.4.5 XVir-N-31 and XVir-N-31-anti-PD-L1 induce the infiltration of immune cells into the tumor area

It was shown for a variety of different OVs that an OV-mediated lysis of tumor cells can induce a potent antitumoral immune response and an infiltration of immune cells into the tumor area (Kiyokawa and Wakimoto 2019, Alayo, Ito et al. 2020, Saha and Rabkin 2020). Additionally, it was found that therapeutic effects mediated by OVs could be supported and even enhanced by an additional treatment with ICIs. The application of anti-PD-L1, anti-PD-1 or anti-CTLA4 antibodies have been shown to be effective and beneficial if used in the combination with different OVs (for detail, see 1.2.4 and (Hardcastle, Mills et al. 2017, Saha, Martuza et al. 2018)). By this background we were interested whether XVir-N-31 and XVir-N-31-anti-PD-L1 were able to induce the infiltration of immune cells into the tumor area and whether this might be enhanced by an additional blockade of the PD-1/PD-L1 axis. To evaluate if there is only a locally increased infiltration of lymphocytes in virus-injected tumors or whether an elevated number of TILs will be observed also in contralateral tumors, we used tissue from the same experiment as for the DAMP stainings (described in the chapters above). Figure 17A and Suppl. Figures 2 and 3 show representative pictures of the different immune cell populations that were investigated. The quantification of TIL subclasses in the tumor area is presented in Figure 17B-H. Focusing on the general population of human immune cells ($CD45^+$), it was found that, compared to the sham treatment, dl309 injection led to a significant but relatively small increase of $CD45^+$ TILs in ipsi- and contralateral tumors (Figure 17B). On the contrary, all cohorts treated with XVir-N-31 showed an approximately at least 4-fold higher number of $CD45^+$ TILs in ipsilateral virus-injected as well as in contralateral untreated tumors. The combination of OVT with the blockade of the PD-1/PD-L1 axis (either by the locally restricted expression of anti-PD-L1 coded by XVir-N-31-anti-PD-L1, or by repeated intraperitoneal injections of Nivolumab, refer to Figure 11) further enhanced the number of $CD45^+$ cells in ipsilateral tumors in the XVir-N-31-anti-PD-L1 cohort and in contralateral tumors in the XVir-N-31 plus Nivolumab and XVir-N-31-anti-PD-L1 cohorts.

Since the strongest cellular immune responses and a specific tumor cell killing is often mediated by $CD3^+$ T cells and especially by $CD3^+/CD8^+$ CTLs, we further investigated the subpopulations of TILs. In all cohorts approximately 75 % of infiltrating $CD45^+$ immune cells were $CD3^+$ T cells with the relative ratio resembling the prior population quite well. Compared to XVir-N-31 the combination of XVir-N-31 plus Nivolumab further increased the $CD3^+$ cell count in ipsilateral tumors (Figure 17C). The majority of TILs were found to be $CD8^+$ CTLs (Figure 17D). Interestingly, probably due to its known immunosuppressive activity, dl309 did not induce $CD8^+$ cell infiltration into the tumor. The number of $CD8^+$ TILs in XVir-N-31 as well as in XVir-N-31 plus Nivolumab cohorts was approximately 10-fold higher in both ipsi- and in contralateral tumors when compared to dl309 and sham cohorts. The amount of $CD8^+$ TILs was further elevated by blocking the PD-1/PD-L1 axis, with significantly more $CD8^+$ TILs in both ipsi- and contralateral tumors in the XVir-N-31-anti-PD-L1 cohort.

Compared to the sham cohort, in the dl309 cohort the number of $CD4^+$ TILs was significantly elevated in both, ipsi- and contralateral tumors. However, in the XVir-N-31 or XVir-N-31-anti-PD-L1 treated cohorts significantly more $CD4^+$ TILs (approximately one third of all $CD3^+$ TILs) were detected than in the dl309 cohort (Figure 17E).

The strong immunostimulatory potential of an XVir-N-31 based OVT is also reflected by the activation status of TILs. Only activated T cells, in this study identified by the expression of

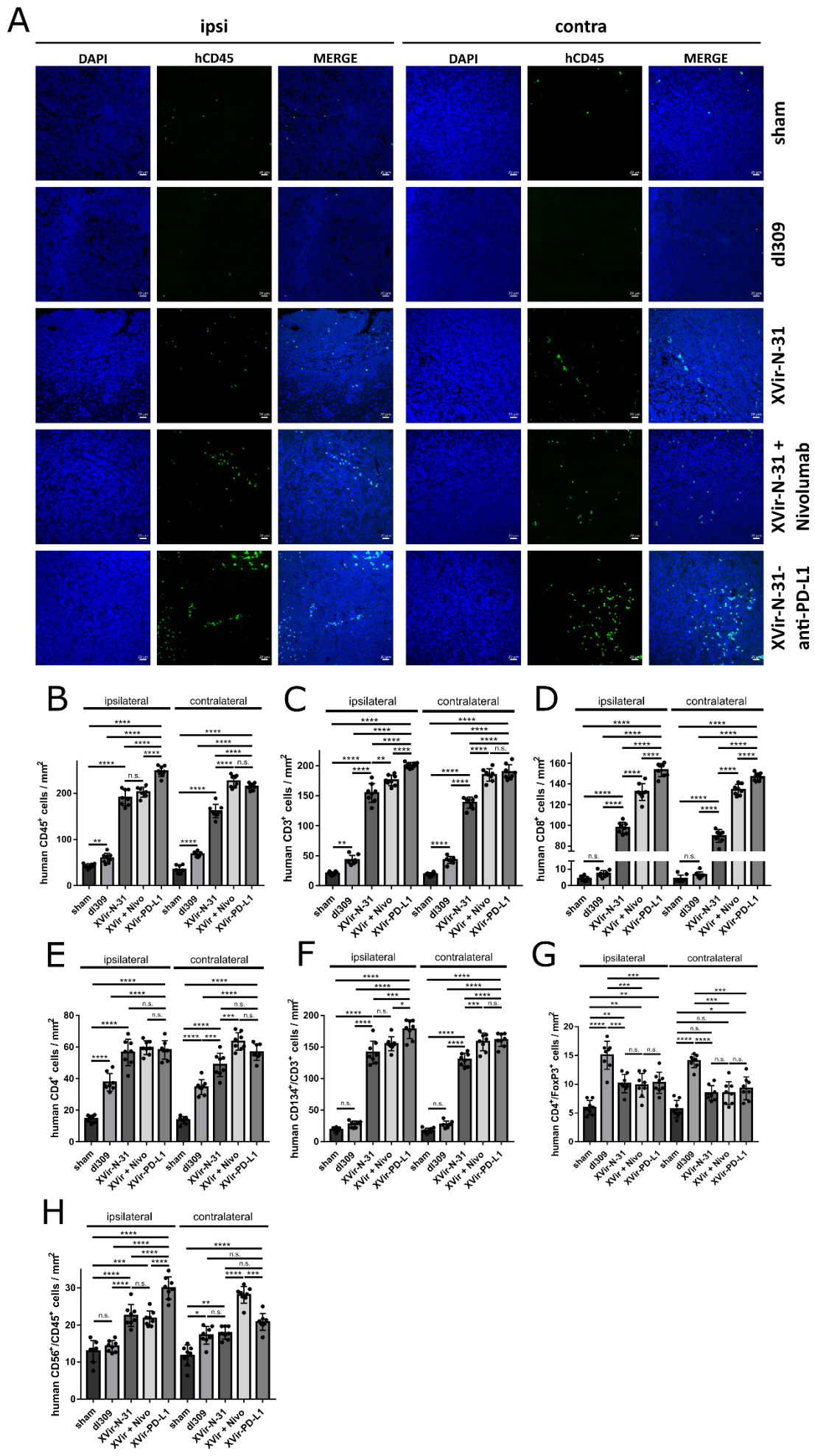
A
ipsi
contra
DAPI
hCD45
MERGE
sham
dl309
XVir-N-31
XVir-N-31 + Nivolumab
XVir-N-31-anti-PD-L1
B
human CD45+ cells / mm2
C
human CD3+ cells / mm2
D
human CD8+ cells / mm2
E
human CD4+ cells / mm2
F
human CD134+/CD3+ cells / mm2
G
human CD4+/FoxP3+ cells / mm2
H
human CD56+/CD45+ cells / mm2
ipsilateral
contralateral
sham
dl309
XVir-N-31
XVir + Nivo
XVir-PD-L1

Figure 17. Intratumoral immune cell invasion. A. Representative immunofluorescence pictures of human immune cell infiltration into U87MG tumors in immuno-humanized NSG mice. Brain sections were stained with DAPI (blue) and anti-human CD45 (green). Pictures were taken 35 days after treatment (refer to Figure 11). **B-H**. Quantification of different immune cell subtypes per mm^2 in GBMs located in the ipsi- or contralateral hemisphere (**B**: human $CD45^+$ cells; **C**: human $CD3^+$ T cells; **D**: human $CD8^+$ cytotoxic T cells; **E**: human $CD4^+$ T helper cells; **F**: human $CD3^+$ T cells expressing the activation marker CD134; **G**: human $CD4^+/FoxP3^+$ regulatory T cells; **H**: human $CD56^+/CD45^+$ NK cells). (XVir-PD-L1: XVir-N-31-anti-PD-L1; n=8 tumors and 5 slices per tumor were analyzed; SEM; ns: not significant; * $p < 0.05$; ** $p < 0.01$, *** $p < 0.001$, **** $p < 0.0001$).

CD134/OX40, are capable of an effective anti-tumor response, while exhausted T cells can even benefit tumor growth. In line with the previous findings, in the cohorts of mice that were injected with XVir-N-31 or XVir-N-31-anti-PD-L1, almost all $CD3^+$ TILs expressed CD134 (Figure 17F). On the contrary, but also in conclusion with its known immuno-suppressive features, in the dl309 cohort CD134 was only expressed on a very small proportion of $CD3^+$ cells. Additionally, in this cohort the number of $FoxP3^+$ T_{regs}, responsible for the suppression of an effective immune response, was significantly higher compared to all other treatment groups (Figure 17G). Even though the number of $FoxP3^+$ cells was slightly elevated in mice treated with XVir-N-31 or XVir-N-31-anti-PD-L1, these cells account for only 5-6 % of all $CD3^+$ cells.

Finally, the impact of an XVir-N-31 based OVT on the infiltration of NK cells as major players and first line defense cells of the innate immune system, was analyzed. In contrast to dl309 injected mice, which showed no (ipsilateral) or an only slightly increased (contralateral) numbers of $CD56^+$ NK cells, XVir-N-31 and XVir-N-31-anti-PD-L1 injected mice showed significantly more NK cells in ipsi- and contralateral tumors (Figure 17H). The only moderate increase in the NK cell count after OVT, compared to the strong increase of $CD3^+$ TILs, indicate that the XVir-N-31 based OVT induce an anti-tumor immune response mainly by cells of the adaptive and only to a lesser amount by cells of the innate immune system. Overall, it was found that XVir-N-31 is able to induce a strong cellular immune response not only locally in virus-injected tumors, but in our mouse model also in tumors that are located far away from the injection side, this mimicking invaded glioma cells. Furthermore, an additional blockade of the PD-1/PD-L1 axis (provided either by Nivolumab or XVir-N-31-anti-PD-L1) increased TIL numbers in the tumor area even further.

3.4.6 XVir-N-31 in a combination with Nivolumab, or XVir-N-31-anti-PD-L1 show an abscopal effect in the reduction of tumor growth

It is frequently discussed that an effective immune response might be a key component for the successful treatment of GBM. Turning the immunosuppressive TME into a “hot”, immunogenic state seems to be extremely beneficial and was already found effective in several cancer entities (Jackson, Choi et al. 2019). Nevertheless, the other important parameter a promising treatment must fulfil, is the effective tumor cell killing and the reduction of the tumor mass. For OVT, this task might be achieved either by the direct lysis of the tumor cells due to viral replication or via tumor cell killing by activated, tumor specific TILs. Therefore, we were finally interested whether an XVir-N-31 based OVT might reduce or delay tumor growth and whether there is a further reduction in tumor growth when blocking the interaction of PD-1 and PD-L1

in addition. While we showed before that Nivolumab monotherapy had no effect on the growth of U87MG tumors (Figure 13D), in this experiment we focused on the same groups and followed the same treatment regime as in the previous experiment (see 3.4.3 and Figure 11). As shown in Figure 18, sham treated control mice showed extremely large tumors in both hemispheres. All virus injected ipsilateral tumors showed a massive size reduction, independently whether a tumor specific OVT (XVir-N-31, XVir-N-31-anti-PD-L1) or an unspecific adenovirus (dl309) was injected. Additionally, no further reduction was observed in ipsilateral tumor by blocking the PD-1/PD-L1 interaction (XVir-N-31 + Nivolumab, XVir-N-31-

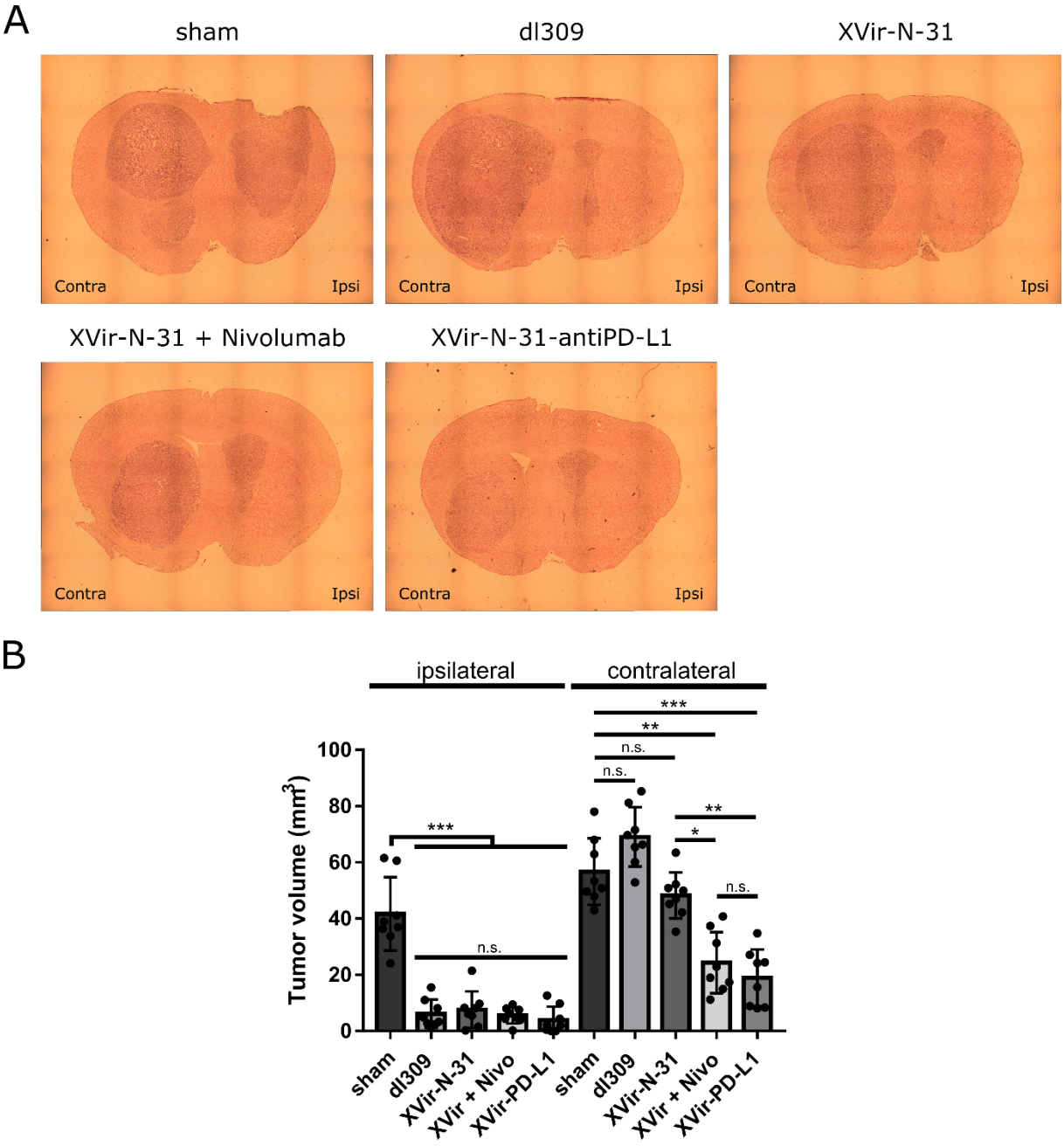

Figure 18. Reduction of tumor growth after OAV injection. A. Representative pictures of brain sections of U87MG tumor bearing, immuno-humanized NSG mice. The ipsilaterally growing tumor was injected with either PBS (sham), $3*10^8$ IFU dl309, XVir-N-31, or XVir-N-31-anti-PD-L1. One group additionally received repeated systemic injections with Nivolumab as indicated in the methods part and Figure 11. **B.** Quantification of the tumor volume (mm^3; XVir-PD-L1: XVir-N-31-anti-PD-L1; n = 8 mice per group, SEM; * p<0.05, ** p< 0.01, *** p<0.001).

anti-PD-L1). This indicates that in ipsilateral tumors the lytic effect mediated by the viruses was sufficient to kill the tumor cells and to reduce the tumor mass.

However, the situation of contralateral tumors was completely different. Contralateral tumors of dl309 and XVir-N-31 treated mice were approximately as big as those of sham treated animals. Interestingly, in the cohorts of mice that received an intratumoral injection of XVir-N-31-anti-PD-L1 into the ipsilateral tumor, or that were ipsilaterally tumor-injected with XVir-N-31 and received Nivolumab in addition, a significantly reduced size of contralateral tumors was visible. This abscopal effect, most likely induced by the previously shown increased infiltration of immune cells, suggests that an XVir-N-31 based OVT in combination with the blockade of the PD-1/PD-L1 axis might show compelling benefits for the treatment of PD-L1 expressing GBM, at least in our animal model.

3.4.7 Enhanced XVir-N-31-anti-PD-L1 mediated immune cell infiltration is dependent on the PD-L1 status of tumors

The results obtained in our immuno-humanized mouse glioma model harboring U87MG PD-L1 positive tumors showed a clear benefit by the treatment with XVir-N-31 or XVir-N-31-anti-PD-L1. Besides the strongly enhanced immune cell infiltration mediated by XVir-N-31, mice intratumorally injected with XVir-N-31-anti-PD-L1 showed even higher TIL numbers in ipsi- as well as in contralateral tumors. Although it was shown that the majority of GBM cells, especially cells of the most malignant mesenchymal subtype, carry PD-L1 on their cell surface, also subpopulations and subtypes of glioblastoma exist that lack the expression of these molecules (Wang, Zhang et al. 2016). To analyze the impact of XVir-N-31-anti-PD-L1 *in vivo* in PD-L1 negative gliomas, we used immuno-humanized NSG mice harboring LN-229 tumors and the treatment regime indicted in Figure 11. LN-229 glioma cells express almost no PD-L1 on their surface (Figure 8). In contrast to the U87MG mouse experiment, this experiment contains only three cohorts: (i) intratumoral injection of PBS into the right sided tumor (sham), (ii) intratumoral right sided tumor injection of XVir-N-31, or (iii) intratumoral right sided tumor injection of XVir-N-31-anti-PD-L1. Immune cell infiltration, especially those of T cells, the most prominent TIL population in the previous U87MG animal experiment, was as before investigated in both, ipsilateral injected as well as in contralateral tumors. In accordance with the previous findings, sham control mice showed only small numbers of human $CD45^+$ TILs in ipsi- and contralateral tumors (Figure 19). Both OAVs increased these cell numbers significantly compared to animals of the sham cohort, both in the ipsi- and contralateral tumors. This indicates an immuno-stimulatory effect of the XVir-N-31 based OVT also in mice bearing PD-L1 negative GBM. Nonetheless, in LN-229 GBM mice XVir-N-31-anti-PD-L1 failed to enhance the number of tumor infiltrating immune cells ($CD45^+$) and of $CD3^+$ T cells compared to XVir-N-31 treated cohort. Still, the ratio was in line with the U87MG experiment, showing approximately 75 % of all TILs being $CD3^+$ T cells (Figure 19B) and a further distribution of two thirds $CD8^+$ CTLs (Figure 19C) and one third $CD4^+$ T helper cells (Figure 19D). Nevertheless, TIL numbers were significantly more abundant in ipsi- as well as in contralateral tumors if the mice received an intratumoral injection of XVir-N-31 or XVir-N-31-anti-PD-L1. Overall, these results point out that $PD\text{-}L1^{neg}$ GBM treated with XVir-N-31 or XVir-N-31-anti-PD-L1 show a significantly enhanced immune cell infiltration in the tumor area of both, virus-injected and untreated contralateral located tumors. However, the additional benefit on immune cell infiltration by

blocking the PD-1/PD-L1 interaction we observed for PD-L1-positive GBM was absent in LN-229 PD-L1 negative GBM.

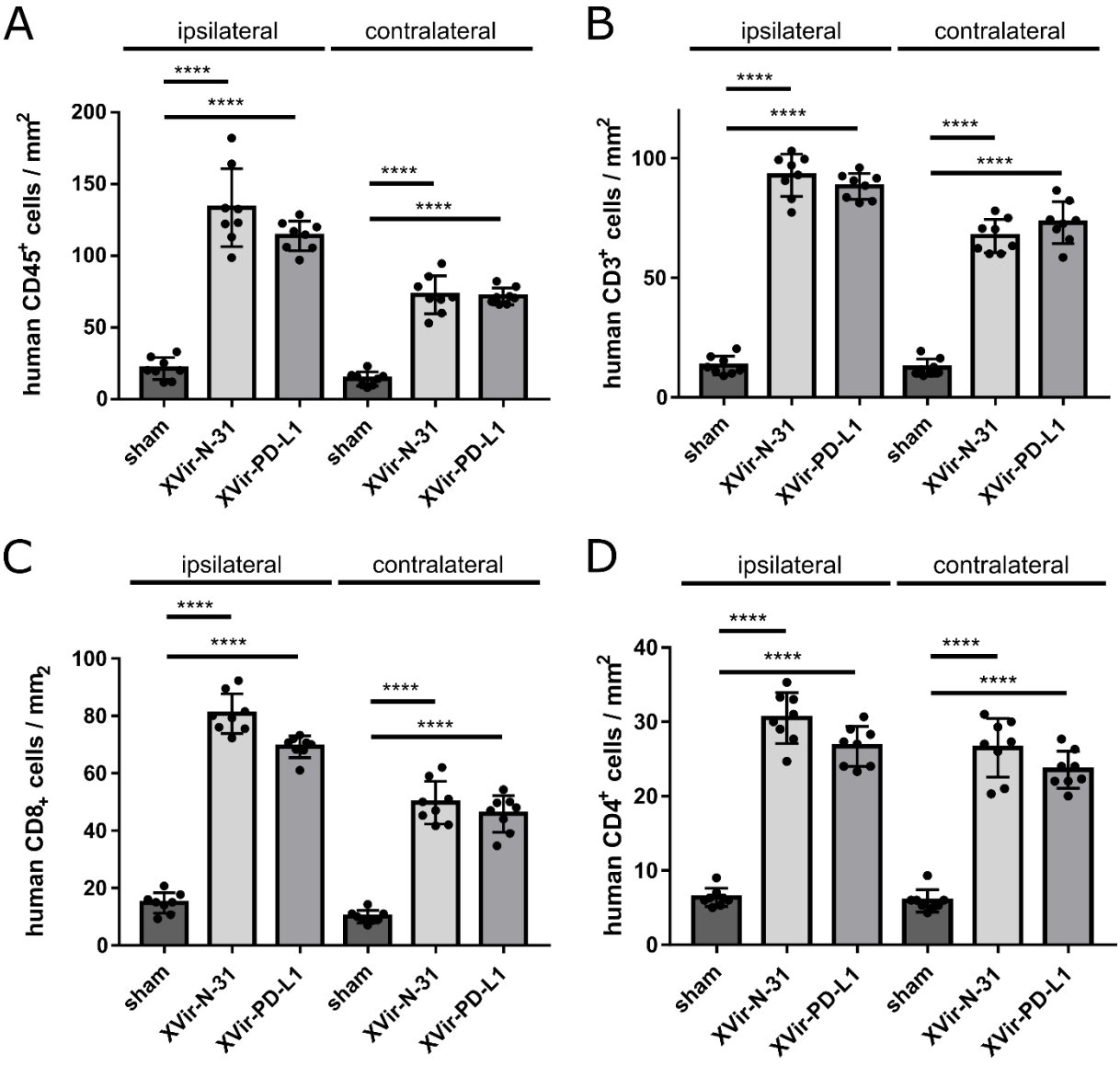

Figure 19. Intratumoral immune cell invasion in LN-229 GBM bearing mice. A-D. Quantification of the infiltration of different immune cells per mm^2 in the ipsilateral injected as well as in the contralateral tumors of LN-229 bearing mice 35 days after treatment (refer to Figure 11). **A**: $CD45^+$ TILs, **B**: $CD3^+$ TILs, **C**: $CD8^+$ TILs, **D**: $CD4^+$ TILs (XVir-PD-L1: XVir-N-31-anti-PD-L1; n=8 tumors and 5 slices per tumor were analyzed; SEM; ns: not significant; * $p < 0.05$, ** $p < 0.01$, *** $p < 0.001$, **** $p < 0.0001$).

4. Discussion

GBM is a devastating disease with so far no cure and is therefore obligatory lethal. Despite best multimodal available therapy, its prognosis is extremely poor and the mOS is still less than 20 months (Stupp, Taillibert et al. 2017). Thus, new therapeutic strategies are urgently needed. OVT is a promising approach to treat GBM and has proven to be potent already in different preclinical models (Fueyo, Gomez-Manzano et al. 2000, Geoerger, Grill et al. 2002). Research of the last decade has revealed that aside of direct tumor oncolysis, especially the immunostimulatory effects of OVs were underestimated. This is an important issue since the induction of a long-lasting immune response is fundamental for a successful treatment of GBM (Zamarin, Holmgaard et al. 2014, Andtbacka, Kaufman et al. 2015). OAVs show several advantages for an effective cancer treatment, including their large packaging capacity and capability of triggering a potent immune response (Gujar, Pol et al. 2018). Nevertheless, a fundamental understanding of the virus-mediated processes leading to an anti-tumor immune response including their influence on and the characterization of the specific cell death induced by OAVs is still missing. Viral replication, oncolysis and the mode of cell death induced by OAVs is dependent on the OAV's specific characteristics. Furthermore, the characteristics of the neoplastic cells and tissue should be considered in advance of the treatment of the tumor with OVs. ICD, which is primarily induced in OAV infected tumor cells, is mainly responsible for the activation of the immune system. It has been shown to be a fundamental key feature to prime and activate the cellular immune response against the tumor (Ma, Ramachandran et al. 2020). With this, the primary therapeutic effect of an OVT is on the one hand the direct virus-mediated cell lysis that occurs during virus replication (oncolysis). On the other hand, the therapeutic effect is expanded by a secondary OAV mediated anti-tumor directed effect evoked by the activation of an anti-tumoral immune response. This secondary effect is highly important since by this even brain infiltrating glioma cells located far away from the virus-treated original tumor will be targeted and eradicated by immune cells.

The aim of this study was to elucidate the impact of the YB-1 dependent OAV XVir-N-31 in the treatment of GBM, with a special focus on its immunostimulatory effects and its benefit for the treatment. XVir-N-31 has been proven to be effective and efficient against GBM cells *in vitro* and *in vivo* (Holzmüller, Mantwill et al. 2011, Mantwill, Naumann et al. 2013), but was so far not analyzed for its immunostimulatory effects in GBM. Additionally, the impact of an XVir-N-31 based OVT in combination with the inhibition of the PD-1/PD-L1 interaction was examined. For this, GBM bearing mice received an OVT using XVir-N-31 in combination with Nivolumab or an XVir-N-31-anti-PD-L1-based OVT, the latter virus being a derivate of XVir-N-31 that codes for a single chain PD-L1 neutralizing antibody.

4.1 XVir-N-31 provides lesser lytic activity than dl309

Due to the high expression of nuclear YB-1 in glioma cells and especially in high grade and recurrent glioma, XVir-N-31 and XVir-N-31-anti-PD-L1 replicate efficiently in GBM cells, this leading to oncolysis (Figure 6). In dl309, being nearly identical to wild type adenovirus, cell lysis is not limited to tumor cells. Whilst the replication deficient adenovirus Ad-NULL, lacking the E1 gene, showed as expected no oncolysis of neither U87MG nor LN-229 cells, infection

of GBM cells with dl309 at low MOI (10-30 MOI) induced strong lysis, especially in U87MG cells (Figure 6B). This might be due to the expression of the E1A13 and ADP genes in the E3 region of dl309, which account to its rapid and successful replication and lytic activity. A deletion in the E3B region in dl309 which distinguishes it from wild type adenovirus, provides its higher cytopathogenicity (Hawkins and Hermiston 2001, Hibma, Real et al. 2009). XVir-N-31 and XVir-N-31-anti-PD-L1 on the other hand, are lacking the E1A13S protein and are therefore dependent on the activation of the E2 late promoter by the nuclear localization of cellular YB-1. Both viruses showed a comparable and MOI dependent, but significantly lower lytic activity than dl309, with an IC_{50} of approximately 30-50 MOI 48 h after infection. Interestingly, XVir-N-31-anti-PD-L1 infection resulted in, dependent on the MOI, almost the same or a slightly reduced cytopathic effect (CPE) compared to XVir-N-31. On a first view this was an unexpected finding since XVir-N-31 lacks the complete E3 region and therefore the adenoviral ADP protein located within that region, whereas XVir-N-31-anti-PD-L1 only lacks the E319K protein but expresses all other adenoviral proteins of the E3 region. Whilst ADP is usually responsible for a more rapid cell lysis (Tollefson, Ryerse et al. 1996), it could be expected that its presence in XVir-N-31-anti-PD-L1 would enhance the viral lytic activity compared to XVir-N-31. Nevertheless, it was shown that the enhanced lytic activity by ADP is mediated by the enhanced induction of apoptosis under control of the E1A proteins (Yun, Kim et al. 2005). As XVir-N-31 and XVir-N-31-anti-PD-L1 lack the immunosuppressive genes E1A13S, E319K and E1B19K, the whole modus of cell death is shifted from apoptosis to ICD (see 3.3 et seqq.; discussed in detail in the following chapter). This suggests that for both OAVs the efficacy of the lytic activity is conducted by (i) the lower reproduction due to the lack of E1A13S, together with (ii) the induction of ICD rather than apoptosis, leaving the expression of ADP of minor importance.

4.2 XVir-N-31 and XVir-N-31-anti-PD-L1 boost the immune response in GBM

In contrast to other cancers like melanoma or squamous cell carcinoma, which present high immunogenicity and a good therapeutic outcome after OVT (Wang, He et al. 2019, Esaki, Goshima et al. 2020), GBMs are highly immunosuppressive and extremely low immunogenic tumors (Pearson, Cuzzubbo et al. 2020). One cause of immunosuppression is the high expression of PD-L1 by glioma cells and cells of the TME. PD-L1 is expressed by the majority of GBMs, especially by the most malignant mesenchymal subtype. However, due to the intratumoral heterogeneity of GBM, only a subpopulation of the tumor cells will express PD-L1 (Chen, Xu et al. 2019). Besides the inhibition of the T cell mediated immune response, PD-L1 expression is also associated with further immunosuppressive effects, e.g., an enhanced infiltration of TAMs and their repolarization to the immunosuppressive M2 phenotype (Zhu, Zhang et al. 2020). Therefore, an additional inhibition of the PD-1/PD-L1 interaction in combination with the XVir-N-31 based OVT might have a beneficial impact on GBM therapy. Recent studies have shown that the combination of virotherapy with ICIs such as anti-PD-1 are capable of overcoming the limitations of both monotherapies and can lead to therapeutic success (Ribas, Dummer et al. 2017, Bourgeois-Daigneault, Roy et al. 2018). In this regard we hypothesize that XVir-N-31-anti-PD-L1 will fulfill several purposes by (i) oncolysis of GBM cells, by (ii) inducing ICD and subsequently an anti-tumoral immune response, along with (iii)

the local expression and secretion of an anti-PD-L1 neutralizing antibody. The locally restricted expression of anti-PD-L1 may thereby possibly minimize or even prevent unwanted adverse events as they have been described in clinical trials where ICIs have been applied systemically.

In the first experiments we demonstrated that the virus-coded single chain PD-L1 neutralizing antibody was secreted from infected cells and that it actively blocked the interaction of PD-1 with PD-L1 (Figure 7). The successful secretion of anti-PD-L1 by XVir-N-31-anti-PD-L1 infected cells is in line with recently described oncoviro-immuno-therapeutic (OVIT) approaches. For example, Dias *et al.* showed the secretion of an anti-CTLA-4 antibody from an OAV where, like in XVir-N-31-anti-PD-L1, the antibody coding sequence was also integrated into the E3 region (Dias, Hemminki et al. 2012).

Subsequently, we were interested in the primary immunostimulatory effects and immune responses provoked by XVir-N-31 and XVir-N-31-anti-PD-L1. It is known that viral infections induce the release of a plethora of immunogenic molecules and inflammatory cytokines, including IFNγ. We therefore examined the release of IFNγ from cocultures of "GBM-cell HLA A/B matched" PBMCs and OAV-infected GBM cells. Whilst infection of U87MG and LN-229 cells with XVir-N-31 increased the IFNγ concentration in these cocultures, a comparable IFNγ concentration was also observed after dl309 infection (Figure 10). This suggests that the primary immunostimulatory and pro-inflammatory boost mediated by the IFNγ release is more likely induced by a viral infection and putatively by a subsequent PAMP release during cell lysis than it is specific for OVs. In this regard the OAV mediated DAMP release and induction of ICD do not seem to play a significant role in the production of IFNγ. Interestingly, the infection of LN-229 cells with XVir-N-31-anti-PD-L1 resulted in a similar concentration of IFNγ in the supernatants of PBMC/LN-229-cocultures. Furthermore, in the above described cocultures the infection of PD-L1^{high} U87MG cells with XVir-N-31-anti-PD-L1 even increased IFNγ levels. It is not completely unraveled whether the source of this increased IFNγ release are glioma cells, cocultured PBMCs or both. Nevertheless, this demonstrates that the additional blockade of the PD-1/PD-L1 interaction, when combined with an adenovirus infection, provides a positive impact on the induction of a proinflammatory boost, at least in PD-L1 expressing GBM.

IFNγ release is one of the first characteristics of the immune response of cells after adenoviral infection and additionally it was shown that IFNγ does not only initiate elevated PD-L1 expression in GBM cells, but also in infiltrating immune cells (Wintterle, Schreiner et al. 2003, Qian, Wang et al. 2018). Therefore, the usage of XVir-N-31-anti-PD-L1 can always be considered for the OVT of GBM. Nevertheless, in further experiments also the amount of IFNγ produced by virus infected GBM cells alone should be measured and should be compared to IFNγ levels produced by cocultures of PBMCs and OAV-infected GBM cells. This would identify whether the increased release after XVir-N-31-anti-PD-L1 infection is caused by GBM cells or PBMCs.

4.3 XVir-N-31 and XVir-N-31-anti-PD-L1 induce ICD

To further investigate the mode of cell death induced by XVir-N-31 and XVir-N-31-anti-PD-L1, we analyzed the release and expression of molecules typical for ICD. HSP70 and HMGB1, intracellular multifunctional proteins, are typical DAMPs when released from cells. YB-1 is a

highly proinflammatory protein. It is involved in the regulation of multiple proliferation pathways, the regulation of angiogenesis and tumor induction and progression. When released from cells it becomes a highly immunogenic protein that is capable of inducing a T cell response in neuroblastoma (Zheng, Jing et al. 2009, Lasham, Print et al. 2012). Additionally, cell surface exposure of CRT is upregulated during ICD, serving as a typical “eat me” signal for immune cells.

In vitro, XVir-N-31 and XVir-N-31-anti-PD-L1 infection induced a significantly elevated release of HMGB1, HSP70 and YB-1 in both analyzed GBM cell lines when compared to dl309 (Figure 9). Compared to dl309, infection of GBM cells with OAVs additionally increased the cell surface exposure of CRT. This shows clearly that XVir-N-31 and XVir-N-31-anti-PD-L1 induce ICD, whereas dl309 does not. This is in line with the findings of Lichtenegger *et al.* in bladder cancer (Lichtenegger, Koll et al. 2019) and can be explained by the expression of the adenoviral E1A13S and E319K proteins. Both proteins are known to possess immunosuppressive functions and are present in dl309, but absent in XVir-N-31. The same is true for the apoptosis inducing protein ADP (located within the E3 region) which induces a more silent and less immunogenic cell death. Whilst E1A13S is known to antagonize the cGas-Sting pathway, crucial to trigger the innate immune system and the expression of inflammatory genes (Anghelina, Lam et al. 2016), E319K inhibits the MHC I exposure on the cell surface, by this interfering with the antigen presentation pathway (Oliveira and Bouvier 2019). Furthermore, the E1B19K protein, expressed in dl309 but absent in both OAVs, inhibits autophagy, which contributes to the OAV mediated ICD (Piya, White et al. 2011). Of note, it has to be mentioned that E1B19K was shown to limit local inflammation induced by innate immune cells (Radke, Grigera et al. 2014). Thus, the role of E1B19K regarding the increase of ICD we observed is so far not completely unraveled and has to be analyzed in more detail in the future. Nevertheless, the deletion of all these proteins in XVir-N-31 or XVir-N-31-anti-PD-L1 could explain the enhanced induction of ICD by these OAVs. Interestingly, although XVir-N-31-anti-PD-L1 expresses (in contrast to XVir-N-31) all proteins of the E3 region except E319K, in infected GBM cells the DAMP release as well as CRT surface exposure was always equal or even slightly elevated compared to XVir-N-31. A reason for this could be the slightly slower viral reproduction of XVir-N-31-anti-PD-L1. Whilst it was shown that 50% cell lysis was achieved approximately 72 hours after infection of GBM cells with XVir-N-31, at the same MOI this takes 82,5 hours for XVir-N-31-anti-PD-L1. This delay can be explained by the extended synthesis of the E3 proteins as well as by the additional expression of anti-PD-L1. It is already known that the size and the location of inserted transgenes can affect adenoviral packaging, replication speed and also titers (Suzuki, Kondo et al. 2015). Over the course of the additional 10,5 hours probably more DAMPs can be released and more CRT can be exposed to the cell surface. Additionally, it might hint that the absence of adenoviral proteins of the E3 region, excluding E319K, are not of great importance for a proper ICD induction. This hypothesis can also be confirmed by the *in vivo* results (discussed in the following chapter).

4.3.1 Induction of ICD by XVir-N-31 and XVir-N-31-anti-PD-L1 *in vivo*

Following these promising *in vitro* results, we investigated the induction of ICD *in vivo*, using our immuno-humanized GBM mouse model (Figure 11). Whilst this model is valid to establish a humanized immune system in mice, a limitation is the onset of GvHD after a certain time.

This onset becomes visible by a sudden burst of $CD45^+$ cells in the murine blood and could influence immune responses. Nevertheless, we showed that this burst occurs at the earliest 80 days after PBMC injection (Supplement Figure 1), which is even later than described before (Ehx, Somja et al. 2018). Since we finished all experiments way earlier, the influence of GvHD effects has been minimized or even completely excluded.

As expected, in PD-$L1^{high}$ U87MG bearing mice 35 days after sham treatment no HMGB1 or HSP70 (Figure 14, Figure 15) staining was detectable in the tumor area. Whilst HMGB1 release after dl309 infection was observed *in vitro*, *in vivo* neither HSP70 nor HMGB1 were detected in the dl309 cohort. This can be explained by the more sensitive measurement of the ELISAs we used in the *in vitro* experiments and the combination of an extremely immunosuppressive TME along with the known immunosuppressive functions of dl309 *in vivo*. This suggests that a wild type adenovirus is not capable of inducing ICD and therefore an enhanced immune response *in vivo*, at least in our animal model. In contrast, XVir-N-31 and XVir-N-31-anti-PD-L1 treated cohorts showed both HMGB1 and to a lesser amount also HSP70 staining in the tumor area. The amount of both DAMPs was further elevated in the XVir-N-31-anti-PD-L1 and XVir-N-31 plus Nivolumab treated cohorts. In line with the *in vitro* findings, XVir-N-31-anti-PD-L1 treatment led to the strongest DAMP expression. Beside the slower replication speed of the virus, this hints that the presence of the E3 proteins, excluding E319K, although having known immunosuppressive functions, do not have a fundamental influence on the expression of DAMPs as HSP70 or HMGB1 and with that on the induction of ICD. This is in line with Nevis, who demonstrated that after adenoviral infection at least HSP70 induction is mediated by E1A proteins (Nevins 1982). Since the dl309 cohort of mice showed no induction of DAMPs, the deletion of E1A13S, E1B19K or E319K in XVir-N-31 and its derivate seem to be essential for the OVT mediated induction of ICD in GBM. The additional blockade of PD-L1 by the anti-PD-L1 antibody, inhibiting the exhaustion of possible infiltrating immune cells, might even boost this induction. This is supported also by the strong expression of both DAMPs after XVir-N-31 injection with the concurrent application of Nivolumab. Overall, this indicates a strong induction of ICD by XVir-N-31, which can be reinforced by the inhibition of the PD-1/PD-L1 interaction.

Remarkably, the induction of ICD was not exclusively found in OAV-injected tumors but was also detected in contralateral tumors. Possible explanations for this abscopal effect are either (i) spreading of the virus to the distant tumor followed by subsequent tumor cell infection and DAMP release or (ii) a general induction of the immune system. In the latter case, activated immune cells attack those tumor cells that have not been targeted by the virus. In contrast, a spreading of the virus might occur at various stages of the experiment, either during the process of injection or from infected cells via the cerebrospinal fluid. Furthermore, it was demonstrated by Kakiuchi *et al.*, that in colon cancer OAVs are transferred via tumor-derived exosomes to metastases located far away from the virus injected tumors. This way, abscopal effects are induced due to oncolysis of metastatic cells by OAVs released from the exosomes (Kakiuchi, Kuroda et al. 2021). Nevertheless, at the time of observation (day 35 after treatment) no hexon staining was detectable in any of the contralateral tumors (Figure 16). Although this is only a snapshot at a fairly late time point, the contemporaneously expression of DAMPs hints that the abscopal effects are rather mediated by an activated immune system than a result of viral replication. This in GBM so far never before described abscopal effect of ICD induction in tumors areas located far away from the virus injection side can be explained by an increased infiltration of activated T lymphocytes also in these areas (Figure 17) and will be discussed in the following chapter. Nevertheless, to exclude the possibility of viral spreading

entirely, in subsequent experiments the evaluation of viral replication should be performed in both tumors at various time points.

As briefly mentioned before, the combined OVT-ICI treatment of GBMs was not only executed using XVir-N-31-anti-PD-L1, but also by using XVir-N-31 plus concurrent repeated systemic applications of Nivolumab. In contrast to virus-expressed anti-PD-L1, Nivolumab blocks PD-1, mainly expressed on the surface of immune cells. Nevertheless, we chose to use Nivolumab and not an anti-PD-L1 antibody like Atezolizumab in our experiments. This was done on purpose since we believed Nivolumab to be the strongest contestant to XVir-N-31-anti-PD-L1 expressed anti-PD-L1. Since we applied Nivolumab intraperitoneally, we hypothesized that Nivolumab will cap PD-1 on immune cells already in the periphery, thereby minimizing exhaustion of TILs by GBM expressed PD-L1 during the infiltration phase. Although in clinical trials Nivolumab was also found intracranially in cerebral cancers after systemic application, we aimed with this to bypass the possible exclusion of molecules like Atezolizumab from the brain by the BBB, as seen for other ICIs (Van Bussel, Beijnen et al. 2019). XVir-N-31-anti-PD-L1 expressed anti-PD-L1, already located in the tumor area, will in contrast bind to PD-L1 on tumor cells, thereby also protecting TILs from exhaustion during the infiltration phase.

Besides the combination treatment with XVir-N-31, we also analyzed the impact of a Nivolumab monotherapy in our immuno-humanized animal model. In patients, treatment with Nivolumab additionally to standard therapy failed to show significant benefits (Reardon, Brandes et al. 2020). In line with that, Nivolumab alone showed no induction of HSP70 and only very weak induction of HMGB1 in the tumor area of U87MG tumor bearing mice (Figure 13A, B). This suggests that the combination of XVir-N-31 with an ICI leads to a strong induction of ICD, whereas the treatment with Nivolumab alone does not have a significant influence on the established immune system and does not induce ICD appropriately, at least in our animal model.

4.4 XVir-N-31 and XVir-N-31-anti-PD-L1 mediate enhanced immune cell infiltration

It is known that treatment of tumors with several OVs, the subsequent oncolysis and induction of ICD is able to launch a strong immune response and to enhance the infiltration of immune cells into the tumor area (Ma, Ramachandran et al. 2020, Saha and Rabkin 2020). In line with these findings, all virus treated cohorts showed significantly more human $CD45^+$ cells in those tumor area the virus was injected in (Figure 17A, B). Interestingly, but also in accord with our previous findings, the XVir-N-31, XVir-N-31-anti-PD-L1 and XVir-N-31 plus Nivolumab cohorts of mice showed significantly more human $CD45^+$ TILs than the dl309 cohort. Since no DAMPs were found in the dl309 cohort, the induction of ICD observed in all other virus treated cohorts seems to be beneficial for an enhanced immune cell infiltration. In line with that, Nivolumab monotherapy, lacking a proper induction of ICD, showed no increased $CD45^+$ TIL numbers in the tumor area (Figure 13C).

Regarding the analysis of the human immune cell subpopulations, most cells in the OAV treated mouse cohorts were $CD3^+$ T cells, with a majority of these cells being $CD8^+$ CTLs (Figure 17C-E). This is of special regard, since Han *et al*. showed that in GBM TILs are usually

a relatively small population and that infiltrating cells are rather $CD4^+$ Th cells with only a small amount of $CD8^+$ CTLs (Han, Ma et al. 2016). Comparable results were found in the sham treated controls of mice, where a comparably small population of immune cells were $CD3^+$ TILs. In dl309 treated animals the majority of $CD3^+$ TILs were $CD4^+$ Th cells.

It was shown that an enhanced tumor infiltration of $CD8^+$ CTLs positively correlates with the survival of patients (Han, Zhang et al. 2014, Rosato, Wijeyesinghe et al. 2019) and that OVT can induce an increased tumor infiltration by these cells (Ribas, Dummer et al. 2017). Whilst dl309 injection had no effect on $CD8^+$ T cell numbers in the tumor area, it seems that the immunostimulatory features of XVir-N-31 and XVir-N-31-anti-PD-L1 are highly beneficial to induce a strong CTL mediated anti-tumor immune cell response. The significantly increased numbers of $CD8^+$ TILs in those cohorts additionally treated with ICIs, especially in XVir-N-31-anti-PD-L1 injected animals, indicate the beneficial role of a concurrent PD-1/PD-L1 blockade. Nevertheless, in all of these cohorts the $CD4^+$ Th cell population was still approximately one third of all $CD3^+$ TILs. Therefore, and since it was shown that the ratio between these populations can influence tumor growth (Shimato, Maier et al. 2012, Wang, Zhou et al. 2021), it would be of further interest for future experiments to identify the subpopulations of these Th cells.

Elevated TIL numbers were not only found in the virus-injected, but also in the contralateral located, untreated GBMs. The proportion of individual immune cell subsets in contralateral tumors reflected those identified in ipsilateral tumors quite well, with only a slightly lesser cell count. Although the XVir-N-31-anti-PD-L1 and the XVir-N-31 plus Nivolumab cohorts showed equal levels of human $CD45^+$ and $CD3^+$ TILs, the amount of $CD8^+$ TILs in contralateral tumors was higher in the XVir-N-31-anti-PD-L1 cohort of mice. Nevertheless, all three OAV treated mouse cohorts showed an overall strong induction of $CD3^+$ TILs and especially $CD8^+$ cytotoxic TILs also in contralateral tumors. This is striking since the infiltration of these cells into the area of contralaterally located GBMs might explain the induction of ICD we observed also there. Jaime-Sanchez *et al*. showed that $CD8^+$ TILs are able to induce a kind of “secondary burst” of ICD after primary cancer vaccination (Jaime-Sanchez, Uranga-Murillo et al. 2020). Based on Jaime-Sanchez´s observation, we hypothesized that in GBMs an intratumoral injection with XVir-N-31 or XVir-N-31-anti-PD-L1 leads, via local tumor cell lysis and ICD, to an activation of the immune system and an enhanced infiltration of immune cells also into small tumor areas of infiltrated GBM cells located far away from the injected primary tumor. Thereby, especially the elevated numbers of $CD8^+$ TILs seem to be responsible for the induction of a probably immune cell mediated cell death in contralateral tumors. In the clinic, this abscopal effect might be extremely beneficial for the treatment of diffuse growing gliomas in which infiltrated tumor cells cannot be directly reached with OAVs.

In accordance with the above-mentioned observations were the elevated numbers of $CD134^+$ cells in the tumor areas of OAV treated animals (Figure 17F). We chose to stain the tumors for CD134/OX40, that is expressed on activated $CD4^+$ and $CD8^+$ T cells, instead of staining for the often-used immune cell activation marker CD69. CD134 is expressed for a longer time period compared to CD69 which is upregulated in activated T cells for approximately only 6h (Cibrián and Sánchez-Madrid 2017). Whilst CD134/OX40 was only expressed on a small subset of all $CD3^+$ T cells in the dl309 cohort of mice, in the XVir-N-31 or XVir-N-31-anti-PD-L1 treated cohorts of mice almost all $CD3^+$ cells showed an additional staining for CD134/OX40 in both, ipsi- and contralateral tumors. This is of central relevance since it was shown that OX40L expression, mediated by an armed virus carrying this gene as a therapeutic gene, is

beneficial for an increased $CD8^+$ T cell response and effector T cell survival (Ylösmäki, Ylösmäki et al. 2021). We believe that XVir-N-31 does not necessarily has to be armed to express OX40L, since the infection of GBM cells with this OAV already induces the infiltration of CD134/$OX40^+$ T cells into the tumor. Although the molecular mechanisms behind these findings are not completely unravelled, in this context the already earlier mentioned deletion of the immunosuppressive genes E1B19K and E319K in the adenoviral genome might play a role (refer to 4.3). Additionally, the known inhibitory functions of E1A13S, being absent in XVir-N-31, and its impact on histone acetylation patterns and the regulation of gene expression might also contribute (Tone, Kojima et al. 2007, Horwitz, Zhang et al. 2008, Pelka, Ablack et al. 2009).

In addition, the expression of CD134 might influence the infiltration of $FoxP3^+$ T_{regs} into the tumor areas (Figure 17G). It is already known that in GBM many TILs belong to the subpopulation of immunosuppressive T_{regs} and that the amount of T_{regs} negatively correlates with patient's survival (Jacobs, Idema et al. 2009, Tumangelova-Yuzeir, Naydenov et al. 2019). Whilst in the sham cohort of mice approximately 25% of $CD3^+$ TILs were FoxP3 positive, in the dl309 cohort 33% of $CD3^+$ TILs were T_{regs}, both in ipsi- and contralateral located tumors. In contrast, in the OAV treated cohorts of mice a significant reduction of $FoxP3^+$ cells both in ipsi- and contralateral tumors (5-6 %) was observed. Kitamura *et al*. showed that an activation of the T cell receptor (TCR) with an concurrent CD134/OX40 co-stimulation abrogated the $Foxp3^+$ T_{reg} mediated suppression of antitumor immunity (Kitamura, Murata et al. 2009). Therefore, the XVir-N-31 induced activation of CD134 might also lead to downregulation of FoxP3 in T cells and subsequently to a reduced tumor infiltration with T_{regs}. Since it was not the scope of this study to elucidate the contributions and the impact of the individual adenoviral proteins on immune cell subpopulations, further studies are needed to investigate the detailed molecular mechanisms. Nevertheless, the impact of YB-1 dependent OAVs on CD134$^+$/$CD8^+$ cytotoxic TILs and $FoxP3^+$ T_{regs} leave exciting prospects for the future.

Finally, the XVir-N-31 and XVir-N-31-anti-PD-L1 based OVT of GBMs provide an additional impact on the infiltration of the tumors with $CD56^+$ NK cells (Figure 17H). Although significantly increased in both tumors, the number of $CD56^+$ NK cells was relatively low, especially compared to infiltrating $CD3^+$ T cells. This indicates an only moderate impact of our OAVs on cells of the innate immune system but shows that also the main cellular anti-tumor immune response is mediated by cells of the adaptive immune system. Since it is reported that NK cells, besides their anti-tumor effects, impede the efficacy of virotherapy in GBM through their fast virus-infected cell killing via natural cytotoxicity receptors (Alvarez-Breckenridge, Yu et al. 2012), the induction of an adaptive immune response might be even beneficial for therapy.

XVir-N-31 and XVir-N-31-anti-PD-L1 increased the number of TILs also in LN-229 (PD-$L1^{neg}$) GBM bearing immuno-humanized mice (Figure 19). In contrast to U87MG (PD-$L1^{high}$), in LN-229 tumors and compared to XVir-N-31, XVir-N-31-anti-PD-L1 injection failed to additionally elevate the amount of $CD3^+$ TILs and their $CD4^+$ and $CD8^+$ subpopulations, both in ipsi- and in contralateral located tumors. This suggests that both OAVs induce a strong cellular adaptive immune response also in PD-L1 negative GBMs, but that the beneficial effect of a concurrent PD-1/PD-L1 axis blockade is restricted to PD-L1-positive GBMs. However, since it was shown that PD-L1 is expressed in the majority of primary and recurrent GBMs at least in a subpopulation of tumor cells (Berghoff, Kiesel et al. 2015), and the already mentioned IFNγ

induced upregulation of PD-L1 (refer to 4.2), an additional ICI can always be considered to treat such a diffuse and heterogeneous cancer like GBM. In this regard, it should be mentioned that a systemic application of ICIs, as performed in previous clinical studies, can lead to strong adverse events in several organs and can elevate morbidity and even mortality (Pan and Haggiagi 2019). As the immunostimulatory effects of XVir-N-31-anti-PD-L1 were found to be equal or even better than those observed for XVir-N-31 plus Nivolumab, but the expression of anti-PD-L1 is restricted to the site of virus injection in the tumor area, severe adverse effects might be minimized. Therefore, the demonstrated therapeutic effects of XVir-N-31-anti-PD-L1 open up a future potential to use XVir-N-31 also as a carrier for inhibitors that target other immune checkpoint proteins.

4.5 Abscopal effect of tumor growth reduction

An effective tumor volume reduction impacting on survival and its associated relieve of symptoms in patients is always the most desired outcome in cancer therapy. Therefore, the analysis of tumor growth following the XVir-N-31 based OVT is of fundamental importance. At least in our experimental mouse model Nivolumab monotherapy, which showed already no proper induction of ICD or enhanced immune cell infiltration, failed to reduce the volume of ipsi- or contralateral tumors (Figure 13D) and therefore provides no benefit. In contrast, an intratumoral injection with dl309, XVir-N-31 or XVir-N-31-anti-PD-L1 resulted into a strong tumor volume reduction in the virus-injected tumors (Figure 18). Considering that no significant difference was observed in dl309 or XVir-N-31 treated cohorts, nor in those cohorts that achieved an additional ICI therapy, the lytic effect of the viruses seemed to be sufficient for the reduction of the tumor. At least in our animal model this shows that, even if XVir-N-31 and XVir-N-31-anti-PD-L1 provide diminished cell lysis capacity compared to dl309, *in vivo* both OAVs are still as effective as dl309. Even more strikingly, the combination of XVir-N-31 and Nivolumab or the single intratumoral injection of XVir-N-31-anti-PD-L1 resulted in a significant tumor volume reduction also of contralaterally located GBMs. This indicates that the OAV mediated induction of ICD, associated with the increased immune cell infiltration in the tumor area, mitigates the grow up or even induces a killing of GBM cells that are located far away from the virus injection side. In contrast, dl309 and XVir-N-31 treated mouse cohorts showed no reduction of contralaterally located tumors. Whilst this was not expected for a dl309 based therapy, it was a clear setback for an XVir-N-31 based OVT, as this therapy showed an induction of ICD as well as an increased infiltration of activated $CD8^+$ T cells also into contralateral tumors. However, the HMGB1 and HSP70 staining in the contralateral tumor area of XVir-N-31 bearing mice was relatively low and the amount of $CD3^+/CD134^+$ TILs was lower than in XVir-N-31-anti-PD-L1 or XVir-N-31 plus Nivolumab treated animals. Therefore, we hypothesize that for an efficient eradication of infiltrating GBM cells located far away from the primary tumor that can be intratumorally injected with OAVs, the induction of a potent ICD and a subsequent strong immune cell infiltration is required. This can be provided by the treatment with XVir-N-31 and a concurrent inhibition of the PD-1 / PD-L1 interaction.

4.6 Conclusion & Outlook

In the present study we analyzed the therapeutic effects of XVir-N-31 in GBM, with a special focus on its immunostimulatory impact. Although *in vitro* XVir-N-31 demonstrates significantly lower cell killing capacity than dl309, *in vivo* the lytic efficacy of both viruses was comparable. The shift from immunogenic silent cell death to an efficient induction of ICD as well as the induction of further immunostimulatory processes are thereby mainly responsible for the therapeutic effect of XVir-N-31 in the treatment of GBM. This is in line with the data obtained for a Herpes simplex virus based OVT, showing that during the treatment the induction of ICD is more important than an efficient virus replication (Workenhe, Simmons et al. 2014, Ma, Ramachandran et al. 2020). Our data give additional information about the importance of several adenoviral proteins for a proper induction of an immune response. It is suggested that the expression of the adenoviral large E1A13S, E1B19K and E319K proteins should be avoided due to their virus-mediated, immunosuppressive effects. Our data evidence that an XVir-N-31 based OVT of GBM leads to a strong activation of the adaptive immune system and enhanced immune cell infiltration in the tumor area, not only in virus injected tumors, but also in tumors far away from the injection side. Additionally, it was shown that the observed immunostimulatory effects can be further enhanced by a concurrent ICI based therapy, which is provided by XVir-N-31-anti-PD-L1. This derivate demonstrates, besides local therapeutic improvements, additional therapeutic effects, including the enhanced induction of ICD, an elevated number of activated TILs and a subsequent tumor growth reduction also in contralaterally located, untreated GBMs. Therefore, we hypothesize that an OVT/ICI combination therapy using XVir-N-31-anti-PD-L1 will be a promising step to improve the therapeutic outcome of GBM patients.

For future directions, an optimal viral replication, an efficient spreading of the virus over the brain or a further improvement of an OVT/ICI combination therapy is of interest. While we demonstrated that viral replication is of lesser importance, our collaboration partners in the group of Prof. Holm (TU Munich) showed an impressive increase of XVir-N-31 replication by an additional treatment of GBM cells with bromodomain or CDK4/6 inhibitors. The treatment of GBM with these inhibitors might in further experiments lead to an optimal and efficient local tumor cell lysis, but also an increased induction of ICD and therefore to enhanced immune responses. A method to increase the spreading of the virus is to cargo it in shuttle cells, which then can be applied intranasally and travel along the olfactory route into the brain and towards infiltrating GBM cells. This application method and approach was already shown to be safe and effective in the treatment of CNS diseases (Danielyan, Schäfer et al. 2009, Chapman, Frey et al. 2013, Drews, Yenkoyan et al. 2019). These “trojan horse” cells, loaded with XVir-N-31, could distribute the virus all over the brain, thereby targeting invaded glioma cells and stimulating the immune system. Finally, the positive effect of OVT with an additional blockade of the PD-1/PD-L1 axis suggests that XVir-N-31 can function as an excellent carrier for inhibitors that target other immune checkpoint proteins, such as CTLA-4 or TIM-3.

Taken all together, the obtained results, in line with previous findings, open up a promising future for the treatment of GBM using XVir-N-31. Based on the data of the actual as well as of former studies, a phase I study to treat recurrent GBM with XVir-N-31 is planned and scheduled to start end of 2022.

5. Supplement

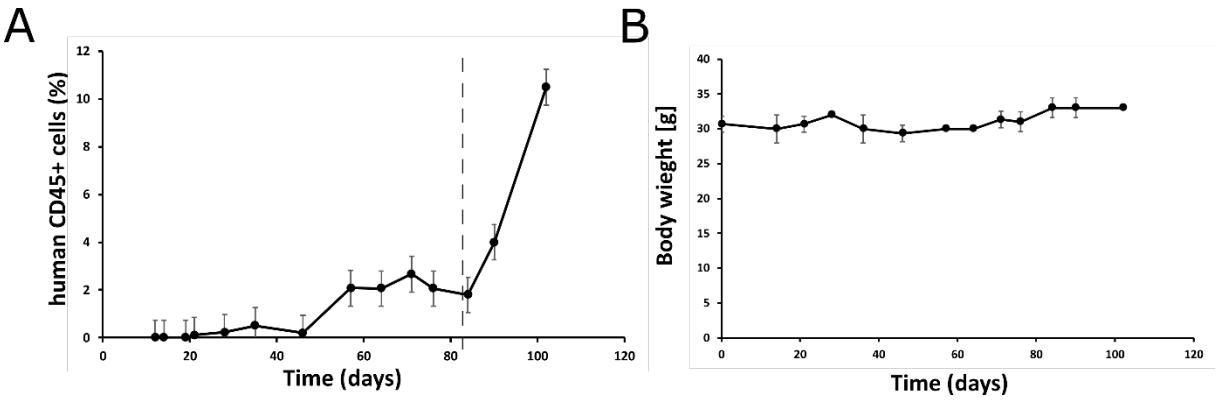

Supplement Figure 1. GvHD signs in an immuno-humanized mouse model. A. First signs of GvHD were determined by the measurement elevated levels of human $CD45^+$ cells in the blood of PBMC injected mice (n=2 mice). **B.** Body weight of PBMC engrafted mice as indicated in A (n= 2 mice).

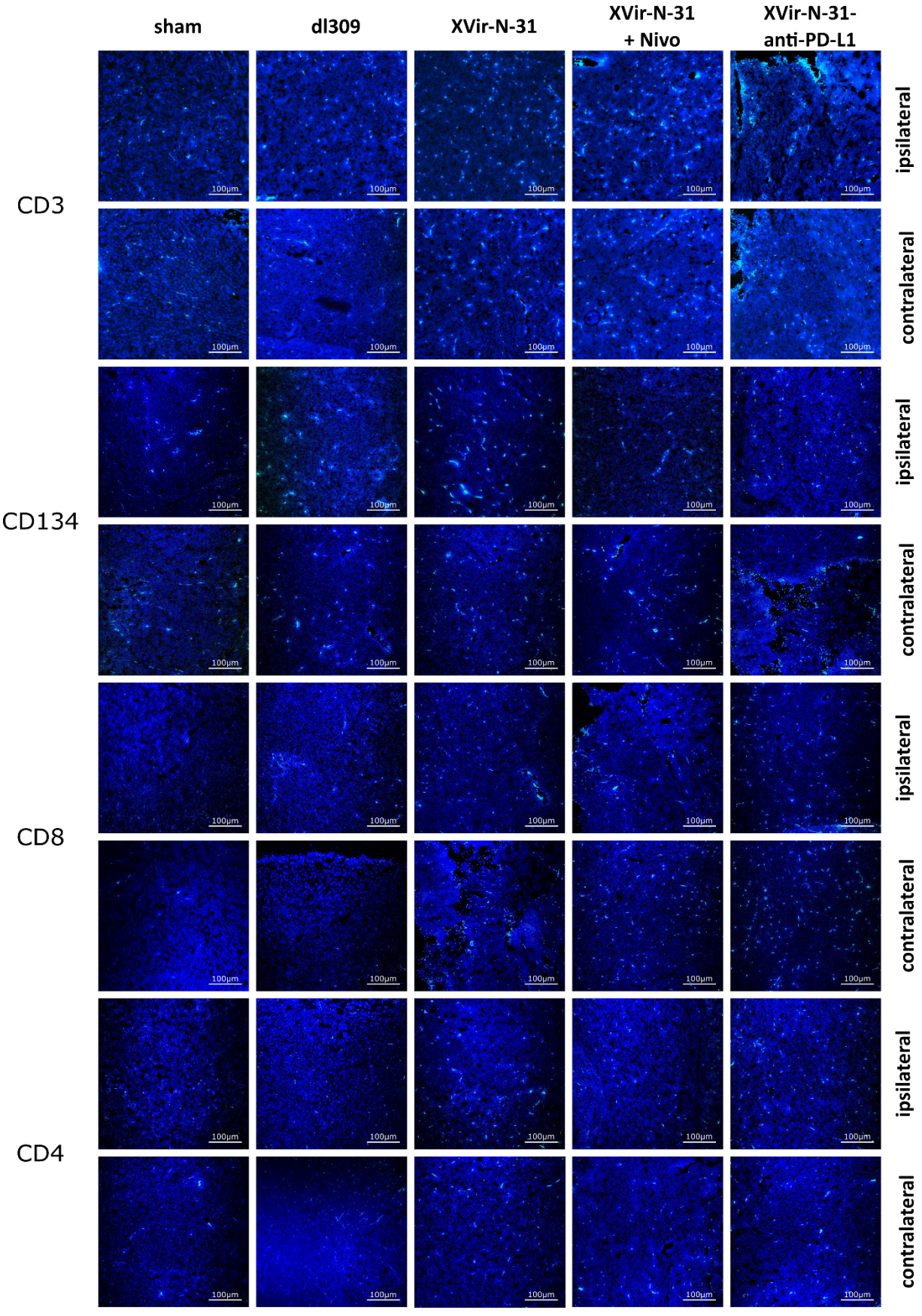
sham
dl309
XVir-N-31
XVir-N-31 + Nivo
XVir-N-31-anti-PD-L1
CD3
CD134
CD8
CD4
ipsilateral
contralateral
ipsilateral
contralateral
ipsilateral
contralateral
ipsilateral
contralateral
100µm

Supplement Figure 2. Intratumoral invasion of different immune cells after intratumoral OAV injection. Representative immunofluorescence pictures of human immune cell infiltration into U87MG tumors in NSG mice. Brain sections were stained with DAPI (blue) and for anti-human CD3 (T cells), CD134 (activated T cells), CD8 (CTLs) and CD4 (T helper cells) (all in green). Pictures were taken 35 days after the injection of virus or sham into the tumor on the ipsilateral (injected) as well as on the contralateral (not injected) side.

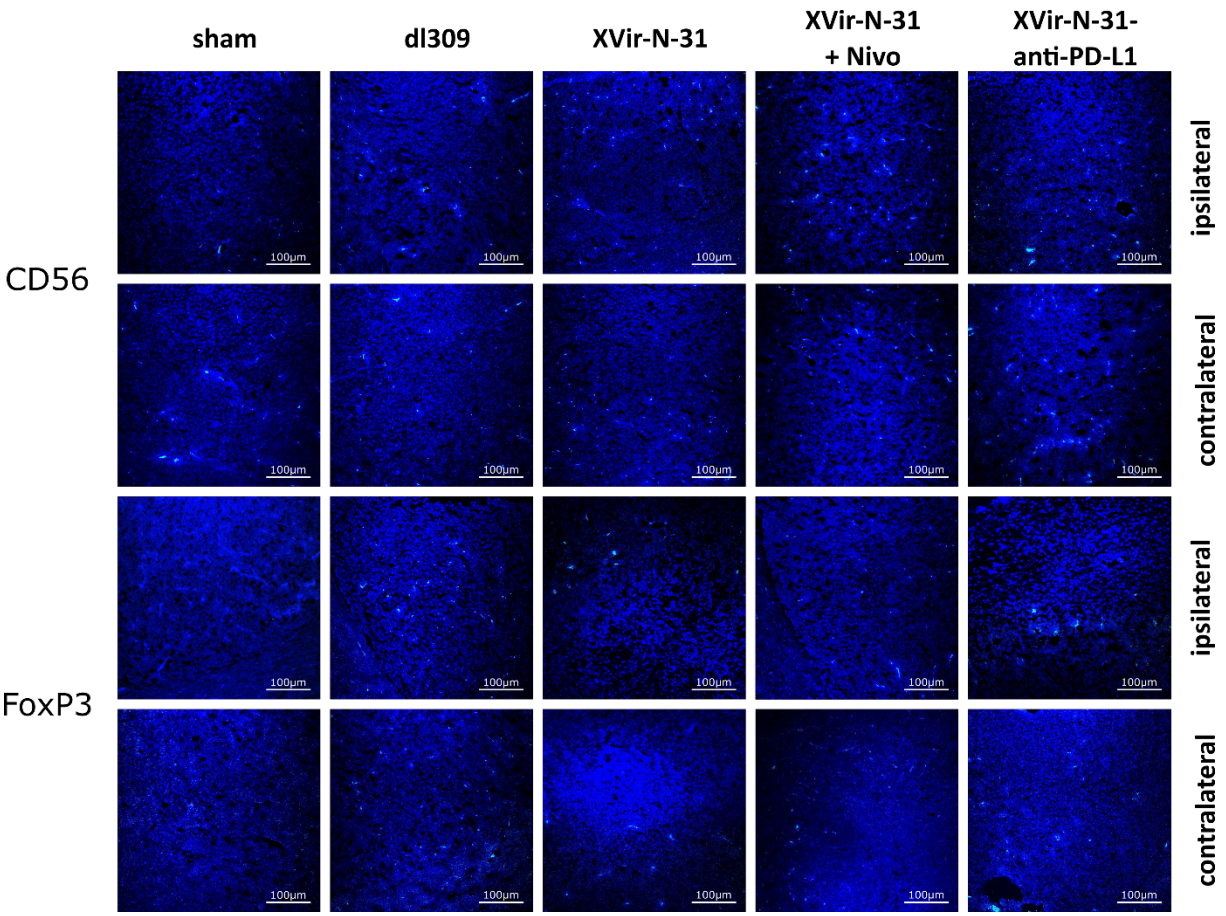

Supplement Figure 3. Intratumoral invasion of NK cells and T_{regs} after intratumoral OAV injection. Representative immunofluorescence pictures of human immune cell infiltration into U87MG tumors in NSG mice. Brain sections were stained with DAPI (blue) and for anti-human CD56 (NK cells) and FoxP3 (T_{regs}) (both in green). Pictures were taken 35 days after the injection of virus or sham into the tumor on the ipsilateral (injected) as well as on the contralateral (not injected) side.

6. Statement of Contributions

Statement of contributions according to § 9 (2):

1. If not otherwise clearly mentioned, all work has been performed by the author of this manuscript**, Moritz Klawitter** (M.A.).

2. All work related to Figure 9A was performed by **Jasmin Buch** (M.A.), under the direct supervision of Moritz Klawitter (as always mentioned in the text).

3. All work related to Figure 13A, B and Figure 15 was performed by **Jakob Rüttinger**, under the direct supervision of Moritz Klawitter (as always mentioned in the text).

4. All work related to Supplement Figure 1A was performed by **Yana Parfyonova** (as mentioned in the text).

All named contributors are aware and appreciate their work to this thesis and declare their permission to publish all data in the given format.

7. References

Ablack, J. N. G., et al. (2010). "Comparison of E1A CR3-Dependent Transcriptional Activation across Six Different Human Adenovirus Subgroups." Journal of Virology **84**(24): 12771-12781.

Ahluwalia, M., et al. (2018). "ATIM-41. PHASE II TRIAL OF A SURVIVIN VACCINE (SurVaxM) For Newly Diagnosed Glioblastoma." Neuro-Oncology **20**(suppl_6): vi10-vi11.

Ahmed, A. and S. W. G. Tait (2020). "Targeting immunogenic cell death in cancer." Molecular Oncology **14**(12): 2994-3006.

Alayo, Q. A., et al. (2020). "Glioblastoma infiltration of both tumor- and virus-antigen specific cytotoxic T cells correlates with experimental virotherapy responses." Scientific Reports **10**(1).

Alvarez-Breckenridge, C. A., et al. (2012). "NK cells impede glioblastoma virotherapy through NKp30 and NKp46 natural cytotoxicity receptors." Nature Medicine **18**(12): 1827-1834.

Andtbacka, R. H. I., et al. (2015). "Talimogene Laherparepvec Improves Durable Response Rate in Patients With Advanced Melanoma." Journal of Clinical Oncology **33**(25): 2780-2788.

Anghelina, D., et al. (2016). "Diminished Innate Antiviral Response to Adenovirus Vectors in cGAS/STING-Deficient Mice Minimally Impacts Adaptive Immunity." Journal of Virology **90**(13): 5915-5927.

Ansell, S. M., et al. (2015). "PD-1 Blockade with Nivolumab in Relapsed or Refractory Hodgkin's Lymphoma." New England Journal of Medicine **372**(4): 311-319.

Antonios, J. P., et al. (2016). "PD-1 blockade enhances the vaccination-induced immune response in glioma." JCI Insight **1**(10).

Apetoh, L., et al. (2007). "The interaction between HMGB1 and TLR4 dictates the outcome of anticancer chemotherapy and radiotherapy." Immunological Reviews **220**(1): 47-59.

Armento, A., et al. (2017). "Carboxypeptidase E transmits its anti-migratory function in glioma cells via transcriptional regulation of cell architecture and motility regulating factors." International Journal of Oncology **51**(2): 702-714.

Atasheva, S. and D. M. Shayakhmetov (2016). "Adenovirus sensing by the immune system." Current Opinion in Virology **21**: 109-113.

Avvakumov, N., et al. (2004). "Comprehensive sequence analysis of the E1A proteins of human and simian adenoviruses." Virology **329**(2): 477-492.

Bandara, L. R. and N. B. La Thangue (1991). "Adenovirus E1a prevents the retinoblastoma gene product from complexing with a cellular transcription factor." Nature **351**(6326): 494-497.

Bauer, H. C., et al. (2014). ""You Shall Not Pass"-tight junctions of the blood brain barrier." Front Neurosci **8**: 392.

Bauerschmitz, G. J., et al. (2006). "Triple-Targeted Oncolytic Adenoviruses Featuring the Cox2 Promoter, E1A Transcomplementation, and Serotype Chimerism for Enhanced Selectivity for Ovarian Cancer Cells." Molecular Therapy **14**(2): 164-174.

Bausart, M., et al. (2022). "Immunotherapy for glioblastoma: the promise of combination strategies." Journal of Experimental & Clinical Cancer Research **41**(1).

Bellmunt, J., et al. (2017). "Pembrolizumab as Second-Line Therapy for Advanced Urothelial Carcinoma." New England Journal of Medicine **376**(11): 1015-1026.

Ben-Israel, H. (2002). "Adenovirus and cell cycle control." Frontiers in Bioscience **7**(1-3): d1369.

Berghoff, A. S., et al. (2015). "Programmed death ligand 1 expression and tumor-infiltrating lymphocytes in glioblastoma." Neuro-Oncology **17**(8): 1064-1075.

Berk, A. J. (1986). "ADENOVIRUS PROMOTERS AND E1A TRANSACTIVATION." Annual Review of Genetics **20**(1): 45-77.

Bielamowicz, K., et al. (2018). "Trivalent CAR T cells overcome interpatient antigenic variability in glioblastoma." Neuro-Oncology **20**(4): 506-518.

Bischoff, J. R., et al. (1996). "An adenovirus mutant that replicates selectively in p53-deficient human tumor cells." Science **274**(5286): 373-376.

Blumenthal, R., et al. (1986). "pH-dependent lysis of liposomes by adenovirus." Biochemistry **25**(8): 2231-2237.

Bourgeois-Daigneault, M. C., et al. (2018). "Neoadjuvant oncolytic virotherapy before surgery sensitizes triple-negative breast cancer to immune checkpoint therapy." Sci Transl Med **10**(422).

Braithwaite, A. W. and I. A. Russell (2001). APOPTOSIS **6**(5): 359-370.

Brat, D. J., et al. (2020). "cIMPACT-NOW update 5: recommended grading criteria and terminologies for IDH-mutant astrocytomas." Acta Neuropathologica **139**(3): 603-608.

Brat, D. J., et al. (2018). "cIMPACT-NOW update 3: recommended diagnostic criteria for "Diffuse astrocytic glioma, IDH-wildtype, with molecular features of glioblastoma, WHO grade IV"." Acta Neuropathologica **136**(5): 805-810.

Burster, T., et al. (2021). "Regulation of MHC I Molecules in Glioblastoma Cells and the Sensitizing of NK Cells." Pharmaceuticals **14**(3): 236.

Burster, T., et al. (2021). "Critical View of Novel Treatment Strategies for Glioblastoma: Failure and Success of Resistance Mechanisms by Glioblastoma Cells." Frontiers in Cell and Developmental Biology **9**.

Cai, J., et al. (2019). "The role of PD-1/PD-L1 axis and macrophage in the progression and treatment of cancer." Journal of Cancer Research and Clinical Oncology **145**(6): 1377-1385.

Candolfi, M., et al. (2009). "Release of HMGB1 in Response to Proapoptotic Glioma Killing Strategies: Efficacy and Neurotoxicity." Clinical Cancer Research **15**(13): 4401-4414.

Cassany, A., et al. (2015). "Nuclear Import of Adenovirus DNA Involves Direct Interaction of Hexon with an N-Terminal Domain of the Nucleoporin Nup214." Journal of Virology **89**(3): 1719-1730.

Cenciarini, M., et al. (2019). "Dexamethasone in Glioblastoma Multiforme Therapy: Mechanisms and Controversies." Frontiers in Molecular Neuroscience **12**.

Chahlavi, A., et al. (2005). "Glioblastomas Induce T-Lymphocyte Death by Two Distinct Pathways Involving Gangliosides and CD70." Cancer Research **65**(12): 5428-5438.

Chanteloup, G., et al. (2020). "Monitoring HSP70 exosomes in cancer patients' follow up: a clinical prospective pilot study." Journal of Extracellular Vesicles **9**(1): 1766192.

Chapman, C. D., et al. (2013). "Intranasal Treatment of Central Nervous System Dysfunction in Humans." Pharmaceutical Research **30**(10): 2475-2484.

Chaurasiya, S., et al. (2021). "Oncolytic Virotherapy for Cancer: Clinical Experience." Biomedicines **9**(4): 419.

Chen, L. and X. Han (2015). "Anti–PD-1/PD-L1 therapy of human cancer: past, present, and future." Journal of Clinical Investigation **125**(9): 3384-3391.

Chen, R. Q., et al. (2019). "The Binding of PD-L1 and Akt Facilitates Glioma Cell Invasion Upon Starvation via Akt/Autophagy/F-Actin Signaling." Frontiers in Oncology **9**.

Chen, Z., et al. (2017). "Cellular and Molecular Identity of Tumor-Associated Macrophages in Glioblastoma." Cancer Research **77**(9): 2266-2278.

Chen, Z. and D. Hambardzumyan (2018). "Immune Microenvironment in Glioblastoma Subtypes." Frontiers in immunology **9**: 1004-1004.

Chiocca, E. A., et al. (2019). "Regulatable interleukin-12 gene therapy in patients with recurrent high-grade glioma: Results of a phase 1 trial." Science Translational Medicine **11**(505): eaaw5680.

Chirmule, N., et al. (1999). "Immune responses to adenovirus and adeno-associated virus in humans." Gene Therapy **6**(9): 1574-1583.

Choi, A., et al. (2016). "From Benchtop to Bedside: A Review of Oncolytic Virotherapy." Biomedicines **4**(3): 18.

Cibrián, D. and F. Sánchez-Madrid (2017). "CD69: from activation marker to metabolic gatekeeper." European Journal of Immunology **47**(6): 946-953.

Cirone, M., et al. (2012). "Primary Effusion Lymphoma Cell Death Induced by Bortezomib and AG 490 Activates Dendritic Cells through CD91." PLoS ONE **7**(3): e31732.

Cloughesy, T. F., et al. (2020). "A randomized controlled phase III study of VB-111 combined with bevacizumab vs bevacizumab monotherapy in patients with recurrent glioblastoma (GLOBE)." Neuro-Oncology **22**(5): 705-717.

Cloughesy, T. F., et al. (2019). "Neoadjuvant anti-PD-1 immunotherapy promotes a survival benefit with intratumoral and systemic immune responses in recurrent glioblastoma." Nature Medicine **25**(3): 477-486.

Crane, C. A., et al. (2010). "TGF- downregulates the activating receptor NKG2D on NK cells and CD8+ T cells in glioma patients." Neuro-Oncology **12**(1): 7-13.

Czolk, R., et al. (2019). "Irradiation enhances the therapeutic effect of the oncolytic adenovirus XVir-N-31 in brain tumor initiating cells." International Journal of Molecular Medicine **44**(4): 1484-1494.

Czolk, R., et al. (2019). "Irradiation enhances the therapeutic effect of the oncolytic adenovirus XVir-N-31 in brain tumor initiating cells." International Journal of Molecular Medicine.

D'Alessio, A., et al. (2019). "Pathological and Molecular Features of Glioblastoma and Its Peritumoral Tissue." Cancers **11**(4): 469.

Daniel and I. Mellman (2013). "Oncology Meets Immunology: The Cancer-Immunity Cycle." Immunity **39**(1): 1-10.

Danielyan, L., et al. (2009). "Intranasal delivery of cells to the brain." Eur J Cell Biol **88**(6): 315-324.

Desai, K., et al. (2019). "The Role of Checkpoint Inhibitors in Glioblastoma." Targeted Oncology **14**(4): 375-394.

Dhingra, A., et al. (2019). "Molecular Evolution of Human Adenovirus (HAdV) Species C." Scientific Reports **9**(1).

Dias, J. D., et al. (2012). "Targeted cancer immunotherapy with oncolytic adenovirus coding for a fully human monoclonal antibody specific for CTLA-4." Gene Therapy **19**(10): 988-998.

Dobes, M., et al. (2011). "Increasing incidence of glioblastoma multiforme and meningioma, and decreasing incidence of Schwannoma (2000-2008): Findings of a multicenter Australian study." Surg Neurol Int **2**: 176.

Domingues, P., et al. (2016). "Tumor infiltrating immune cells in gliomas and meningiomas." Brain, Behavior, and Immunity **53**: 1-15.

Drews, H. J., et al. (2019). "Intranasal Losartan Decreases Perivascular Beta Amyloid, Inflammation, and the Decline of Neurogenesis in Hypertensive Rats." Neurotherapeutics **16**(3): 725-740.

Dubinski, D., et al. (2016). "CD4+T effector memory cell dysfunction is associated with the accumulation of granulocytic myeloid-derived suppressor cells in glioblastoma patients." Neuro-Oncology **18**(6): 807-818.

Dunn-Pirio, A. M. and G. Vlahovic (2017). "Immunotherapy approaches in the treatment of malignant brain tumors." Cancer **123**(5): 734-750.

Ehx, G., et al. (2018). "Xenogeneic Graft-Versus-Host Disease in Humanized NSG and NSG-HLA-A2/HHD Mice." Frontiers in immunology **9**: 1943.

Eigenbrod, S., et al. (2014). "Molecular stereotactic biopsy technique improves diagnostic accuracy and enables personalized treatment strategies in glioma patients." Acta Neurochir (Wien) **156**(8): 1427-1440.

Eliseeva, I. A., et al. (2011). "Y-box-binding protein 1 (YB-1) and its functions." Biochemistry (Moscow) **76**(13): 1402-1433.

Ellingson, B. M., et al. (2018). "Validation of postoperative residual contrast-enhancing tumor volume as an independent prognostic factor for overall survival in newly diagnosed glioblastoma." Neuro-Oncology **20**(9): 1240-1250.

Esaki, S., et al. (2020). "Oncolytic activity of HF10 in head and neck squamous cell carcinomas." Cancer Gene Therapy **27**(7-8): 585-598.

Fausther-Bovendo, H. and G. P. Kobinger (2014). "Pre-existing immunity against Ad vectors." Human Vaccines & Immunotherapeutics **10**(10): 2875-2884.

Fecci, P. E., et al. (2007). "Systemic CTLA-4 Blockade Ameliorates Glioma-Induced Changes to the CD4+ T Cell Compartment without Affecting Regulatory T-Cell Function." Clinical Cancer Research **13**(7): 2158-2167.

Ferris, R. L., et al. (2016). "Nivolumab for Recurrent Squamous-Cell Carcinoma of the Head and Neck." New England Journal of Medicine **375**(19): 1856-1867.

Filley, A. C., et al. (2017). "Recurrent glioma clinical trial, CheckMate-143: the game is not over yet." Oncotarget **8**(53): 91779-91794.

Flies, D. B. and L. Chen (2007). "The New B7s: Playing a Pivotal Role in Tumor Immunity." Journal of Immunotherapy **30**(3): 251-260.

Fontana, A., et al. (1991). "Expression of TGF-beta 2 in human glioblastoma: a role in resistance to immune rejection?" Ciba Found Symp **157**: 232-238; discussion 238-241.

Francisco, L. M., et al. (2010). "The PD-1 pathway in tolerance and autoimmunity." Immunological Reviews **236**(1): 219-242.

Fucikova, J., et al. (2021). "Calreticulin and cancer." Cell Research **31**(1): 5-16.

Fueyo, J., et al. (2003). "Preclinical Characterization of the Antiglioma Activity of a Tropism-Enhanced Adenovirus Targeted to the Retinoblastoma Pathway." JNCI Journal of the National Cancer Institute **95**(9): 652-660.

Fueyo, J., et al. (2000). "A mutant oncolytic adenovirus targeting the Rb pathway produces anti-glioma effect in vivo." Oncogene **19**(1): 2-12.

Garber, K. (2006). "China Approves World's First Oncolytic Virus Therapy For Cancer Treatment." JNCI: Journal of the National Cancer Institute **98**(5): 298-300.

Gea, Z. (2018). "Abstract–interim results of a phase II multicenter study of the conditionally replicative oncolytic adenovirus DNX-2401 with pembrolizumab (Keytruda) for recurrent glioblastoma; CAPTIVE STUDY (LEYNOTE-192)." Neuro-Oncology **20**(suppl_6): vi6.

Geletneky, K., et al. (2017). "Oncolytic H-1 Parvovirus Shows Safety and Signs of Immunogenic Activity in a First Phase I/IIa Glioblastoma Trial." Molecular Therapy **25**(12): 2620-2634.

Geoerger, B., et al. (2002). "Oncolytic Activity of the E1B-55 kDa-deleted Adenovirus ONYX-015 Is Independent of Cellular p53 Status in Human Malignant Glioma Xenografts1." Cancer Research **62**(3): 764-772.

Ghebremedhin, B. (2014). "Human adenovirus: Viral pathogen with increasing importance." European Journal of Microbiology and Immunology **4**(1): 26-33.

Ghiringhelli, F. O., et al. (2005). "Tumor cells convert immature myeloid dendritic cells into TGF-β–secreting cells inducing CD4+CD25+ regulatory T cell proliferation." Journal of Experimental Medicine **202**(7): 919-929.

Gianchecchi, E. and A. Fierabracci (2018). "Inhibitory Receptors and Pathways of Lymphocytes: The Role of PD-1 in Treg Development and Their Involvement in Autoimmunity Onset and Cancer Progression." Frontiers in immunology **9**.

Giberson, A. N., et al. (2012). "Chromatin structure of adenovirus DNA throughout infection." Nucleic Acids Research **40**(6): 2369-2376.

Gieryng, A., et al. (2017). "Immune microenvironment of gliomas." Laboratory Investigation **97**(5): 498-518.

Gonzalez-Pastor, R., et al. (2021). "Understanding and addressing barriers to successful adenovirus-based virotherapy for ovarian cancer." Cancer Gene Therapy **28**(5): 375-389.

Green, D. R. (2017). "Cell death and the immune system: getting to how and why." Immunological Reviews **277**(1): 4-8.

Gujar, S., et al. (2018). "Antitumor Benefits of Antiviral Immunity: An Underappreciated Aspect of Oncolytic Virotherapies." Trends in Immunology **39**(3): 209-221.

Haile, L. A., et al. (2012). "Immune Suppression: The Hallmark of Myeloid Derived Suppressor Cells." Immunological Investigations **41**(6-7): 581-594.

Hambardzumyan, D., et al. (2016). "The role of microglia and macrophages in glioma maintenance and progression." Nature Neuroscience **19**(1): 20-27.

Han, S., et al. (2016). "Rescuing defective tumor-infiltrating T-cell proliferation in glioblastoma patients." Oncology Letters **12**(4): 2924-2929.

Han, S., et al. (2014). "Tumour-infiltrating CD4+ and CD8+ lymphocytes as predictors of clinical outcome in glioma." British Journal of Cancer **110**(10): 2560-2568.

Hanssen, L., et al. (2013). "YB-1 Is an Early and Central Mediator of Bacterial and Sterile Inflammation In Vivo." The Journal of Immunology **191**(5): 2604-2613.

Hardcastle, J., et al. (2017). "Immunovirotherapy with measles virus strains in combination with anti-PD-1 antibody blockade enhances antitumor activity in glioblastoma treatment." Neuro-Oncology **19**(4): 493-502.

Hawkins, L. and T. Hermiston (2001). "Gene delivery from the E3 region of replicating human adenovirus: evaluation of the E3B region." Gene Therapy **8**(15): 1142-1148.

Hegi, M. E., et al. (2005). "MGMTGene Silencing and Benefit from Temozolomide in Glioblastoma." New England Journal of Medicine **352**(10): 997-1003.

Heise, C., et al. (2000). "An adenovirus E1A mutant that demonstrates potent and selective systemic anti-tumoral efficacy." Nature Medicine **6**(10): 1134-1139.

Hemminki, O., et al. (2012). "Ad3-hTERT-E1A, a Fully Serotype 3 Oncolytic Adenovirus, in Patients With Chemotherapy Refractory Cancer." Molecular Therapy **20**(9): 1821-1830.

Hibma, M. H., et al. (2009). "Increased apoptosis and reduced replication efficiency of the E3 region-modified dl309 adenovirus in cancer cells." Virus Res **145**(1): 112-120.

Hindupur, S. V., et al. (2020). "STAT3/5 Inhibitors Suppress Proliferation in Bladder Cancer and Enhance Oncolytic Adenovirus Therapy." International Journal of Molecular Sciences **21**(3): 1106.

Hoeben, R. C. and T. G. Uil (2013). "Adenovirus DNA Replication." Cold Spring Harbor Perspectives in Biology **5**(3): a013003-a013003.

Holm, P. S., et al. (2002). "YB-1 Relocates to the Nucleus in Adenovirus-infected Cells and Facilitates Viral Replication by Inducing E2 Gene Expression through the E2 Late Promoter." Journal of Biological Chemistry **277**(12): 10427-10434.

Holm, P. S., et al. (2004). "Multidrug-resistant Cancer Cells Facilitate E1-independent Adenoviral Replication." Cancer Research **64**(1): 322-328.

Holzmüller, R., et al. (2011). "YB-1 dependent virotherapy in combination with temozolomide as a multimodal therapy approach to eradicate malignant glioma." International Journal of Cancer **129**(5): 1265-1276.

Horwitz, G. A., et al. (2008). "Adenovirus Small e1a Alters Global Patterns of Histone Modification." Science **321**(5892): 1084-1085.

Huang, B., et al. (2021). "Current Immunotherapies for Glioblastoma Multiforme." Frontiers in immunology **11**.

Huber, A., et al. (2018). "Current State of Dendritic Cell-Based Immunotherapy: Opportunities for in vitro Antigen Loading of Different DC Subsets?" Frontiers in immunology **9**.

Huebener, P., et al. (2014). "High-Mobility Group Box 1 Is Dispensable for Autophagy, Mitochondrial Quality Control, and Organ Function In Vivo." Cell Metabolism **19**(3): 539-547.

Huettner, C., et al. (1997). "Interleukin 10 is expressed in human gliomas in vivo and increases glioma cell proliferation and motility in vitro." Anticancer Res **17**(5a): 3217-3224.

Hulina, A., et al. (2018). "Extracellular Hsp70 induces inflammation and modulates LPS/LTA-stimulated inflammatory response in THP-1 cells." Cell Stress and Chaperones **23**(3): 373-384.

Hussain, S. F., et al. (2006). "The role of human glioma-infiltrating microglia/macrophages in mediating antitumor immune responses1." Neuro-Oncology **8**(3): 261-279.

Hutter, G., et al. (2019). "Microglia are effector cells of CD47-SIRPα antiphagocytic axis disruption against glioblastoma." Proceedings of the National Academy of Sciences **116**(3): 997-1006.

Iacob, G. and E. B. Dinca (2009). "Current data and strategy in glioblastoma multiforme." Journal of medicine and life **2**(4): 386-393.

Ishida, Y., et al. (1992). "Induced expression of PD-1, a novel member of the immunoglobulin gene superfamily, upon programmed cell death." The EMBO Journal **11**(11): 3887-3895.

Ishii, N., et al. (1999). "Frequent Co-Alterations ofTP53, p16/CDKN2A, p14ARF,PTENTumor Suppressor Genes in Human Glioma Cell Lines." Brain Pathology **9**(3): 469-479.

Jackson, C., et al. (2011). "Challenges in Immunotherapy Presented by the Glioblastoma Multiforme Microenvironment." Clinical and Developmental Immunology **2011**: 1-20.

Jackson, C. M., et al. (2019). "Mechanisms of immunotherapy resistance: lessons from glioblastoma." Nature Immunology **20**(9): 1100-1109.

Jacobs, J. F. M., et al. (2009). "Regulatory T cells and the PD-L1/PD-1 pathway mediate immune suppression in malignant human brain tumors." Neuro-Oncology **11**(4): 394-402.

Jaime-Sanchez, P., et al. (2020). "Cell death induced by cytotoxic CD8+T cells is immunogenic and primes caspase-3–dependent spread immunity against endogenous tumor antigens." Journal for ImmunoTherapy of Cancer **8**(1): e000528.

Jhanji, V., et al. (2015). "Adenoviral keratoconjunctivitis." Survey of Ophthalmology **60**(5): 435-443.

Kajon, A. and J. Lynch (2016). "Adenovirus: Epidemiology, Global Spread of Novel Serotypes, and Advances in Treatment and Prevention." Seminars in Respiratory and Critical Care Medicine **37**(04): 586-602.

Kakiuchi, Y., et al. (2021). "Local oncolytic adenovirotherapy produces an abscopal effect via tumor-derived extracellular vesicles." Mol Ther **29**(10): 2920-2930.

Kicielinski, K. P., et al. (2014). "Phase 1 Clinical Trial of Intratumoral Reovirus Infusion for the Treatment of Recurrent Malignant Gliomas in Adults." Molecular Therapy **22**(5): 1056-1062.

Kielbik, M., et al. (2021). "Calreticulin—Multifunctional Chaperone in Immunogenic Cell Death: Potential Significance as a Prognostic Biomarker in Ovarian Cancer Patients." Cells **10**(1): 130.

Kitajima, S., et al. (2020). "Tumor Milieu Controlled by RB Tumor Suppressor." International Journal of Molecular Sciences **21**(7): 2450.

Kitamura, N., et al. (2009). "OX40 costimulation can abrogate Foxp3⁺regulatory T cell-mediated suppression of antitumor immunity." International Journal of Cancer **125**(3): 630-638.

Kiyokawa, J. and H. Wakimoto (2019). " Preclinical And Clinical Development Of Oncolytic Adenovirus For The Treatment Of Malignant Glioma ." Oncolytic Virotherapy **Volume 8**: 27-37.

Kolaczkowska, E. and P. Kubes (2013). "Neutrophil recruitment and function in health and inflammation." Nature Reviews Immunology **13**(3): 159-175.

Koodie, L., et al. (2019). "Rodents Versus Pig Model for Assessing the Performance of Serotype Chimeric Ad5/3 Oncolytic Adenoviruses." Cancers **11**(2): 198.

Kuwano, M., et al. (2003). "The basic and clinical implications of ABC transporters, Y-box-binding protein-1 (YB-1) and angiogenesis-related factors in human malignancies." Cancer Science **94**(1): 9-14.

Laevskaya, A., et al. (2021). "Metabolome-Driven Regulation of Adenovirus-Induced Cell Death." International Journal of Molecular Sciences **22**(1): 464.

Land, W. G. (2015). "The Role of Damage-Associated Molecular Patterns in Human Diseases: Part I - Promoting inflammation and immunity." Sultan Qaboos Univ Med J **15**(1): e9-e21.

Lang, F. F., et al. (2018). "Phase I Study of DNX-2401 (Delta-24-RGD) Oncolytic Adenovirus: Replication and Immunotherapeutic Effects in Recurrent Malignant Glioma." Journal of Clinical Oncology **36**(14): 1419-1427.

Larocca, C. J. and S. G. Warner (2018). "Oncolytic viruses and checkpoint inhibitors: combination therapy in clinical trials." Clinical and Translational Medicine **7**(1): 35.

Lasham, A., et al. (2012). "YB-1: oncoprotein, prognostic marker and therapeutic target?" Biochemical Journal **449**(1): 11-23.

Le Rhun, E., et al. (2018). "Associations of anticoagulant use with outcome in newly diagnosed glioblastoma." Eur J Cancer **101**: 95-104.

Leece, R., et al. (2017). "Global incidence of malignant brain and other central nervous system tumors by histology, 2003–2007." Neuro-Oncology **19**(11): 1553-1564.

Li, H., et al. (2009). "Cancer-Expanded Myeloid-Derived Suppressor Cells Induce Anergy of NK Cells through Membrane-Bound TGF-β1." The Journal of Immunology **182**(1): 240-249.

Li, J. and J. Gu (2019). "Efficacy and safety of ipilimumab for treating advanced melanoma: A systematic review and meta-analysis." J Clin Pharm Ther **44**(3): 420-429.

Lichtenegger, E., et al. (2019). "The Oncolytic Adenovirus XVir-N-31 as a Novel Therapy in Muscle-Invasive Bladder Cancer." Hum Gene Ther **30**(1): 44-56.

Lichtenstein, D. L., et al. (2004). "FUNCTIONS AND MECHANISMS OF ACTION OF THE ADENOVIRUS E3 PROTEINS." International Reviews of Immunology **23**(1-2): 75-111.

Louis, D. N., et al. (2016). "The 2016 World Health Organization Classification of Tumors of the Central Nervous System: a summary." Acta Neuropathologica **131**(6): 803-820.

Louis, D. N., et al. (2021). "The 2021 WHO Classification of Tumors of the Central Nervous System: a summary." Neuro-Oncology **23**(8): 1231-1251.

Louveau, A., et al. (2015). "Structural and functional features of central nervous system lymphatic vessels." Nature **523**(7560): 337-341.

Lutz, P., et al. (1997). "The product of the adenovirus intermediate gene IX is a transcriptional activator." Journal of Virology **71**(7): 5102-5109.

Ly, K. I., et al. (2020). "Imaging of Central Nervous System Tumors Based on the 2016 World Health Organization Classification." Neurol Clin **38**(1): 95-113.

Ma, J., et al. (2020). "Characterization of virus-mediated immunogenic cancer cell death and the consequences for oncolytic virus-based immunotherapy of cancer." Cell Death & Disease **11**(1).

Malkki, H. (2016). "Glioblastoma vaccine therapy disappointment in Phase III trial." Nature Reviews Neurology **12**(4): 190-190.

Mantwill, K., et al. (2013). "YB-1 dependent oncolytic adenovirus efficiently inhibits tumor growth of glioma cancer stem like cells." Journal of Translational Medicine **11**(1): 216.

Markert, J. M., et al. (2009). "Phase Ib Trial of Mutant Herpes Simplex Virus G207 Inoculated Pre-and Post-tumor Resection for Recurrent GBM." Molecular Therapy **17**(1): 199-207.

McGranahan, T., et al. (2019). "Current State of Immunotherapy for Treatment of Glioblastoma." Current Treatment Options in Oncology **20**(3).

Melcher, A., et al. (1998). "Tumor immunogenicity is determined by the mechanism of cell death via induction of heat shock protein expression." Nature Medicine **4**(5): 581-587.

Melin, B. S., et al. (2017). "Genome-wide association study of glioma subtypes identifies specific differences in genetic susceptibility to glioblastoma and non-glioblastoma tumors." Nature Genetics **49**(5): 789-794.

Melzer, M., et al. (2017). "Oncolytic Vesicular Stomatitis Virus as a Viro-Immunotherapy: Defeating Cancer with a “Hammer” and “Anvil”." Biomedicines **5**(4): 8.

Muster, V. and T. Gary (2020). "Incidence, Therapy, and Bleeding Risk—Cancer- Associated Thrombosis in Patients with Glioblastoma." Cancers **12**(6): 1354.

Nabors, L. B., et al. (2020). "Central Nervous System Cancers, Version 3.2020, NCCN Clinical Practice Guidelines in Oncology." Journal of the National Comprehensive Cancer Network **18**(11): 1537-1570.

Nduom, E. K., et al. (2015). "Immunosuppressive mechanisms in glioblastoma: Fig. 1." Neuro-Oncology **17**(suppl 7): vii9-vii14.

Nevins, J. R. (1982). "Induction of the synthesis of a 70,000 dalton mammalian heat shock protein by the adenovirus E1A gene product." Cell **29**(3): 913-919.

Ohgaki, H. and P. Kleihues (2013). "The Definition of Primary and Secondary Glioblastoma." Clinical Cancer Research **19**(4): 764-772.

Oliveira, E. R. A. and M. Bouvier (2019). "Immune evasion by adenoviruses: a window into host–virus adaptation." FEBS Letters **593**(24): 3496-3503.

Omuro, A. and L. M. DeAngelis (2013). "Glioblastoma and Other Malignant Gliomas: A Clinical Review." JAMA **310**(17): 1842-1850.

Omuro, A., et al. (2018). "Nivolumab with or without ipilimumab in patients with recurrent glioblastoma: results from exploratory phase I cohorts of CheckMate 143." Neuro-Oncology **20**(5): 674-686.

Ostrom, Q. T., et al. (2019). "Risk factors for childhood and adult primary brain tumors." Neuro-Oncology **21**(11): 1357-1375.

Ostrom, Q. T., et al. (2014). "CBTRUS Statistical Report: Primary Brain and Central Nervous System Tumors Diagnosed in the United States in 2007-2011." Neuro-Oncology **16**(suppl 4): iv1-iv63.

Pan, P. C.-W. and A. Haggiagi (2019). "Neurologic Immune-Related Adverse Events Associated with Immune Checkpoint Inhibition." Current Oncology Reports **21**(12).

Parajuli, P. (2013). "Role of IL-17 in Glioma Progression." Journal of Spine & Neurosurgery.

Parsa, A. T., et al. (2007). "Loss of tumor suppressor PTEN function increases B7-H1 expression and immunoresistance in glioma." Nature Medicine **13**(1): 84-88.

Patsoukis, N., et al. (2020). "Revisiting the PD-1 pathway." Science Advances **6**(38): eabd2712.

Paudel, Y. N., et al. (2019). "Enlightening the role of high mobility group box 1 (HMGB1) in inflammation: Updates on receptor signalling." Eur J Pharmacol **858**: 172487.

Pearson, J. R. D., et al. (2020). "Immune Escape in Glioblastoma Multiforme and the Adaptation of Immunotherapies for Treatment." Frontiers in immunology **11**.

Pelka, P., et al. (2009). "Identification of a second independent binding site for the pCAF acetyltransferase in adenovirus E1A." Virology **391**(1): 90-98.

Pellegatta, S., et al. (2018). "Constitutive and TNFα-inducible expression of chondroitin sulfate proteoglycan 4 in glioblastoma and neurospheres: Implications for CAR-T cell therapy." Science Translational Medicine **10**(430): eaao2731.

Peng, M., et al. (2019). "Neoantigen vaccine: an emerging tumor immunotherapy." Molecular Cancer **18**(1).

Pereira, M. B., et al. (2018). "Transcriptional characterization of immunological infiltrates and their relation with glioblastoma patients overall survival." OncoImmunology **7**(6): e1431083.

Pham, T., et al. (2018). "An Update on Immunotherapy for Solid Tumors: A Review." Annals of Surgical Oncology **25**(11): 3404-3412.

Piccinini, A. M. and K. S. Midwood (2010). "DAMPening Inflammation by Modulating TLR Signalling." Mediators of Inflammation **2010**: 1-21.

Piya, S., et al. (2011). "The E1B19K Oncoprotein Complexes with Beclin 1 to Regulate Autophagy in Adenovirus-Infected Cells." PLoS ONE **6**(12): e29467.

Poli, A., et al. (2013). "Targeting glioblastoma with NK cells and mAb against NG2/CSPG4 prolongs animal survival." Oncotarget **4**(9): 1527-1546.

Polyzoidis, S. and K. Ashkan (2014). "DCVax®-L—Developed by Northwest Biotherapeutics." Human Vaccines & Immunotherapeutics **10**(11): 3139-3145.

Pombo Antunes, A. R., et al. (2020). "Understanding the glioblastoma immune microenvironment as basis for the development of new immunotherapeutic strategies." eLife **9**.

Pouwels, S. D., et al. (2014). "DAMPs activating innate and adaptive immune responses in COPD." Mucosal Immunology **7**(2): 215-226.

Preusser, M., et al. (2015). "Prospects of immune checkpoint modulators in the treatment of glioblastoma." Nature Reviews Neurology **11**(9): 504-514.

Qian, J., et al. (2018). "The IFN-γ/PD-L1 axis between T cells and tumor microenvironment: hints for glioma anti-PD-1/PD-L1 therapy." Journal of Neuroinflammation **15**(1).

Radke, J. R., et al. (2014). "Adenovirus E1B 19-Kilodalton Protein Modulates Innate Immunity through Apoptotic Mimicry." Journal of Virology **88**(5): 2658-2669.

Radogna, F. and M. Diederich (2018). "Stress-induced cellular responses in immunogenic cell death: Implications for cancer immunotherapy." Biochemical Pharmacology **153**: 12-23.

Randall, R. E. and S. Goodbourn (2008). "Interferons and viruses: an interplay between induction, signalling, antiviral responses and virus countermeasures." Journal of General Virology **89**(1): 1-47.

Ranger, A. M., et al. (2014). "Familial syndromes associated with intracranial tumours: a review." Child's Nervous System **30**(1): 47-64.

Razavi, S. M., et al. (2016). "Immune Evasion Strategies of Glioblastoma." Front Surg **3**: 11.

Reardon, D. A., et al. (2020). "Effect of Nivolumab vs Bevacizumab in Patients With Recurrent Glioblastoma." JAMA Oncology **6**(7): 1003.

Reardon, D. A., et al. (2016). "Glioblastoma Eradication Following Immune Checkpoint Blockade in an Orthotopic, Immunocompetent Model." Cancer Immunology Research **4**(2): 124-135.

Reardon, D. A., et al. (2017). "Phase 2 study to evaluate safety and efficacy of MEDI4736 (durvalumab [DUR]) in glioblastoma (GBM) patients: An update." Journal of Clinical Oncology **35**(15_suppl): 2042-2042.

Rehman, H., et al. (2016). "Into the clinic: Talimogene laherparepvec (T-VEC), a first-in-class intratumoral oncolytic viral therapy." Journal for ImmunoTherapy of Cancer **4**(1).

Ribas, A., et al. (2017). "Oncolytic Virotherapy Promotes Intratumoral T Cell Infiltration and Improves Anti-PD-1 Immunotherapy." Cell **170**(6): 1109-1119.e1110.

Rius-Rocabert, S., et al. (2020). "Oncolytic Virotherapy in Glioma Tumors." International Journal of Molecular Sciences **21**(20): 7604.

Rivera Vargas, T. and L. Apetoh (2017). "Danger signals: Chemotherapy enhancers?" Immunol Rev **280**(1): 175-193.

Roa, W., et al. (2004). "Abbreviated Course of Radiation Therapy in Older Patients With Glioblastoma Multiforme: A Prospective Randomized Clinical Trial." Journal of Clinical Oncology **22**(9): 1583-1588.

Robert-Guroff, M. (2007). "Replicating and non-replicating viral vectors for vaccine development." Current Opinion in Biotechnology **18**(6): 546-556.

Rodriguez, A., et al. (2017). "Chimeric antigen receptor T-cell therapy for glioblastoma." Transl Res **187**: 93-102.

Roesch, S., et al. (2018). "When Immune Cells Turn Bad—Tumor-Associated Microglia/Macrophages in Glioma." International Journal of Molecular Sciences **19**(2): 436.

Rognoni, E., et al. (2009). "Adenovirus-based virotherapy enabled by cellular YB-1 expression in vitro and in vivo." Cancer Gene Therapy **16**(10): 753-763.

Rosato, P. C., et al. (2019). "Virus-specific memory T cells populate tumors and can be repurposed for tumor immunotherapy." Nature Communications **10**(1).

Roth, W., et al. (1999). "Locoregional Apo2L/TRAIL eradicates intracranial human malignant glioma xenografts in athymic mice in the absence of neurotoxicity." Biochem Biophys Res Commun **265**(2): 479-483.

Russell, S. J., et al. (2012). "Oncolytic virotherapy." Nature Biotechnology **30**(7): 658-670.

Russell, W. C. (2009). "Adenoviruses: update on structure and function." Journal of General Virology **90**(1): 1-20.

Saha, D., et al. (2018). "Oncolytic herpes simplex virus immunovirotherapy in combination with immune checkpoint blockade to treat glioblastoma." Immunotherapy **10**(9): 779-786.

Saha, D. and S. D. Rabkin (2020). Immunohistochemistry for Tumor-Infiltrating Immune Cells After Oncolytic Virotherapy, Springer New York**:** 179-190.

Salinas, R. D., et al. (2020). "Potential of Glioblastoma-Targeted Chimeric Antigen Receptor (CAR) T-Cell Therapy." CNS Drugs **34**(2): 127-145.

Salter, M. W. and B. Stevens (2017). "Microglia emerge as central players in brain disease." Nature Medicine **23**(9): 1018-1027.

Schalper, K. A., et al. (2019). "Neoadjuvant nivolumab modifies the tumor immune microenvironment in resectable glioblastoma." Nature Medicine **25**(3): 470-476.

Scheffel, T. B., et al. (2021). "Immunosuppression in Gliomas via PD-1/PD-L1 Axis and Adenosine Pathway." Frontiers in Oncology **10**.

Scheinecker, C., et al. (2020). "Treg cells in health and autoimmune diseases: New insights from single cell analysis." Journal of Autoimmunity **110**: 102376.

Schreiber, R. D., et al. (2011). "Cancer Immunoediting: Integrating Immunity’s Roles in Cancer Suppression and Promotion." Science **331**(6024): 1565-1570.

Schwartzbaum, J. A., et al. (2006). "Epidemiology and molecular pathology of glioma." Nature Clinical Practice Neurology **2**(9): 494-503.

Seifried, L. A., et al. (2008). "pRB-E2F1 Complexes Are Resistant to Adenovirus E1A-Mediated Disruption." Journal of Virology **82**(9): 4511-4520.

Sharma, P., et al. (2017). "Primary, Adaptive, and Acquired Resistance to Cancer Immunotherapy." Cell **168**(4): 707-723.

Shimato, S., et al. (2012). "Profound tumor-specific Th2 bias in patients with malignant glioma." BMC Cancer **12**(1): 561.

Srivastava, M. K., et al. (2010). "Myeloid-Derived Suppressor Cells Inhibit T-Cell Activation by Depleting Cystine and Cysteine." Cancer Research **70**(1): 68-77.

Stupp, R., et al. (2009). "Effects of radiotherapy with concomitant and adjuvant temozolomide versus radiotherapy alone on survival in glioblastoma in a randomised phase III study: 5-year analysis of the EORTC-NCIC trial." Lancet Oncol **10**(5): 459-466.

Stupp, R., et al. (2005). "Radiotherapy plus Concomitant and Adjuvant Temozolomide for Glioblastoma." New England Journal of Medicine **352**(10): 987-996.

Stupp, R., et al. (2017). "Effect of Tumor-Treating Fields Plus Maintenance Temozolomide vs Maintenance Temozolomide Alone on Survival in Patients With Glioblastoma." JAMA **318**(23): 2306.

Sung, H., et al. (2021). "Global Cancer Statistics 2020: GLOBOCAN Estimates of Incidence and Mortality Worldwide for 36 Cancers in 185 Countries." CA: A Cancer Journal for Clinicians **71**(3): 209-249.

Suzuki, M., et al. (2015). "Preferable sites and orientations of transgene inserted in the adenovirus vector genome: The E3 site may be unfavorable for transgene position." Gene Therapy **22**(5): 421-429.

Takasu, A., et al. (2016). "Immunogenic cell death by oncolytic herpes simplex virus type 1 in squamous cell carcinoma cells." Cancer Gene Therapy **23**(4): 107-113.

Tan, A. C., et al. (2020). "Management of glioblastoma: State of the art and future directions." CA: A Cancer Journal for Clinicians **70**(4): 299-312.

Taylor, O. G., et al. (2019). "Glioblastoma Multiforme: An Overview of Emerging Therapeutic Targets." Front Oncol **9**: 963.

Tesileanu, C. M. S., et al. (2020). "Survival of diffuse astrocytic glioma, IDH1/2 wildtype, with molecular features of glioblastoma, WHO grade IV: a confirmation of the cIMPACT-NOW criteria." Neuro-Oncology **22**(4): 515-523.

Tollefson, A. E., et al. (1996). "The E3-11.6-kDa adenovirus death protein (ADP) is required for efficient cell death: characterization of cells infected with adp mutants." Virology **220**(1): 152-162.

Tone, Y., et al. (2007). "OX40 Gene Expression Is Up-Regulated by Chromatin Remodeling in Its Promoter Region Containing Sp1/Sp3, YY1, and NF-κB Binding Sites." The Journal of Immunology **179**(3): 1760-1767.

Toth, K. and W. S. M. Wold (2010). "Increasing the Efficacy of Oncolytic Adenovirus Vectors." Viruses **2**(9): 1844-1866.

Tucha, O., et al. (2000). "Cognitive deficits before treatment among patients with brain tumors." Neurosurgery **47**(2): 324-333; discussion 333-324.

Tumangelova-Yuzeir, K., et al. (2019). "Mesenchymal Stem Cells Derived and Cultured from Glioblastoma Multiforme Increase Tregs, Downregulate Th17, and Induce the Tolerogenic Phenotype of Monocyte-Derived Cells." Stem Cells International **2019**: 1-15.

Ueda, R., et al. (2009). "Dicer-regulated microRNAs 222 and 339 promote resistance of cancer cells to cytotoxic T-lymphocytes by down-regulation of ICAM-1." Proceedings of the National Academy of Sciences **106**(26): 10746-10751.

Van Bussel, M. T. J., et al. (2019). "Intracranial antitumor responses of nivolumab and ipilimumab: a pharmacodynamic and pharmacokinetic perspective, a scoping systematic review." BMC Cancer **19**(1).

Van Meir, E. G. (1995). "Cytokines and tumors of the central nervous system." Glia **15**(3): 264-288.

Verhaak, R. G. W., et al. (2010). "Integrated Genomic Analysis Identifies Clinically Relevant Subtypes of Glioblastoma Characterized by Abnormalities in PDGFRA, IDH1, EGFR, and NF1." Cancer Cell **17**(1): 98-110.

Wang, H., et al. (2017). "Metabolic Regulation of Tregs in Cancer: Opportunities for Immunotherapy." Trends in Cancer **3**(8): 583-592.

Wang, H., et al. (2021). "Different T-cell subsets in glioblastoma multiforme and targeted immunotherapy." Cancer Letters **496**: 134-143.

Wang, S., et al. (2019). "Antigen presentation and tumor immunogenicity in cancer immunotherapy response prediction." eLife **8**.

Wang, S. and Y. Zhang (2020). "HMGB1 in inflammation and cancer." Journal of Hematology & Oncology **13**(1).

Wang, Z., et al. (2016). "Molecular and clinical characterization of PD-L1 expression at transcriptional level via 976 samples of brain glioma." OncoImmunology **5**(11): e1196310.

Wei, J., et al. (2011). "Hypoxia Potentiates Glioma-Mediated Immunosuppression." PLoS ONE **6**(1): e16195.

Weller, M., et al. (2017). "European Association for Neuro-Oncology (EANO) guideline on the diagnosis and treatment of adult astrocytic and oligodendroglial gliomas." The Lancet Oncology **18**(6): e315-e329.

Wen, P. Y., et al. (2020). "Glioblastoma in adults: a Society for Neuro-Oncology (SNO) and European Society of Neuro-Oncology (EANO) consensus review on current management and future directions." Neuro-Oncology **22**(8): 1073-1113.

Wintterle, S., et al. (2003). "Expression of the B7-Related Molecule B7-H1 by Glioma Cells: A Potential Mechanism of Immune Paralysis1." Cancer Research **63**(21): 7462-7467.

Workenhe, S. T., et al. (2014). "Immunogenic HSV-mediated oncolysis shapes the antitumor immune response and contributes to therapeutic efficacy." Mol Ther **22**(1): 123-131.

Woroniecka, K. I., et al. (2018). "T-cell Dysfunction in Glioblastoma: Applying a New Framework." Clinical Cancer Research **24**(16): 3792-3802.

Wu, A., et al. (2010). "Glioma cancer stem cells induce immunosuppressive macrophages/microglia." Neuro-Oncology **12**(11): 1113-1125.

Yan, H., et al. (2009). "IDH1andIDH2Mutations in Gliomas." New England Journal of Medicine **360**(8): 765-773.

Yi, Y., et al. (2016). "Glioblastoma Stem-Like Cells: Characteristics, Microenvironment, and Therapy." Frontiers in Pharmacology **7**.

Ylösmäki, E., et al. (2021). "Characterization of a novel OX40 ligand and CD40 ligand-expressing oncolytic adenovirus used in the PeptiCRAd cancer vaccine platform." Molecular Therapy - Oncolytics **20**: 459-469.

Yun, C.-O., et al. (2005). "ADP-overexpressing adenovirus elicits enhanced cytopathic effect by induction of apoptosis." Cancer Gene Therapy **12**(1): 61-71.

Zagzag, D., et al. (2005). "Downregulation of major histocompatibility complex antigens in invading glioma cells: stealth invasion of the brain." Laboratory Investigation **85**(3): 328-341.

Zamarin, D., et al. (2014). "Localized Oncolytic Virotherapy Overcomes Systemic Tumor Resistance to Immune Checkpoint Blockade Immunotherapy." Science Translational Medicine **6**(226): 226ra232-226ra232.

Zeng, J., et al. (2013). "Anti-PD-1 Blockade and Stereotactic Radiation Produce Long-Term Survival in Mice With Intracranial Gliomas." International Journal of Radiation Oncology*Biology*Physics **86**(2): 343-349.

Zhang, S., et al. (2016). "The Role of Myeloid-Derived Suppressor Cells in Patients with Solid Tumors: A Meta-Analysis." PLoS ONE **11**(10): e0164514.

Zhang, W. and M. J. Imperiale (2003). "Requirement of the Adenovirus IVa2 Protein for Virus Assembly." Journal of Virology **77**(6): 3586-3594.

Zhao, Y., et al. (2021). "Oncolytic Adenovirus: Prospects for Cancer Immunotherapy." Frontiers in Microbiology **12**.

Zheng, J., et al. (2009). "Discovery of YB-1 as a new immunological target in neuroblastoma by vaccination in the context of regulatory T cell blockade." Acta biochimica et biophysica Sinica **41**(12): 980-990.

Zheng, J., et al. (2009). "Discovery of YB-1 as a new immunological target in neuroblastoma by vaccination in the context of regulatory T cell blockade." Acta Biochimica et Biophysica Sinica **41**(12): 980-990.

Zhu, P., et al. (2017). "Survival benefit of glioblastoma patients after FDA approval of temozolomide concomitant with radiation and bevacizumab: A population-based study." Oncotarget **8**(27): 44015-44031.

Zhu, Z., et al. (2020). "PD-L1-Mediated Immunosuppression in Glioblastoma Is Associated With the Infiltration and M2-Polarization of Tumor-Associated Macrophages." Frontiers in immunology **11**.

8. Acknowledgement

First and foremost, I would like to thank Prof. Dr. Ulrike Naumann for giving me the opportunity to perform my doctoral work and thesis in her department. Besides that, I also want to thank her for her excellent supervision and her guidance whenever I needed it. Thank you so much, Uli!

Furthermore, I would like to thank Prof. Dr. Ulrich Lauer and Prof. Dr. Stephan Huber for their help throughout my whole project as members of my advisory board. Their help and input contributed notably to this work.

Many thanks also to Prof. Dr. Per Sonne Holm and Maximilian Ehrenfeld, our cooperation partners from the TU Munich for their assistance and their excellent work that contributed to this project.

Additionally, I want to express my gratitude to Jasmin Buch and Jakob Rüttinger, which I supervised during my project and who contributed to this work. You did an excellent job and I wish you all the best for your future projects!

Apart of that, I would like to thank also all members of the neurooncology research group, present and past. All of you were amazing colleagues and good friends and I miss you already. Special thanks thereby to Nikhil Ranjan, who helped me a lot in the beginning and to Ali El-Ayoubi, who shared hours and hours of perfectly scientific as well as non-scientific moments with me and became an amazing friend.

Finally, I would like to thank my girlfriend, Leonie Dany, my whole family, Eric, Helene and Nathalie Klawitter, Helga and Dominik Martiniak and all of my friends. You all supported me unconditionally and all the time. I am grateful and honoured to have you in my life. Thank you for everything!